Inaugural dissertation

for

obtaining the doctoral degree

of the

Combined Faculty of Mathematics, Engineering and Natural Sciences

of the

Ruprecht-Karls-University

Heidelberg

Presented by

M.Sc. Anna-Clara Schnell

born in: Herrenberg, Germany

Oral examination: 14.12.2023

Virus Venetian masked ball: Does the Hepatitis Delta Virus use different helper viruses?

Referees:

Prof. Dr. Dr. h.c. Ralf Bartenschlager

Prof. Dr. Oliver T. Fackler

Abstract

Changes in viral host cell tropism by e.g. changing receptor usage can lead to altered disease manifestations, requiring different treatment modalities. Hepatitis Delta virus (HDV), a small hepatotropic RNA virus, is known to depend on hepatitis B virus (HBV) envelope proteins for envelopment and spread. However, as HDV possesses the ability to replicate in non-hepatic cells and since envelopment of HDV was recently proposed to be mediated by non-HBV viruses, there might be an increased potential for altered host cell tropism of HDV due to differential envelope protein usage. This would have major clinical implications, as currently only HBV positive carriers are screened for HDV and specific therapeutic options only target HBV-dependent spread.

Viruses that were proposed to mediate envelopment of HDV include hepatitis C virus (HCV) and vesicular stomatitis virus (VSV). As HDV is known for its liver tropism, I focused primarily on hepatitis C virus (HCV) as potential HBV-independent helper and aimed to evaluate the following questions: a) Does HDV make use of HCV envelope proteins? b) Can HDV be rendered susceptible for alternative helper usage by modification of HBV specificity determinants in HDV? c) What is the zoonotic potential of HDV via utilisation of non-human hepadnaviral helper viruses?

I made use of different human cell culture systems based on RNA transfection or viral infection. Thereby, I was able to show efficient co-replication and co-infection of HDV and HCV in the same cell. However, production of HCV enveloped HDV particles was not observed. Based on plasmid transfection, I showed that HDV preferentially uses HBV with little, if any, envelopment by HCV or VSV. Based on sequence comparison to an animal Delta-like agent putatively using HBV-independent spread, I hypothesised that determinants specifically targeting the HBV envelope might hinder HDV from using alternative viral envelopes. However, eliminating HBV specificity determinants from HDV did not render HDV competent to use non-HBV envelopes. As the HDV-HBV interaction is mediated by a tryptophan-rich domain on HBV envelope proteins, I examined HCV and VSV envelope proteins for the presence of similar determinants. However, algorithm-based protein structure prediction did not detect such determinants, which is consistent with the almost exclusive envelopment of HDV by HBV. Last, I investigated various non-human hepadnaviruses for their capacity to provide helper function for HDV. To this end, I produced non-infectious self-assembling particles exclusively consisting of envelope proteins and preliminarily investigated secretion of HDV RNA mediated by these particles.

Taken together, the data presented in this study support the current view that HDV most likely utilises exclusively HBV as helper virus, further arguing for co-evolution of these two viruses.

Kurzfassung

Veränderungen im viralen Wirtszelltropismus durch beispielsweise veränderte Rezeptorbindungsspezifität können ein verändertes Krankheitsbild sowie angepasste Behandlungsmöglichkeiten bedingen. Hepatitis Delta Virus (HDV), ein kleines RNA Virus, ist hinsichtlich seiner Umhüllung und Verbreitung abhängig von Hepatitis B Virus (HBV). Da für HDV gezeigt werden konnte, dass eine Replikation in verschiedenen Zelltypen möglich ist und darüber hinaus eine mögliche HBV-unabhängige Verbreitung von HDV postuliert wurde, ist ein erhöhtes Risiko für veränderten Zelltropismus abhängig von der genutzten Hülle denkbar. Sollte dies der Fall sein, sind gravierende klinische Auswirkungen zu erwarten, da bisher lediglich HBV positive Patienten auf HDV getestet werden und darüber hinaus spezifische Behandlung von HDV nur auf HBV-umhülltes HDV abzielt.

Bisher wurde eine mögliche Umhüllung von HDV unter anderem durch Hepatitis C Virus und Vesicular Stomatitis Virus (VSV) postuliert. Da HDV für seinen Leber-Tropismus bekannt ist, habe ich mich in dieser Arbeit auf HCV als mögliches HBV-unabhängiges Helfervirus konzentriert, um folgende Fragen zu beantworten: a) Nutzt HDV Hüllproteine von HCV für die Umhüllung? b) Kann durch Veränderung der HBV-spezifischen Determinanten im HDV Genom eine Nutzung anderer Hüllproteine ermöglicht werden? c) Wie ist das zoonotische Potenzial von HDV durch Nutzung tierischer HBV ähnlicher Hüllproteine einzuschätzen?

In dieser Arbeit nutzte ich verschiedene Zellkultursysteme basierend auf RNA Transfektion oder viraler Infektion. In diesen Systemen konnte ich eine effiziente Ko-Replikation und Ko-Infektion von HDV und HCV in der gleichen Zelle nachweisen. Dennoch war die Bildung von HCV umhüllten HDV Partikeln nicht zu beobachten. In einem Plasmid-Transfektionssystem konnte ich weiterhin zeigen, dass HDV bevorzugt HBV Hüllproteine im Gegensatz zu HCV oder VSV Hüllproteinen nutzt. Ausgehend von einem Sequenzvergleich zwischen HDV und einem tierischen HDV ähnlichen Virus, welches vermutlich einen HBV-unabhängigen Verbreitungsweg nutzt, stellte ich die Hypothese auf, dass die Determinanten für spezifische HBV/HDV Interaktion für die Nutzung anderer Hüllproteine hinderlich sein könnten. Nach Eliminierung dieser Determinanten konnte dennoch keine Umhüllung von HDV mit HCV Hüllproteinen beobachtet werden. Da die Interaktion zwischen HDV und HBV durch eine Tryptophan-reiche Domäne auf den HBV Hüllproteinen vermittelt wird, habe ich HCV und VSV Hüllproteine auf ähnliche Determinanten hin untersucht. Die Untersuchung mittels Algorithmus-basierter Proteinstrukturvorhersage konnte in beiden Proteinen keine solchen Determinanten detektieren, was mit der nahezu ausschließlichen Umhüllung von HDV durch HBV Hüllproteine übereinstimmt. Zuletzt untersuchte ich weitere Hepadnaviren hinsichtlich ihrer

Umhüllungskapazität für HDV. Hierzu konnte ich die Produktion von nicht-infektiösen Partikeln, welche nur aus Hüllproteinen bestehen, nachweisen und untersuchte die Sekretion von HDV RNA durch diese Partikel in einem Pilotexperiment.

Zusammenfassend lässt sich sagen, dass die Daten dieser Arbeit den bisherigen Kenntnisstand stützen, dass HDV vermutlich nur von HBV abhängig ist, was wiederum auf eine Ko-Evolution beider Viren hindeutet.

Contents

List of Figures

List of Tables

List of abbreviations

AA	Amino acid
ADAR1	Adenosine deaminase acting on RNA 1
agHDV	Antigenomic HDV RNA
AGL	Antigenic loop
AMDV	Astatotilapia HBV
ANOVA	Analysis of variance
APOBEC3G	Apolipoprotein B mRNA editing enzyme catalytic polypeptide 3G
ApoE	Apolipoprotein E
APS	Ammoniumperoxosulfate
ATP	Adenosinetriphosphate
BgHBV	Bluegill HBV
BHDAg	BHDV antigen
BHDV	Bat HDV
BSA	Bovine serum albumin
cccDNA	Covalently closed circular DNA
CD81	Cluster of differentiation 81
CIC	Co-infection coefficient
CSKV	Coho salmon HBV
CV	Column volume
CYL	Cytosolic loop
d.p.i.	Days post infection
d.p.t.	Days post transfection
DAA	Directly acting antivirals
DAPI	4',6-Diamidin-2-phenylindol
DEPC	Diethylpolycarbonate
DHBV	Duck HBV
DMEM	Dulbecco's modified Eagle medium
DMSO	Dimethylsulphoxide
DNA	Desoxyribonucleic acid
dNTP	Desoxynucleotide triphosphate
DR	Direct repeat
dslDNA	Double stranded linear DNA

DTT ..... Dithiothreitol
ECL ..... Enhanced chemiluminescence
EDTA ..... Ethylenediaminetetraacetic acid
EGFR ..... Epidermal growth factor receptor
EGTA ..... Ethylene glycol-bis(β-aminoethyl ether)-N,N,N,N-tetraacetic acid
ELISA ..... Enzyme linked immunosorbant assay
EMA ..... European Medicines Agency
ER ..... Endoplasmatic reticulum
ESCRT ..... Endosomal sorting complex required for transport
FCS ..... Fetal calf serum
flHCV ..... Full length HCV RNA
fw ..... Forward
GAG ..... Glycosaminoglycan moieties
GFP ..... Green fluorescent protein
gHDV ..... Genomic HDV RNA
gt ..... Genotype
HA ..... Hemagglutinin
HAV ..... Hepatitis A virus
HBcAg ..... Hepatitis B core antigen
HBsAg ..... Hepatitis B surface antigen
HBV ..... Hepatitis B virus
HBx ..... Hepatitis B X protein
HCC ..... Hepatocellular carcinoma
HCV ..... Hepatitis C virus
HDAg ..... Hepatitis Delta Antigen
HDV ..... Hepatitis D virus
HeHBV ..... Heron HBV
HEPES ..... 2(4-(2-hydroxyethyl)-1-piperazine)ethanesulfonic acid
HEV ..... Hepatitis E virus
HIV ..... Human immunodeficiency virus
HSPG ..... Heparan sulfate proteoglycan
HVR-1 ..... Hypervariable region 1
IF ..... Immunofluorescence
IFN ..... Interferon
IgG ..... Immunoglobulin G
IRES ..... Internal ribosomal entry site
kb ..... Kilo base pairs

LB ..... Luria Broth
LB-Amp ..... LB medium + 1mg/mL Ampicillin
LDLR ..... Low density lipoprotein receptor
LFB ..... Lonafarnib
LSEC ..... Liver sinusoidal endothelial cell
MEM ..... Minimum essential medium
miR ..... microRNA
MOI ..... Multiplicity of infection
mRNA ..... Messenger RNA
MVB ..... Multivesicular body
NANBH ..... Non-A-Non-B-Hepatitis
NCBI ..... National Center for Biotechnology Information
NEAA ..... Non-essential amino acids
NEB ..... New England Biolabs
NLS ..... Nuclear localisation signal
NPHV ..... Nonprimate hepacivirus
NS ..... Non-structural protein
NTCP ..... Sodium taurocholate co-transporting peptide
ORF ..... Open reading frame
PBS ..... Phosphate buffered saline
PCR ..... Polymerase chain reaction
PEG ..... Polyethylenglycol
PFA ..... Paraformaldehyde
pgRNA ..... Pregenomic RNA
PNK ..... Polynucleotidkinase
qPCR ..... Quantitative PCR
rcDNA ..... Relaxed circular DNA
rev ..... Reverse
RNA ..... Ribonucleic acid
RNA Pol II ... RNA polymerase II
RNP ..... Ribonucleoparticle
RRHBV ..... Rice rat HBV
rSAP ..... Recombinant shrimp alkaline phosphatase
RT-qPCR ..... Reverse transcription followed by qPCR
SDS ..... Sodiumdodecylsulfate
sgHCV ..... Subgenomic HCV RNA
SIC ..... Super-infection coefficient

SkHBV ..... Skink HBV
SLHBV ..... Spiny lizard HBV
SRB1 ..... Scavenger receptor B1
SVP ..... Subviral particle
TAE ..... Tris-acetate-EDTA
TBE ..... Tris-borate-EDTA
TFHBV ..... Tibetan frog HBV
TGS ..... Tris-glycine-SDS
TMB ..... Tetramethylbenzidine
TMDV ..... Mexican tetra HBV
TN ..... Tris-NaCl
TRD ..... Tryptophan-rich domain
Trp ..... Tryptophan
TSG101 ..... Tumor susceptibility gene 101
UTR ..... Untranslated region
UV ..... Ultra violet
VSV ..... Vesicular stomatitis virus
WHV ..... Woodchuck HBV
wt ..... Wildtype

1 Introduction

Viral host tropism is determined by the ability of a virus to replicate in a certain host and cell type, which can be restricted at any stage of the viral replication cycle [144]. Various viruses have been observed to have altered tropism by e.g. changing receptor binding specificity. This is classically driven by local changes in the viral receptor binding proteins as described for influenza- and coronaviruses [178, 128]. In contrast, snatching an envelope in order to mediate tropism is not a common phenomenon. Paired with the ability to replicate in many cell types, this would have major clinical implications such as delayed identification of new infections, an unknown or even more severe disease pattern and/or altered treatment options. As such a phenomenon has been postulated for hepatitis D virus known for its almost exclusive human liver tropism [150], there is an urgent need to further investigate the importance of this observation.

1.1 Hepatitis viruses

Infection of the liver can occur by different viral agents. Sharing their narrow tropism for the human liver and inducing local inflammation, they are called hepatitis viruses (derived from the Greek words *hepar* – liver and *itis* – inflammation). Viral infection represents the most common cause for liver disease, even before alcohol or toxin intake or certain medications. The chronic damage of the liver caused by persistent viral infection can lead to fibrosis, cirrhosis, and hepatocellular carcinoma (HCC), which is the third leading cause of cancer-related deaths worldwide. Although vaccination or treatment is available against several hepatitis viruses, the numbers of viral hepatitis cases are constantly increasing. By 2015, numbers of deaths related to viral hepatitis reached approximately 1,34 million worldwide, surpassing the numbers of deaths related to HIV or tuberculosis and leading to a major global health burden [213, 21, 6].
To date, five hepatitis viruses with different geno- and serotypes have been identified: hepatitis virus A, B, C, D, and E. They originate from different taxa and therefore differ in replication strategy, particle composition, routes of transmission, and chronicity of infection.

The only hepatitis virus causing exclusively acute infections is hepatitis A virus (HAV). Hepatitis E virus (HEV) causes mostly acute infections, but can establish chronicity in immunosuppressed individuals. Both viruses possess a single stranded RNA genome of positive polarity and are transmitted via the fecal-oral route. HAV [164] belongs to

the family of *Picornaviridae*, whereas HEV [161] belongs to the family of *Hepeviridae*. Both viruses are considered non-enveloped, although HEV can occur in a so-called quasi-enveloped form being associated with cellular membranes [133]. Clinical appearance of HAV and HEV infection is very similar and can include elevation of liver parameters, jaundice, hepatomegaly, as well as non-specific symptoms like fever, nausea, loss of appetite and abdominal pain. In rare cases, a fulminant hepatitis with elevated risk of death can occur. Many infections occurring in young children are asymptomatic or exhibit only very mild symptoms, whereas disease severity increases with age. Vaccination is available for HAV and HEV, with the HEV vaccine only being available in China [164, 161].

Infection with hepatitis virus B, C, and D (HBV, HCV, HDV) can lead to an acute hepatitis but also in a certain number of patients develop into a chronic disease. These viruses are described in more detail below.

1.1.1 Hepatitis B virus

HBV was the first isolated hepatitis virus, although HAV and HBV were previously recognised as two different types of viral hepatitis [50]. Belonging to the family of *Hepadnaviridae*, HBV was first detected in 1970 by David S. Dane using electron microscopy [55] and is therefore also called *Dane-particle*.

Particle structure and genome organisation

The virus particle of HBV measures approximately 42nm in diameter and consists of an envelope surrounding a capsid that harbors the viral genome. The envelope is built from a lipid bilayer and the hepatitis B surface antigen (HBsAg), which is produced in three different variants known as S, M, and L protein. The icosahedral capsid is comprised of the capsid or core protein, referred to as HBcAg. The capsid spontaneously forms from stable core homodimers, adopting either T4 (120 dimers) or, to a lower extend, T3 (90 dimers) symmetry [34, 106]. The viral DNA is located inside the capsid. It comprises of a partial double strand that is covalently coupled to the viral polymerase protein via the 5'-end of the complete (-)DNA strand [56]. The 3,2kb genome is characterised by its extremely high coding capacity. This is due to overlapping open reading frames (ORFs), where every nucleotide contains protein coding information (see figure 1.1B). Additionally, all regulatory elements for expression and replication are also overlapping with protein coding regions. From the viral genome, five RNA species are produced, resulting in the translation of a total of seven distinct proteins. These proteins include the previously mentioned surface proteins S, M, and L, as well as the core protein, the polymerase, the X protein, and the HBeAg [136].

In addition to the infectious particle, a great excess of empty envelopes are released from infected cells. These so-called subviral particles (SVPs) are not infectious and

outnumber the Dane-particles by 100 to 10000 fold [172, 173]. With approximately 20nm diameter measurement, they display a much smaller size than the viral particles. SVPs can occur in a spherical or filamentous morphology, depending on the proportion of S:M:L proteins present [75]. In the instance of the infectious HBV particle, this ratio equals 5:3:2, whereas in the filamentous SVPs it equals 4:1:1. However, the spherical particles primarily consist of S protein with approximately 10% M protein and a limited number of L molecules [112]. While decoying the host immune response is a popular and evident notion, their potential significance in infected patients is still under debate [78]. A schematic representation of HBV viral and subviral particles and the genome organisation is shown in Fig. 1.1.

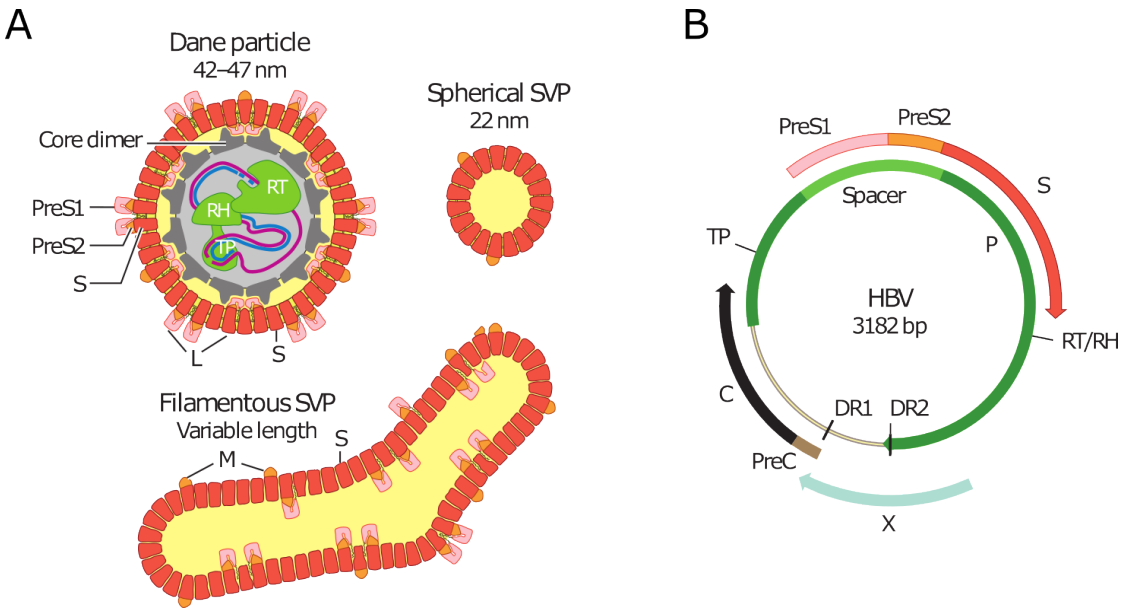

Figure 1.1: HBV particle morphology and genome organisation.
A) Schematic representation of complete viral particles and subviral particles. Virions consist of all three envelope proteins (S, M, L) as well as the inner capsid harboring the viral genome and polymerase. In contrast, subviral particles contain the envelope proteins (mainly S) but lack the inner capsid and viral genome. B) Schematic representation of the HBV genome. The different overlapping ORFs are depicted in different colors. Figure was taken and adapted from Seitz et. al. [173]

Replication cycle

An overview of the replication cycle is shown in Fig. 1.2. The main target cells and replication site of HBV are hepatocytes. In the composition of the entire organ, these cells are separated from the direct blood stream by a layer of endothelial cells and an intracellular space known as the space of Disse. The initial attachment of the virus to

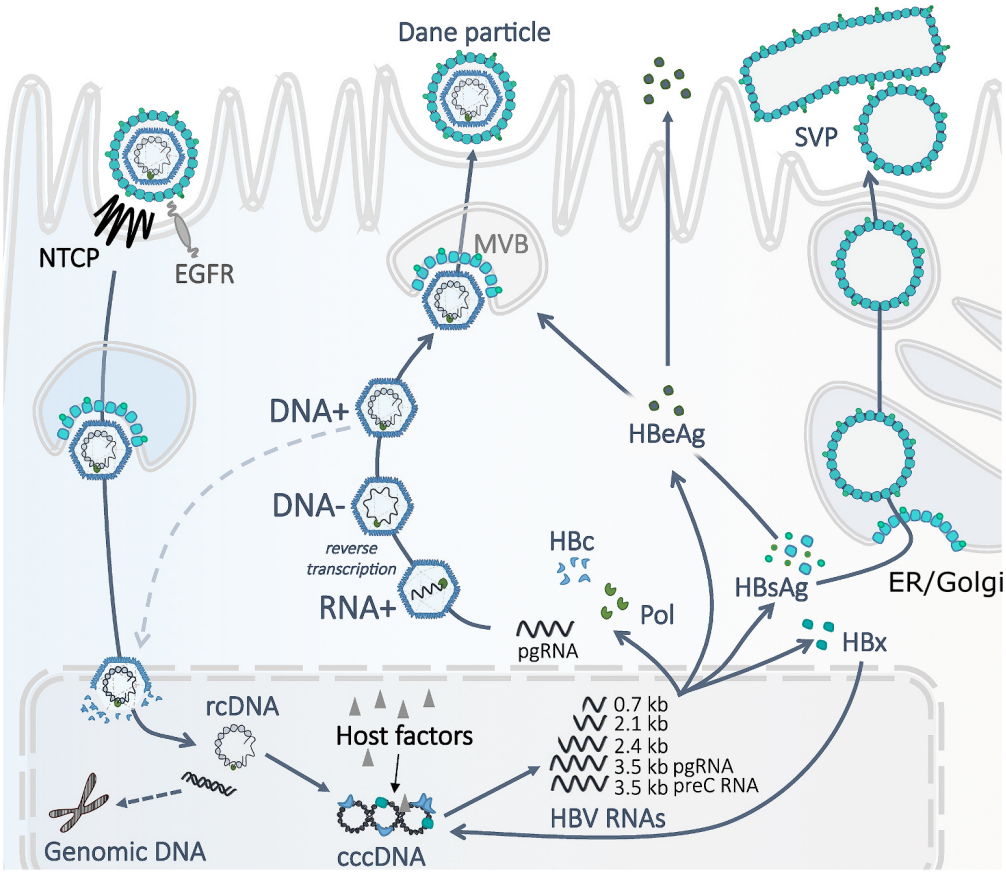

Figure 1.2: HBV replication cycle.
For detailed description see main text. In brief, HBV uptake is mediated by binding to NTCP and EGFR. The capsid with the viral DNA is transported to the nucleus. There, the DNA is released and repaired to covalently closed circular DNA (cccDNA), which serves as a template for transcription. Amplification of new genomes happens within the protected capsid shell in the nucleus, starting from freshly produced pregenomic RNA (pgRNA). Viral particles exit the cells via association with HBsAg and the multivesicular body (MVB) pathway. Subviral particles produced from self assembling HBsAg are secreted via the conventional secretory pathway. Figure was taken and adapted from Tsukuda et. al.[196]

hepatocytes is mediated by interaction of the preS1 domain of the L protein and the antigenic loop (AGL) of the S protein with glycosaminoglycan (GAG) on heparan sulfate proteoglycans (HSPGs) [182, 108, 171]. However, it remains unknown how incoming viruses reach the final target cells. Recent research indicates that they do not diffuse randomly into the space of Disse, but rather utilise a more targeted mechanism by hijacking the hosts' lipid transport mechanisms. This transport might include infection of liver resident macrophages, also known as Kupffer cells, and re-deposition of viral particles in the space of Disse [45]. There is evidence, that, as described for other hepatotropic pathogens, receptors on the sinusoidal side of liver sinusoidal endothelial cells (LSECs) might play a role as well [100].

In preparation to virus entry, the myristoylated N-terminus of preS1 binds to the sodium taurocholate co-transporting peptide (NTCP), which has been identified as the specific HBV receptor and is almost exclusively expressed on hepatocytes [216, 189]. More recent research indicates, that epidermal growth factor receptor (EGFR) plays a co-factor role during receptor mediated endocytosis of the virus by interacting with NTCP [81]. This process is probably dependent on the clathrin pathway [79]. However, a previous study in HepaRG cells claims participation of caveolin-1 for virus entry [122].

The details of viral capsid release to the cytoplasm and transport to the nucleus are not well understood. Several studies suggest that the capsid is transported along the endocytic pathways to late endosomes, where it is released and transported to the nuclear pore using the host cell's transporting machinery on dynein molecules [71, 146]. Whether the intact capsid is then imported into the nucleus or disassembles at the nuclear pore to release the genome, is unclear as well. Inside the nucleus, the host cell enzyme machinery removes the viral polymerase and repairs the partially double stranded DNA molecule to a complete circular double strand, the so called covalently closed circular DNA (cccDNA). Additional association with histones and other host proteins contributes to the mimicry of a mini-chromosome [170]. The cccDNA remains within the nucleus as an episome and serves as a template for production of all viral RNAs. Transcription is performed by the host cell's RNA polymerase II (RNA Pol II) leading to a total of five RNA species carrying 5'-cap and 3'-poly(A) features that are exported to the cytoplasm. These RNA species differ in length (2x ≈3,5kbp; 2,4kbp; 2,1kbp; 0,7kbp) and function. The three small RNAs have protein coding function only (L; M/S; X), whereas one ≈3,5kbp RNA, also known as pregenomic RNA (pgRNA) translates into core and polymerase (Pol) proteins and serves as a template for virus genome replication [172, 35]. The other ≈3,5kbp mRNA encodes for a non-assembling version of preCore/Core that is further processed and secreted as HBeAg [135].

The production of Pol and core is tightly regulated. Translation of Pol starts with a +1 frameshift from an internal start codon within the core frame [23]. This translation initiation appears very inefficient and leads to the production of several hundred core proteins before only a few polymerase proteins are translated [35]. The polymerase initiates packaging of itself and pgRNA into self-assembling capsids by binding to a 5'-hairpin loop on the pgRNA, called epsilon (ϵ) loop [9, 88]. In addition, several host

factors are packaged into the capsid, such as heat shock proteins Hsp90, Hsc70 and Hsp40 serving as chaperones. In an overexpression setting, also DNA synthesis blocking factors like APOBEC3G are packaged into virions [175]. Inside this protective environment, a protein priming mechanism initiates replication of the viral genome. Therefore, HBV utilises the N-terminal hydroxyl group on a tyrosine residue in the TP domain of Pol to synthesise the first five nucleotides. The newly synthesised DNA is then transferred to the complementary sequence (DR1) on the 3'-end of pgRNA (first template switch) and the (-) DNA strand is synthesised [137]. The RNA template is degraded in parallel by the RNaseH domain of Pol until the the last 15-18 nucleotides. These are cap protected and then transferred to the complementary sequence (DR2) on the 5'-end of the template (second template switch) [69]. This step is performed in the majority of cases, resulting in the synthesis of the (+) DNA strand until the end of the template (-) DNA strand. There, the newly synthesised DNA is re-transferred to the DR1 region on the 3'-end of the (-) DNA strand to permit completion of the (+) DNA strand and circularisation of the molecule, which is then called relaxed circular DNA (rcDNA) [210]. If the second template switch does not happen, double stranded linear DNA (dslDNA) is formed, that can integrate into the host genome. This dslDNA is either packaged into infectious particles and secreted, or re-imported into the nucleus of the same cell [197].

Envelopment of mature capsids containing rcDNA and secretion of viral particles is mediated via multivesicular bodies (MVBs) and the ESCRT-complex [204]. Similarly, filamentous SVPs are also secreted via this pathway, while the smaller spherical SVPs are secreted via the general secretory pathway across the ER and Golgi apparatus. The mechanism responsible for directing these particles to their respective pathway is likely regulated by the amount of L protein on the particle surface [83, 78]. Studies have revealed, that HBsAg, which does not contain a recruiting motif for ESCRT proteins itself, interacts with α-taxilin via the preS1 domain. This, in turn, recruits TSG101 as a subunit of ESCRT-I. In order to facilitate this process, α-taxilin is upregulated in infected cells by HBx and L-HBsAg [76]. Newly formed viruses are then released in an immature form that hides the preS domain inside the particle and therefore cannot bind to NTCP. Only after circulating in the blood stream for a certain time, the preS domain flips to the outer side of the virus particle rendering it infectious [174].

Epidemiology and pathogenesis

Approximately 300 million people are chronically infected with HBV worldwide. The prevalence largely differs between regions with rates ranging from less than 1% in Western Europe and Northern America to as high as 10% in Sub-Saharan Africa and Southeast Asia. HBV is described to manifest in ten different genotypes (gtA-J) each with various subgenotypes and different geographical distribution. In the European context, gtA and gtD are the most prevalent genotypes, whereas regions of Asia are characterised by elevated prevalence of gtB and gtC [215, 162].

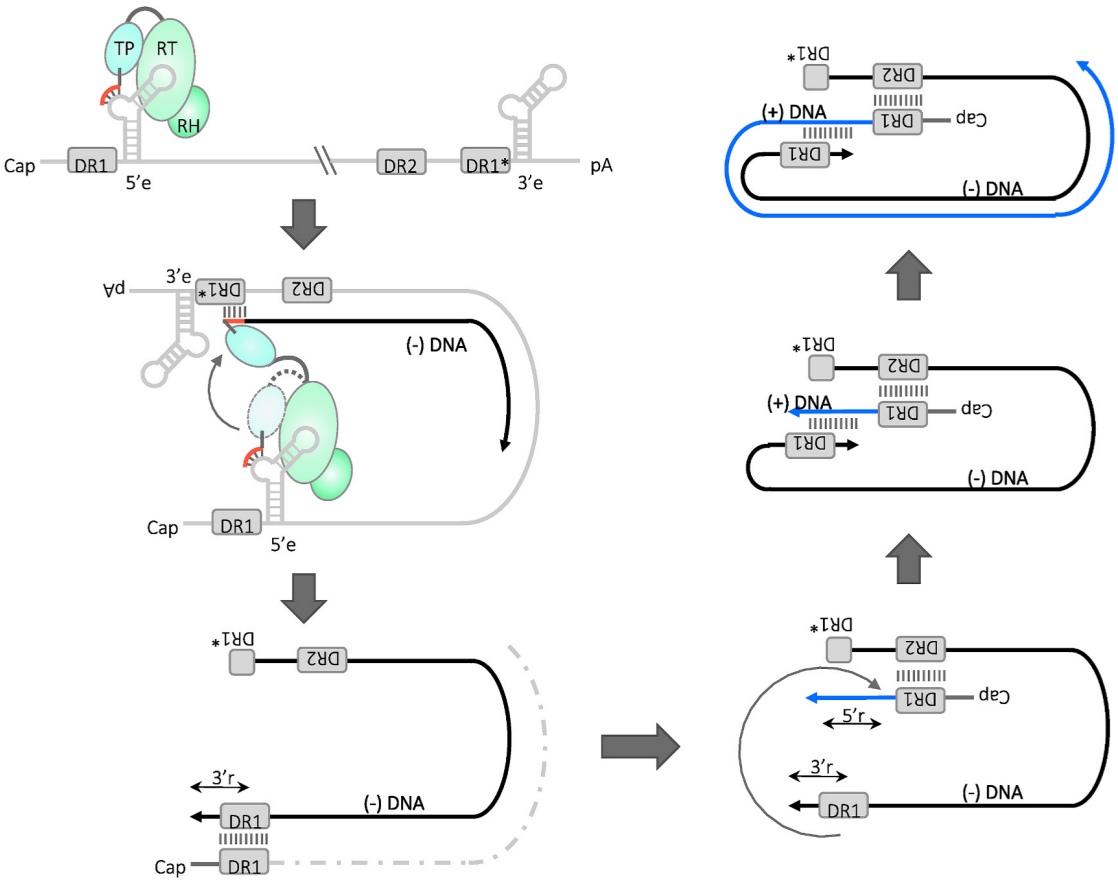

Figure 1.3: Genome replication of HBV.
For detailed description see main text. In brief, replication starts with protein priming of Pol at the 5'-ϵ loop. After synthesis of the first nucleotides, the first template switch to the 3'-DR1 is performed, followed by synthesis of the (-) DNA strand and parallel degradation of the RNA template. Synthesis of the (+) DNA strand is iniated after the second template switch to the 5'-DR2 sequence. A third template switch to the 3'-DR1 allows completion of the (+) DNA strand and circularisation to the relaxed circular DNA (rcDNA). Figure was taken from Tsukuda et. al. [196].

Infection with HBV occurs via vertical transmission at giving birth or direct contact to contaminated body fluid. If infected in early childhood, the risk for developing a chronic infection is about 95%, whereas it decreases with age. Viral particles are extremely stable and can survive outside of the host for approximately seven days [215]. Acute infection is most often not recognised due to rather mild and unspecific symptoms. In contrast, chronic infection can lead to severe disease outcomes including liver fibrosis, cirrhosis, and HCC. The very high risk of developing severe HCC (25% of chronic HBV carriers develop HCC) makes HBV infection therefore a major life threat causing approximately 800.000 deaths per year [20]. Notably, the severe disease does not originate from a high viral cytopathogenicity, but rather from the immune response targeting infected cells, while not being able to fully eliminate the virus [192].

An effective vaccine consisting of recombinant HBsAg is available since 1981 and can provide lifelong protection from infection [192]. Therapeutic options for chronic HBV infections are limited to PEGylated interferon alpha (PEG-IFN-α) and nucleot(s)ide analogues interfering with the viral replication. However, response rates for PEG-IFN-α differ by HBV genotype. In addition, this therapy is accompanied with considerable side effects and low viral clearance rates of only 10-15%. Nucleot(s)ide analogues are more effective in reducing viral and inflammatory markers, if given in combination of different drugs to increase the resistance barrier. However, treatment has to be continued lifelong, as the viral reservoir cccDNA is not targeted, leading to a quick relapse after treatment discontinuation [103, 188, 192].

1.1.2 Hepatitis C virus

Hepatitis C virus was identified in 1989 as the causative agent of Non-A-Non-B-Hepatitis (NANBH) that was associated with blood transfusions [51, 28]. It belongs to the family of *Flaviviridae* and is the sole human member of the Hepacivirus genus [131, 114].

Particle structure and genome organisation

Infectious HCV particles present irregular spherical morphologies with diameters ranging from 40-100nm. They consist of a nucleocapsid harboring the viral RNA and a lipid bilayer embedded with the envelope proteins E1 and E2. Furthermore, HCV particles are associated with cholesterol and cholesterylesters as well as different apolipoproteins like apolipoprotein E (ApoE), ApoB, and ApoA-I, and therefore referred to as lipoviroparticle [19, 127, 107]. The viral genome (see Fig. 1.4) consists of a single stranded RNA molecule of approximately 9,6kb with positive polarity. It contains a single open reading frame flanked by 5'- and 3'-untranslated regions (UTRs), which is translated from an internal ribosomal entry site (IRES) within the 5'-UTR. The translated polyprotein is further processed by host and viral proteases into three structural proteins (E1, E2, Core) and seven non-structural proteins (p7, NS2, NS3, NS4A, NS4B, NS5A, NS5B)

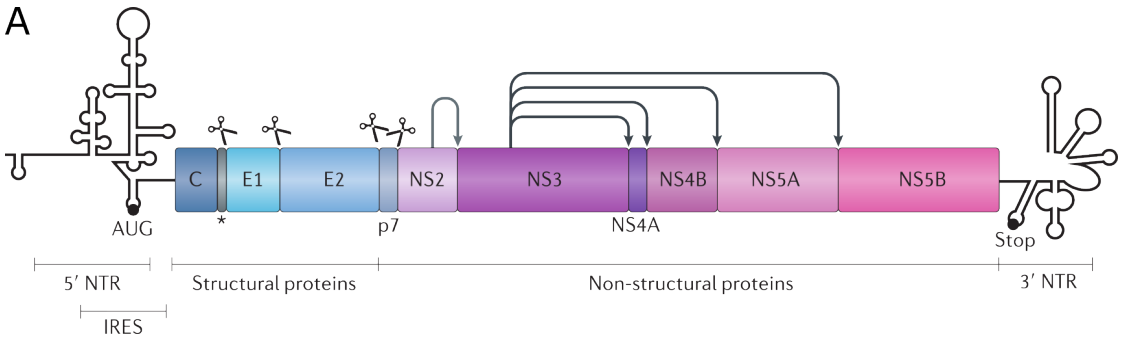

Figure 1.4: HCV genome organisation.
Schematic representation of the HCV RNA genome. Cleaving sites for host peptidases are indicated with scissors, cleaving sites for the viral protease are indicated by arrows. Figure was taken and adapted from Neufeldt et. al. [142]

[142, 131]. Additionally, the HCV genome harbors two binding sites for the human microRNA miR122, which is known to be present in high abundance within the liver. Binding of miR122 to the 5'-UTR site greatly enhances viral replication [85], thereby presenting a potential target for antiviral therapy. However, miR122 plays an important role as a tumor suppressor being downregulated in many hepatocellular carcinomas. This observation finally led to the discontinuation of clinical trials investigating the potential therapeutic targeting of miR122 [193].

Replication cycle

HCV particles circulating in the bloodstream of infected patients enter the space of Disse by passing through the fenestrated epithelium. The initial attachment to hepatocytes is facilitated by interaction of ApoE with HSPGs [10] and the low density lipoprotein receptor (LDLR) [2, 39]. The Scavenger receptor B1 (SRB1) plays an essential role in the initial attachment and serves as viral entry receptor by binding to HCV E2 [190]. Other receptor molecules involved in the HCV entry process are CD81 as well as claudin-1 and occludin, both being located at tight junctions between hepatocytes [154, 47, 155]. The virus-receptor-complex is internalised by clathrin-mediated endocytosis [48]. Subsequently, the viral genome is released into the host cell cytoplasm via pH-dependent fusion of the viral envelope and the endosomal membrane [176].

In a first step of the replication cycle, the polyprotein is produced by the host cell translation machinery starting from the type III IRES in the 5'-UTR. The structural proteins are separated from the non-structural proteins by the host signal peptide peptidase and the signal peptidase, while the non-structural proteins are cleaved by the viral NS2 and NS3/NS4A protease [115]. Extensive membrane rearrangement, mainly induced by NS4B and NS5A, results in the formation of the so-called membranous web, which is the replication site of HCV. This arrangement of single-, double- and multi-membrane

structures provides a shielding environment that protects the viral genome and replication intermediates from detection by the host immune system [166, 42, 60]. Assembly of viral particles most likely occurs at lipid droplets in close proximity to the replication factories. These lipid droplets get tightly wrapped by ER membranes and colocalise with E1, E2, p7, NS2, NS3 and NS5A upon virus replication [107, 84, 130, 118]. The exact spatiotemporal course of the assembly process is still not fully resolved. Most likely, newly formed genomes and core proteins are guided by several non-structural proteins to ER-sites enriched in E1E2 and bud into the ER lumen. There, they associate with lipoproteins and follow the conventional secretory pathway out of the cell [149]. An overview of the replication cycle is shown in Fig. 1.5.

Epidemiology and pathogenesis

HCV is a global health concern with approximately 58 million people being chronically infected and 1,5 million patients newly infected every year. The prevalence varies across different regions, with the highest prevalence in the Eastern Mediterranean and European regions [212]. The virus is classified into seven genotypes (gt1-7) and several subgenotypes with gt1 and gt3 being the most prevalent ones [163]. Since HCV is a blood borne disease, the major route of infection is through the use of improperly sterilised needles in healthcare or drug usage, as well as through contaminated blood products.
Acute HCV infection is usually asymptomatic and presents with flu-like symptoms, while the minority of patients experience hepatitis specific symptoms. The initial infection is cleared in only 30% of cases. The majority of patients suffer from chronic infection that largely remains undetected for several years, but strongly elevates risk of developing cirrhosis and liver cancer [163]. Currently, there is no effective vaccine available against HCV. Treatment with directly acting antivirals (DAAs) has shown high efficiency with approximately 95% cure rates within 24 weeks. However, access to diagnosis and treatment is limited due to high medication cost, particularly in high and middle income countries [212].

1.1.3 Hepatitis D virus

Hepatitis D virus (HDV) was first identified in 1977, after being wrongly classified as a novel antigen marker in HBV infected patients. It was later recognised as a separate virus that depends on HBV envelope proteins for spread, leading to its classification as a satellite virus [110].

Particle structure and genome organisation

The HDV particle presents a diameter of 35-37nm, thereby ranging between the size of HBV SVPs and viral particles [160]. It consists of an outer envelope and an RNA

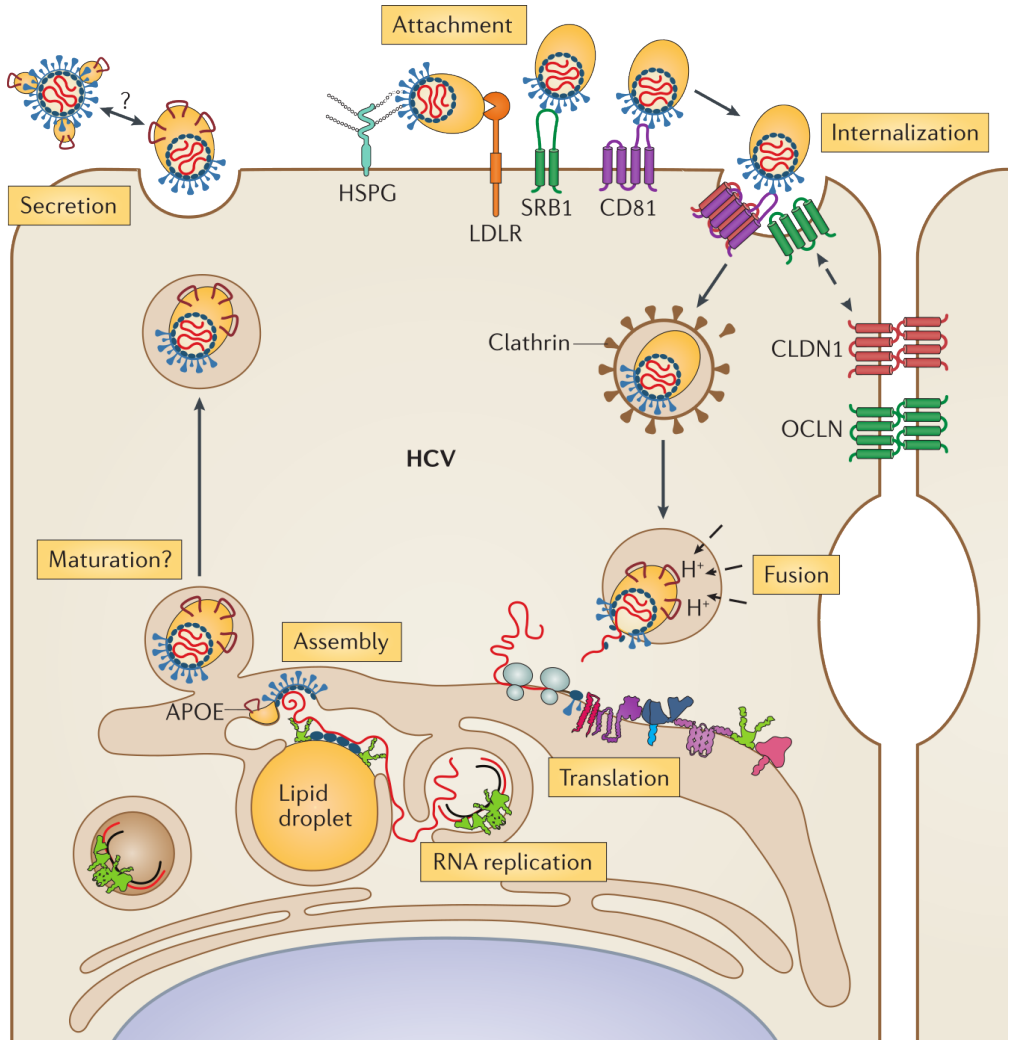

Figure 1.5: HCV replication cycle.
See main text for detailed description. In brief, HCV enters target cells after binding to several receptors (SRB1, CD81, claudin-1, occludin) followed by internalisation. After pH-dependent release of the viral genome into the cytoplasm, the polyprotein is translated and processed. Re-arrangement of cellular membranes results in formation of the membranous web, that, in turn, serves as shielding environment for viral genome replication. Assembly occurs at lipid droplets and results in production of lipid-associated infectious particles that are secreted out of the cell via the conventional secretory pathway. Figure was taken from Neufeldt et. al. [142]

genome that is decorated with 70-200 copies of the Hepatitis Delta Antigen (HDAg) forming a ribonucleoparticle (RNP) [64, 168]. The envelope consists of a lipid bilayer and S, M, and L proteins from HBV [159, 110].

The circular RNA genome of HDV is approximately 1,7kb in length and single stranded with negative polarity. It is characterised by a high degree of self-complementarity and strong secondary structures with approximately 70% intramolecular base pairing. The rod shaped molecule further presents a very stable structure, which has a long half-life time of several days and is relatively resistant to RNase treatment [27, 126, 97]. The viral genome encodes for a single ORF that is translated into two forms of HDAg: S-HDAg and the C-terminally extended L-HDAg. Production of L-HDAg occurs later in the replication cycle and is induced by editing of the RNA antigenome by the host enzyme Adenosine Deaminase Acting on RNA 1 (ADAR1). This process leads to a read-through of an amber stop codon and thereby elongation of the HDAg by approximately 19 amino acids (AA) [117, 156]. Both, S-HDAg and L-HDAg, possess RNA binding capacity, but they have different effects on RNA replication: S-HDAg promotes replication, while L-HDAg inhibits replication [25]. Furthermore, L-HDAg undergoes farnesylation at the cystein residue C211/212 (depending on the genotype) in its C-terminal elongation and mediates interaction with HBsAg for envelopment and spread [145, 203]. A schematic overview of the HDV genome and particle structure is shown in Fig. 1.6.

Replication cycle

As HDV and HBV share the same envelope proteins, the entry mechanism of both viruses is considered very similar. Initial attachment occurs at HSPGs, whereas specific binding of L to NTCP induces uptake of viral particles (see section 1.1.1). After release, the viral RNP is transported to the nucleus. This process is potentially mediated by the nuclear localisation signal (NLS) on HDAg, which allows nuclear uptake by the host cells' import machinery [29, 186].

Amplification of the viral genome occurs in a double rolling circle mechanism, mediated by the host cells' RNA Pol II and potentially RNA polymerase I [27, 22, 129]. Initially, the antigenome is produced, which can also serve as a template for the rolling circle amplification. To this end, multimeric copies of genome and antigenome are generated. The ribozyme activity in the genomic and antigenomic RNA itself subsequently processes them into unit length copies [98, 121].
In addition to genomic and antigenomic RNA, a shorter RNA that is capped and polyadenylated is produced and exported from the nucleus and mediates production of HDAg [77]. In the course of viral replication, the amber stop codon UAG in the antigenome is edited by ADAR1 to a UGG codon, encoding for a tryptophan instead and allowing for production of L-HDAg [117, 156]. Re-imported HDAg associates with newly formed HDV RNA and mediates nuclear export via interaction with the TAP/Aly export machinery exclusively for genomic RNA [80, 120].

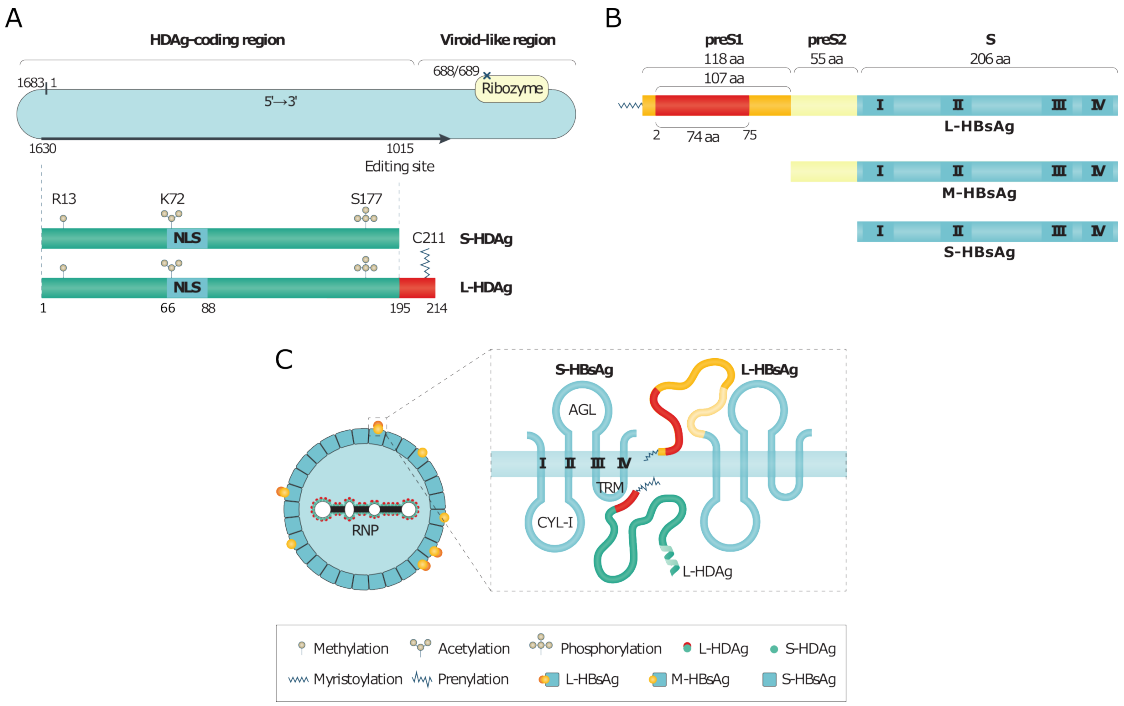

Figure 1.6: HDV genome organisation and particle structure.
A) Schematic representation of the HDV genome and C) the virus particle. In addition, the HBV envelope proteins and the interaction between HDAg and envelope proteins are shown in B). Figure taken and adapted from Lempp et. al. [110]

Secretion of infectious HDV particles requires the presence of suitable envelope proteins, such as HBsAg. Interestingly, envelopment and secretion of the HDV RNP can occur with S alone, while S, M, and L proteins are required for envelopment of the HBV capsid. Therefore, HDV is thought to exit the cell via the conventional secretory pathway along the ER and Golgi apparatus together with HBV SVPs. Of note, as S-only enveloped HDV particles lack the preS1 domain, they remain non-infectious [65, 181, 4, 220].
In addition, a recent study proposed propagation of HDV by helper envelope proteins distinct from HBsAg, such as HCV E1E2 or vesicular stomatitis virus G protein (VSV-G) [150]. Cell division mediated spread has been described for HDV as a mechanism to maintain persistent infection. Thereby, viral genomes are distributed upon cell division to daughter cells keeping up the reservoir for ongoing replication. This mechanism is sensitive to interferon treatment as further *in vitro* data suggest [57, 219].

Further experimental and clinical evidence suggests that HDV might not present exclusive human liver tropism. On the one hand, HDV is able to replicate in non-hepatic human cell culture systems such as HeLa or HEK293T cells, but also in murine hepatocytes [74, 109]. On the other hand, HDV has been detected in salivary gland tissue of patients suffering from a chronic autoimmune disease, called Sjögrens syndrome. Those patients further tested negative for any HBV marker and anti-HDAg antibodies [207]. Of note, this data was only confirmed and further investigated by one study from the same research group [72].

Epidemiology and pathogenesis

Approximately 5% of chronic HBV carriers are also diagnosed positive for HDV. Similar to HBV, the prevalence of HDV strongly differs across geographical locations, with hotspots in Mongolia, the republic of Moldova and several countries in Western and Central Africa [214]. HDV can be classified into eight genotypes (gt1-8), which differ in replication fitness and preferences for HBV genotypes for envelopment [203]. As HDV relies on HBV for envelopment and spread, the major infection route is through direct contact with contaminated blood products or usage of improperly sterilised needles. Unlike to HBV, mother to child transmission of HDV is rare [214].
Clinical appearance of HDV infection is very similar to HBV, with an acute infection being characterised by unspecific hepatitis symptoms such as fatigue, fever, nausea, and jaundice. Chronic infection is linked to a more severe liver disease progression and higher rates of cirrhosis and HCC development [214].

Vaccination against HBV is also effective in preventing HDV infection. Treatment of chronic HDV infection includes PEG-IFN-α, which is, similar to HBV, accompanied by severe side effects [214]. In 2020, the entry inhibitor Bulevirtide has been approved by the European Medicine Agency (EMA) as a novel treatment option that can be administered alone or in combination with nucleotide analogues targeting HBV [46]. Clinical studies further demonstrated a synergistic effect of Bulevirtide and PEG-IFNα [91, 206], which is likely due to their targeting of both routes of HDV persistance: *de novo* infection

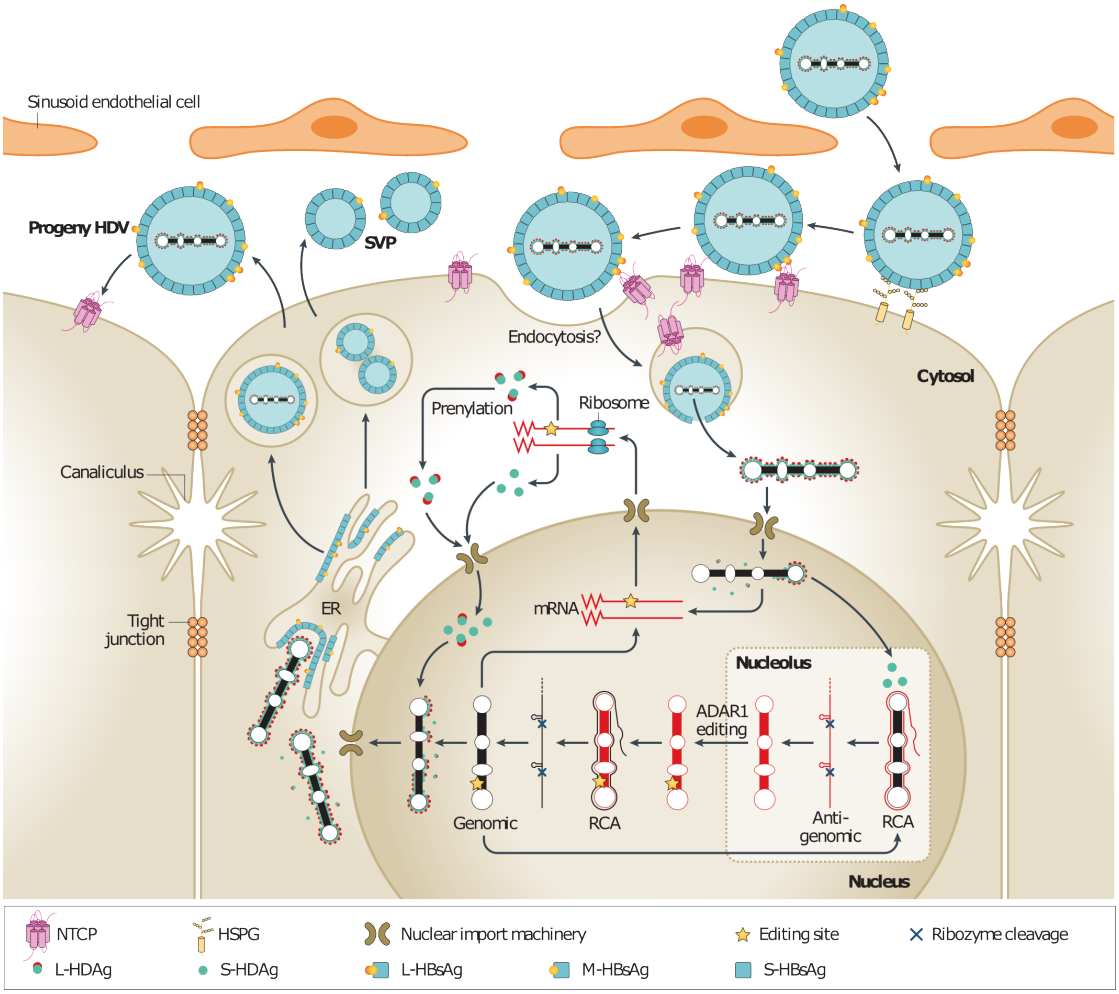

Figure 1.7: Replication cycle of HDV.
See main text for detailed description. In brief, HDV enters hepatocytes in the same way as HBV via binding to NTCP followed by internalisation. Rolling circle amplification of the viral genome occurs in the nucleus. Editing of the antigenome is performed by the host enzyme ADAR1 resulting in the production of C-terminally elongated L-HDAg. Newly produced genomes associate with HDAg, are packaged by HBsAg, and released from the cell. Figure was taken from Lempp et. al. [110]

and cell division mediated spread. Furthermore, Lonafarnib, which targets the cellular farnesyltransferase and thereby inhibits formation of progeny HDV particles, is currently under clinical investigation. After completing phase III clinical studies in combination therapy with the HIV protease inhibitor Ritonavir, Lonafarnib has been granted PRIME designation and orphan drug status by EMA [219, 43].

1.1.4 Co-infections

All three chronically infecting hepatitis viruses (HBV, HCV, HDV) can be detected not only as single but also co-infections with each other. Co-infections are considered more complex, as multiple viruses can hijack the same cell and potentially compete for resources.

HBV/HCV

With a global prevalence of approximately 1-15%, HBV/HCV co-infection is relatively common. The majority of cases results from super-infection rather than acute co-infection, with HCV super-infection being more common than HBV super-infection. Altough existing studies are contradicting, HBV/HCV co-infection is mostly associated with higher disease severity and mortality rates [125].
Direct viral interaction between HBV and HCV has not been described in different cell culture models, indicating that each virus replicates independently from the respective other one [217, 11]. In contrast, in animal and clinical studies, interference between the two viruses has been obswerved, with HBV replication being suppressed [116, 209]. This might be due to the direct interaction between viral proteins, as hypothesized for HCV core inhibiting HBV, as well as the host's immune response [93]. The exact mechanism is still unclear, but *in vitro* studies have shown, that the innate immune response is not modulated in HBV/HCV co-infection [132], indicating a more prominent role for the adaptive immune system.

HBV/HDV

As HDV is able to replicate but not able to infect and exit host cells on its own, it almost exclusively occurs in conjunction with an ongoing or previous HBV infection [110, 152, 26]. Co-infection with HBV is often associated with an acute infection that is quickly resolved. However, super-infection of HDV on an already established HBV infection often results in chronicity and is associated with more severe and accelerated liver disease progression [201]. As mentioned above, approximately 5% of chronic HBsAg carrier test positive for HDV [214].

HBV/HCV/HDV

Triple infections of HBV, HCV, and HDV are mostly detected in highly endemic regions such as Mongolia or Taiwan, with prevalence rates ranging from approximately 12% to 30% [221, 194]. Similar to double infections, triple infections tend to result in more severe liver disease outcome and lower treatment response rates [208]. The presence of HBV and HCV in triple infections provides an opportunity for HDV to come in contact with an enveloped non-HBV virus within the same patient. Given the rather high prevalence of triple infections, the potential for HCV mediated transmission of HDV proposed by Perez-Vargas et. al. [150] would be similarly high. However, the topic of HBV/HCV/HDV triple infection is generally understudied and focuses on small study groups, limiting the available knowledge.

1.2 Non-human hepatitis virus-like agents

Non-human hepatitis virus-like agents have been identified in various animal species, although their origin and evolution are not well understood yet. The evolution of hepadnaviruses, for example, has been extensively investigated, indicating that the common ancestor of those viruses replicated approximately 432 million years ago, around the time of separation between ray-finned fishes (*Actinopterygii*) and lobe-finned fishes (*Sarcopterygii*, including mammals) [104]. In contrast, for animal hepaciviruses and Delta-like agents, the current knowledge is still limited, as new agents are being identified one by one in different host species.

1.2.1 HBV-like viruses

HBV-like viruses were initially known to infect mammals and birds. However, in the past decade, new hepadnaviruses infecting fish and amphibian species have been identified [68, 37]. With advancements in computing capacity and efficient screening of sequencing databases, more HBV-like viruses have been identified. Comparative sequence analysis has further revealed the existence of a non-enveloped virus family called Nackednaviruses, suggesting that the common ancestor of all known HBV-like viruses and Nackednaviruses did not possess an envelope [104].
Enveloped HBV-like viruses are classified into five clades: Avihepadnaviruses (infecting birds), Herpetohepadnaviruses (infecting amphibians and reptiles), Orthohepadnaviruses (infecting mammals), Metahepadnaviruses (infecting fish) and Parahepadnaviruses (infecting fish). Parahepadnaviruses represent the oldest clade, that diverged from the others about 360 million years ago. Metahepadnaviruses represent the closest related sister clade of the Orthohepadnaviruses. Analysis of virus-host evolution reveals that Avi-, Herpeto- and Orthohepadnaviruses most likely co-evolved with their hosts with only a

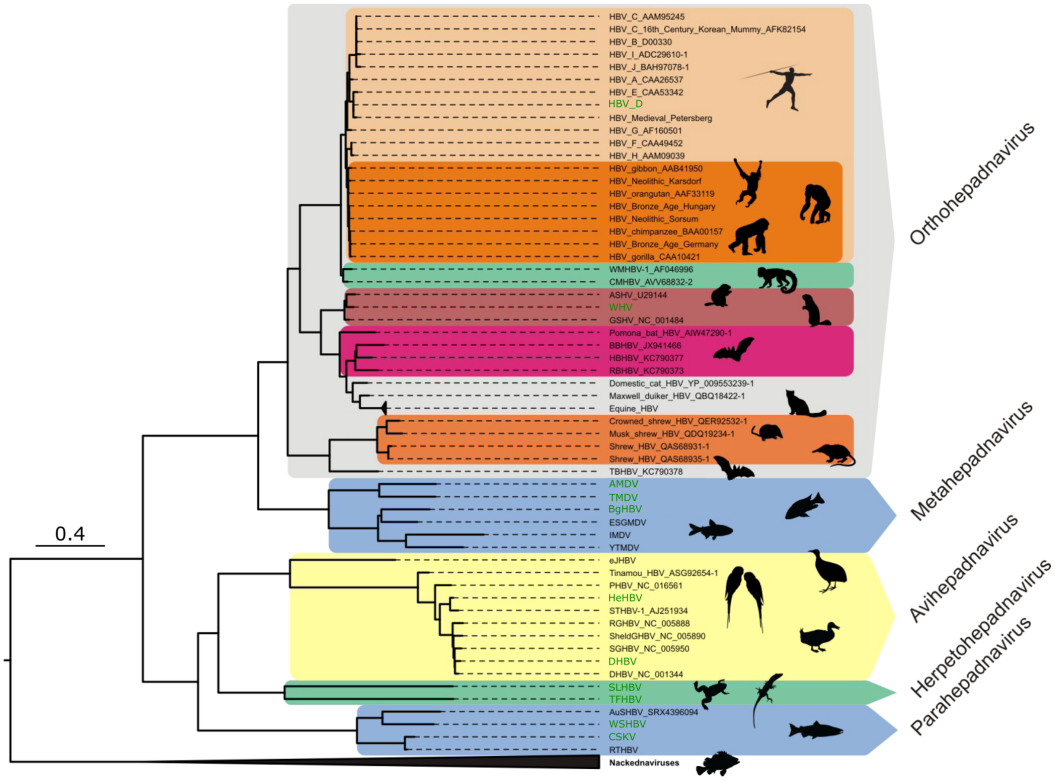

Figure 1.8: Phylogenetic tree of hepadnaviruses.
The phylogenetic analysis is based on the core protein, with the scale bar indicating numbers of substituted AA per site. Hepadnaviruses involved in the S protein investigation in section 4.3 are marked in green. Figure was taken and adapted from Taji et. al. [185]

few major host jumps. In contrast, Meta- and Parahepadnaviruses as well as Nackednaviruses exhibit a more complex evolution pattern with several major host jumps [104]. A phylogenetic tree of several hepadnaviruses is shown in Fig. 1.8.

HBV-like viruses most likely share major characteristics regarding replication strategy and particle production with the human HBV. To this end, duck HBV (DHBV) served as a model organism for studying HBV until suitable cell culture systems supporting the entire HBV replication cycle were established [62, 54]. However, there are also profound differences between different hepadnavirus clades, such as the number of encoded proteins or the morphology of viral and subviral particles [104, 54]. For example, both, HBV and DHBV, express subviral particles but they differ in size and stability. HBV exhibits two types of SVPs with a much smaller diameter than viral particles (see section 1.1.1), while DHBV presents only one type of SVPs, which are similar in size to the viral particles [54]. The presence or absence of an intramolecular loop on the S protein, known as the a-determinant, is likely responsible for these morphological differences. Located

between transmembrane domains II and III, the a-determinant resides on the outer side of the virus particle being a major immunogenicity determinant [184]. Depending on its extension, it might further influence the strength of the induced membrane curvature and thereby particle morphology.

There are further differences regarding the envelope proteins themselves and their topology that are best studied for HBV and DHBV. HBV envelope proteins exist in three different forms S, M, and L sharing the S-ORF, which is N-terminally elongated by preS2 and preS1-preS2 to form M and L proteins, respectively (see Fig. 1.1). In contrast, DHBV possesses only S and L proteins that differ by a single N-terminal preS elongation [157]. L proteins of both viruses are myristoylated, which is in turn important for infectivity [200, 63, 123]. HBV and DHBV share a dual membrane topology of L [66, 101], but it has been proposed that HBV possesses four transmembrane domains, whereas DHBV carries only three [179]. Other Hepadnaviruses possess an S-ORF and at least one putative N-terminal preS part as well (S. Seitz, unpublished data). So far, no experimental data is available regarding membrane topology or myristoylation of those proteins.

1.2.2 HCV-like viruses

For several decades, HCV was considered the only member of the genus hepacivirus. However, in 2011, another hepacivirus was discovered in canine nasal swabs even in the absence of liver disease symptoms [89]. Shortly after the discovery of this so called non-primate hepacivirus (NPHV), evidence was found that this virus most likely originated from horses and might have been transmitted accidentally to dogs through contaminated horse blood products such as vaccines [16]. Subsequently, novel hepaciviruses have been identified in various other species, including rodents [90, 53], bats [158], cattle [33, 7], non-human primates [105], fish [177] and birds [218, 59]. Evolutionary analysis of these animal hepaciviruses and their hosts indicates several inter-species transmission events and a potential zoonotic origin of HCV [191, 70].

All known animal hepaciviruses share similarities in genome organisation and putative protein structure. Potential binding sites for miR122 have been identified in most of those viruses. However, it is still unclear whether animal hepaciviruses utilise miR122 in the same way as HCV [70].
Differences also exist in the diversification of hepacivirus genomes. For example, HCV is highly diversified, whereas the most closely related equine HCV (NPHV or EqHCV) shows a rather high sequence stability. The sequence of the HCV envelope glycoproteins E1E2 is frequently mutated in the so called hypervariable region 1 (HVR-1). High mutation rates in this region as well as the very dense glycosylation pattern is connected to efficient immune evasion and chronicity of HCV. Interestingly, an HVR-1-like sequence is missing in EqHCV, which also shows a lower rate of chronic infections [67].

1.2.3 HDV-like viruses

HDV-like viruses, also termed Delta-like agents, have recently been identified in birds through metagenomics analysis, making the first identification of these viruses in non-human animal species [211]. Shortly after, an increasing number of Delta-like agents has been found in various taxa with the exception of non-human primates [73, 147, 82, 13]. The origin of Delta-like agents is still unclear, but evidence suggests that these viruses diversify through host jumping instead of co-evolution with their hosts [13].

Delta-like agents share key similarities in genome size, circularisation, and polarity, and are most likely actively replicating in their respective hosts. As for HDV, these viruses have only one ORF that probably does not encode for an envelope protein. Therefore, these viruses are considered to be dependent on a helper mechanism for particle production and spread [140, 24]. However, a putative helper virus might be distinct from any hepadnavirus, making the very close association of HDV and HBV unique to the human virus. In addition and potentially also due to a helper-independent spreading mechanism, Delta-like agents do not present a very strict liver tropism [73, 211]. However, the exact mechanisms underlying virus transmission are not known yet. Unpublished data in our group suggests a potential hepacivirus-mediated transmission of a bat Delta-like agent (BHDV), as this virus has been found in a bat (*Peropteryx macrotis*) and a rodent, both in presence of the same animal hepacivirus. Other potential spreading strategies include the usage of other helper viruses (either actively replicating or endogenous viral elements) or extracellular vesicles [147, 82].

1.3 Aim of the study

Hepatitis D virus spread is known to be mediated by HBV envelope proteins. However, a recent study reports the spread of HDV in an HBV-independent manner [150]. If confirmed, this finding would have major clinical implications, as current screening of HDV is primarily focused on HBsAg positive carriers. In addition, HDV infection might affect non-hepatic tissue, depending on the the presence of a helper virus leading to various diseases of unknown origin.
Recently discovered non-human Delta-like agents share structural and genetical similarities with HDV, but appear to be independent of hepadnaviral envelope proteins. This implies: i) these non-human Delta-like agents might employ different spreading strategies (either utilising a different viral envelope or being envelope-independent) and ii) those strategies might be unavailable for HDV (e.g. due to steric hindrance or unavailability of protein interactions). On the helper virus side, non-human hepadnaviruses from the related genus of Metahepadnaviruses share sequence and structural similarities with the human HBV, raising the possibility that HDV might be able to utilise such non-human HBV envelope proteins for spread.

Therefore, this study aims to answer the following three major questions:

a) Can HDV use envelope proteins of human non-HBV helper viruses (such as HCV) for its spread?

b) Can HDV be rendered susceptible to alternative helper usage by modifying HBV specificity determinants?

c) What is the zoonotic potential of HDV by utilising non-human hepadnaviral helpers?

In order to address these questions, I made use of different cell culture models based on transfection or viral infection. I further included bioinformatic tools to perform sequence comparison and investigate protein structure predictions.

2 Materials

2.1 Antibiotics

Table 2.1: Antibiotics

Name	**Concentration**	**Purpose**	**Composition/supplier**
Ampicillin	1mg/mL	Bacterial selection	Sigma-Aldrich, St. Louis, USA
Blasticidin S hydrochloride	5µg/mL	Eukaryotic selection	MP Biomedicals, USA
Doxycycline	2µM	Induction of virus production	Sigma-Aldrich, St. Louis, USA
Geneticin (G418)	1mg/mL	Eukaryotic selection	ThermoFisher Scientific, Waltham, USA
Puromycin	1µg/mL	Eukaryotic selection	Sigma-Aldrich, St. Louis, USA

2.2 Antibodies

2.2.1 Antibodies for IF

Table 2.2: Primary antibodies for IF

Target	Name	Clonality	Species	Supplier	Dilution
HA	H3663	Monoclonal	Mouse	Sigma-Aldrich, St. Louis, USA	1:200
HBsAg	HBC34	Monoclonal	Human	Discontinued	1:1000
HBcAg	DAKO	Polyclonal	Rabbit	Discontinued	1:3000
HCV E2	Hybridoma	Monoclonal	Rat	Minh Tu Pham	1:20
HCV NS5A	9E10	Monoclonal	Mouse	Kind gift from C. Rice	1:3000
HDAg	FD3A7	monoclonal	Rabbit	Kind gift from S. Urban	1:2000
VSV-G	I1 hybridoma	Monoclonal	Mouse	Vibhu Prasad	1:20

Table 2.3: Secondary antibodies for IF

Target	Fluorophore	Species	Supplier	Dilution
Human IgG	AlexaFluor 488	Goat	ThermoFisher Scientific, Waltham, USA	1:1000
Human IgG	AlexaFluor 555	Goat	ThermoFisher Scientific, Waltham, USA	1:1000
Mouse IgG	AlexaFluor 488	Goat	ThermoFisher Scientific, Waltham, USA	1:1000
Mouse IgG	AlexaFluor 555	Goat	ThermoFisher Scientific, Waltham, USA	1:1000

Table 2.3: Continued Secondary antibodies for IF

Target	Fluorophore	Species	Supplier	Dilution
Mouse IgG	AlexaFluor 647	Donkey	ThermoFisher Scientific, Waltham, USA	1:1000
Rabbit IgG	AlexaFluor 488	Goat	ThermoFisher Scientific, Waltham, USA	1:1000
Rabbit IgG	AlexaFluor 647	Donkey	ThermoFisher Scientific, Waltham, USA	1:1000
Rat IgG	AlexaFluor 488	Goat	ThermoFisher Scientific, Waltham, USA	1:1000
Rat IgG	AlexaFluor 647	Goat	ThermoFisher Scientific, Waltham, USA	1:1000

2.2.2 Antibodies for western blot

Table 2.4: Primary antibodies for western blot

Target	Name	Clonality	Species	Supplier	Dilution
α-tubulin	T5168	Monoclonal	Mouse	Sigma-Aldrich, St. Louis, USA	1:8000
HA	H3663	Monoclonal	Mouse	Sigma-Aldrich, St. Louis, USA	1:2000
HBsAg	HBD87	Polyclonal	Human	Discontinued	1:8000
HCV E2	N/A	Monoclonal	Rabbit	Minh Tu Pham	1:5000
HDAg	FD3A7	Monoclonal	Rabbit	Kind gift from S. Urban	1:2000

Table 2.5: Secondary antibodies for western blot

Target	Enzyme	Species	Supplier	Dilution
Human IgG	HRP	Goat	Abcam, Cambridge, UK	1:5000
Mouse IgG	HRP	Goat	Sigma-Aldrich, St. Louis, USA	1:10000
Rabbit IgG	HRP	Goat	Sigma-Aldrich, St. Louis, USA	1:20000

2.3 Buffers and solutions

Table 2.6: Buffers and solutions

Name	Composition/supplier
Cell freezing medium	FCS (heat inactivated) + 10% DMSO
Cytofix/Cytoperm solution	BD, Heidelberg, Germany
Cytomix	120mM KCl; 0.15mM CaCl2; 10mM K2HPO4/KH2PO4 (pH 7.6); 25mM Hepes (1M stock solution, cell culture grade); 2mM EGTA; 5mM MgCl2; adjust pH to 7.6 with KOH, sterilize by filtration and store at room temperature
DMEM, high glucose	ThermoFisher Scientific, Waltham, USA
DMEM/F12 HEPES	ThermoFisher Scientific, Waltham, USA
ELISA coating buffer	13mM Na_2CO_3, 88mM $NaHCO_3$; pH 9,2
ELISA washing buffer	PBS + 0,05% Tween20
ELISA blocking buffer	PBS + 0,05% Tween20 + 1% BSA
ELISA dilution buffer	PBS + 0,05% Tween20 + 0,1% BSA
Fetal Calf Serum (FCS)	Capricorn Scientific, Ebsdorfergrund, Germany
FCS for HEK cells	PAN Biotech, Aidenbach, Germany

Table 2.6: Continued Buffers and solutions

Name	Composition/supplier
GeneRuler 1kb Plus DNA ladder	ThermoFisher Scientific, Waltham, USA
HEPES (1M)	ThermoFisher Scientific, Waltham, USA,
Hydrocortisone hemisuccinate	Sigma-Aldrich, St. Louis, USA
Insulin, recombinant human	Sigma-Aldrich, St. Louis, USA
Laemmli Buffer (6X)	9,75mL Tris 0,5M (pH6.8), 15mL Glycerol, 15mL 10% SDS, 3,75mL β-mercaptoethanol, 30mg Bromophenol blue, 6.5mL H2O
LB Agar	300mL LB Medium + 4,5g Agar
L-gluatmine (200mM)	ThermoFisher Scientific, Waltham, USA
Loading Dye RNA (2X)	ThermoFisher Scientific, Waltham, USA
Loading Dye DNA (6X, purple)	New England Biolabs (NEB), Frankfurt a.M., Germany
Luciferase assay buffer	10mL Glycyl Glycin (0,5M stock pH7,8), 30mL KPO_4 buffer pH7,8 (0,1M stock), 3mL $MgSO_4$ (1M stock), 4mL EGTA (0,2M stock pH7,8), 153mL H_2O
Luciferase lysis buffer	5mL Triton X-100, 25mL Glycyl Glycin (0,5M), 7,5mL $MgSO_4$ (1M stock), 10mL EGTA (0,2M stock), 50mL Glycerol (99%), 402,5mL H_2O
Luria Broth (LB) Medium	50g Bacto-Trypton, 25g Yeast extract, 25g NaCl in 5L ddH2O and autoclaved
MEM non-essential amino acids (NEAA, 100X)	ThermoFisher Scientific, Waltham, USA
OptiMEM reduced serum medium	ThermoFisher Scientific, Waltham, USA
Paraformaldehyde (4%)	Powder dissolved to 4% (w/v) in PBS at 60°C under constant stirring
Phosphate buffered saline (PBS, 10X)	80mM NA2HPO4, 1.4M NaCl, 2.7mM KCl, 1.76mM KH2PO4
PBS-T	PBS (1x), 0.1% (v/v) Tween-20

Table 2.6: Continued Buffers and solutions

Name	Composition/supplier
Penicillin/Streptomycin (100x)	ThermoFisher Scientific, Waltham, USA
Polyethyleneglycol (PEG, 40%)	40% (w/v) PEG8000 in PBS, sterile filtered
Polymerase buffer (10X)	New England Biolabs (NEB), Frankfurt a.M., Germany
Resolving gel buffer	1,5M Tris Base 0,4% SDS pH 8.8
RiboRuler High Range RNA ladder	ThermoFisher Scientific, Waltham, USA
Sodium pyruvate (100mM)	ThermoFisher Scientific, Waltham, USA
Stacking gel buffer	1M Tris Base 0,8% SDS pH 6.8
TMB substrate set	BioLegend, San Diego, USA
Tris-acetate-EDTA buffer (TAE, 50X)	2M Tris, 2M Acetic Acid, 50mM EDTA, pH 8.3
Tris-borate-EDTA buffer (TBE, 10X)	1M Tris, 1M Boric acid, 20mM EDTA
Tris-glycine-SDS buffer (TGS, 10X)	150mM Tris, 1.92M Glycine, 1% w/v SDS
TN buffer	20mM Tris, 140mM NaCl (pH 7.4)
TN2140	20mM Tris, 2140mM NaCl (pH 7.4)
Transfer buffer (10X)	25mM Tris Base (pH 8.3), 150mM Glycine
Trypsin-EDTA (0,05%)	ThermoFisher Scientific, Waltham, USA
Williams‘ E medium, no glutamine	ThermoFisher Scientific, Waltham, USA

2.4 Cell lines and cultivating media

Table 2.7: Cell lines

Cell line	Characteristics	Selection
HEK239T	Immortalised human embryonic kidney cell line [38]	N/A

Table 2.7: Continued Cell lines

Cell line	Characteristics	Selection
HepAD38	HepG2 derived cell line that harbours a Tet-inducible integration of HBV gtD; produces infectious particles of HBV [99]	1mg/mL Geneticin
HepaRG	Human hepatoma cell line derived from an HCV infected patient suffering from HCC [62]	N/A
HepaRG-FGFR4	HepaRG stably expressing FGFR4	5µg/mL Blasticidin
HepaRG-NTCP	HepaRG stably expressing NTCP	1µg/mL Puromycin
Hep56.1D-NTCP	Murine hepatoma cell line derived from a C57BL/6J mouse [95], stably expressing NTCP	1mg/mL Geneticin
HepG2	Human liver carcinoma cell line derived from a 15 year old patient [1]	N/A
HepG2-NTCP	HepG2 stably expressing the HBV receptor NTCP; kind gift from S. Urban	1µg/mL Puromycin
Huh7	Human hepatoma cell line; derived from a 57-year old patient suffering from HCC [134]	N/A
Huh7-D	Huh7 stably replicating HDV; kind gift from S. Urban	1mg/mL Geneticin
Huh7-END	Huh7 stably expressing the HB2.7 construct, NTCP and stably replicating HDV; produces infectious HDV particles; kind gift from S. Urban	5µg/mL Blasticidin, 1µg/mL Puromycin, 1mg/mL Geneticin
Huh7-S	Huh7 stably expressing S-HDAg; kind gift from S. Urban	5µg/mL Blasticidin
Huh7-HB2.7	Huh7 stably expressing a subgenomic HBV fragment; produces HBV subviral particles and HBx	5µg/mL Blasticidin
Huh7-NTCP	Huh7 stably expressing the HBV receptor NTCP	1mg/mL Geneticin

Table 2.7: Continued Cell lines

Cell line	Characteristics	Selection
Huh7-CD81-NTCP	Huh7 stably expressing the main receptors of HCV (CD81) and HBV (NTCP)	1mg/mL Geneticin, 5µg/mL Blasticidin

Table 2.8: Cultivating media

Basal medium	Supplements	Cultivated cells
DMEM	10% FCS (heat inactivated), 100U/mL penicillin, 100µg/mL streptomycin, 1X NEAA	Huh7 derivatives, HepG2 derivatives, HEK293T, Hep56.1D derivatives
DMEM/F12	10% FCS (heat inactivated), 100U/mL penicillin, 100µg/mL streptomycin, 1X NEAA, 2mM L-glutamine, 1mM sodium pyruvate, 2µg/mL doxycycline (remove to induce virus production)	HepAD38
Williams' E	10% FCS (heat inactivated), 100U/mL penicillin, 100µg/mL streptomycin, 2mM L-glutamine, 50µM hydrocortisone-hemisuccinate, 5µg/mL insulin	HepaRG derivatives

2.5 Chemicals and reagents

Table 2.9: Chemicals and reagents

Name	Composition/supplier
Acetic acid	Carl Roth, Karlsruhe, Germany
Adenosinetriphosphate (ATP), 100mM	Sigma-Aldrich, St. Louis, USA
Agarose	Sigma-Aldrich, St. Louis, USA
Ammoniumperoxosulfate (APS)	Carl Roth, Karlsruhe, Germany

Table 2.9: Continued Chemicals and reagents

Name	Composition/supplier
β-Mercaptoethanol	Sigma-Aldrich, St. Louis, USA
Bovine Serum Albumin (BSA) heat shock fraction, pH7, protease free	Sigma-Aldrich, St. Louis, USA
Bromophenolblue	AppliChem, Darmstadt, Germany
Calcium Chloride (CaCl2)	AppliChem, Darmstadt, Germany
Chloroform	Carl Roth, Karlsruhe, Germany
4',6-Diamidin-2-phenylindol (DAPI)	Sigma-Aldrich, St. Louis, USA, D9542
Diethylpolycarbonate (DEPC)	Carl Roth, Karlsruhe, Germany
Dimethylsulphoxide (DMSO)	VWR International, Darmstadt, Germany
Dithiothreitol (DTT), 1M	Sigma-Aldrich, St. Louis, USA
D-Luciferin	PJK Biotech, Kleinblittersdorf, Germany
dNTPs (10mM)	VWR International, Darmstadt, Germany
ECL Substrate (Clarity Western)	Bio-Rad Laboratories, Hercules, USA
Ethanol absolute 96%	Sigma-Aldrich, St. Louis, USA
Ethylendiaminontetraaceticacid (EDTA)	AppliChem, Darmstadt, Germany
EGTA	AppliChem, Darmstadt, Germany
FluoromountG	Southern Biotech, Birmingham, USA
Glycerol	Sigma-Aldrich, St. Louis, USA
Isopropanol	Sigma-Aldrich, St. Louis, USA
iTaq Universal probes supermix	Bio-Rad Laboratories, Hercules, USA
Potassium Chloride (KCl)	AppliChem, Darmstadt, Germany
Potassiumdihydrogenphosphate (KH_2PO_4)	Carl Roth, Karlsruhe, Germany

Table 2.9: Continued Chemicals and reagents

Name	**Composition/supplier**
Dipotassiumhydrogenphosphate (K_2HPO_4)	Carl Roth, Karlsruhe, Germany
Potassiumphosphate (KPO_4)	Carl Roth, Karlsruhe, Germany
Potassiumhydroxide (KOH)	Carl Roht, Karlsruhe, Germany
Glycerol	Merck, Darmstadt, Germany
Glycine	AppliChem, Darmstadt, Germany
Glycylglycine	Sigma-Aldrich, St. Louis, USA
Magnesium Chloride ($MgCl_2$)	AppliChem, Darmstadt, Germany
Magnesiumsulfate ($MgSO_4$)	Merck, Darmstadt, Germany
Methanol	Sigma-Aldrich, St. Louis, USA
Midori Green Advance	Biozym, Hessisch Oldendorf, Germany
Milk powder	Carl Roth, Karlsruhe, Germany
MyrcludexB (Bulevirtide)	Kind gift from S. Urban
Sodiumcarbonate (Na_2CO_3)	Carl Roth, Karlsruhe, Germany
Sodiumchloride (NaCl)	VWR International, Darmstadt, Germany
Sodiumhydrogencarbonate ($NaHCO_3$)	Carl Roth, Karlsruhe, Germany
Disodiumhydrogenphosphate (Na2HPO4)	Carl Roth, Karlsruhe, Germany
Protein Standard (PrecisionPlus Dual Color)	Bio-Rad Laboratories, Hercules, USA
Rotiphorese Gel 40 (29:1)	Carl Roth, Karlsruhe, Germany
Phenol	Carl Roth, Karlsruhe, Germany
Sodiumdodecylsulfate (SDS) 10%	SERVA Electrophoresis, Heidelberg, Germany
Sulfuric acaid (H_2SO_4; 2N)	AppliChem, Darmstadt, Germany

Table 2.9: Continued Chemicals and reagents

Name	Composition/supplier
Tetramethylethylendiamine (TEMED)	AppliChem, Darmstadt, Germany
TritonX-100	AppliChem, Darmstadt, Germany
Tris Base	Carl Roth, Karlsruhe, Germany
Tween-20	AppliChem, Darmstadt, Germany
TransIT-LT1 transfection reagent	Mirus Bio, Madison, USA
Water, DNase, RNase free	MP Biomedicals Germany, Eschwege, Germany

2.6 Consumables

Table 2.10: Consumables

Name	Supplier
Amicon Ultra 100k filter units (4mL, 15mL)	Merck, Darmstadt, Germany
Bacterial plates (10cm)	Corning, New York, USA
Cell culture flasks (T25, T75, T175, T875)	Corning, New York, USA
Cell culture plates (6-Well, 12-Well, 24-Well, 96-Well)	Greiner Bio-One, Frickenhausen, Germany
CellStar® Cell culture dishes (6cm, 10cm, 15cm)	Greiner Bio-One, Frickenhausen, Germany
Costar aspirating pipets	Corning, New York, USA
Coverslips (12mm)	Th. Geyer, Renningen, Germany
Cryotubes (1,5mL)	Greiner Bio-One, Frickenhausen, Germany
Extra thick filter paper	Bio-Rad Laboratories, Hercules, USA
Face mask	Meditrade, Kiefersfelden, Germany

Table 2.10: Continued Consumables

Name	Supplier
Filter (0,2µm, 0,45µm)	GE Healthcare, Chicago, USA
Filter tips (10µL, 200µL, 1000µL)	Biozym, Hessisch Oldendorf, Germany
GenePulser® electroporation cuvette (0,2cm)	Bio-Rad Laboratories, Hercules, USA
Gloves, nitrile	Starlab, Hamburg, Germany
Gloves, long, nitrile	ShieldScientific, Bennekom, Netherlands
Hard-Shell® 96-Well plates	Bio-Rad Laboratories, Hercules, USA
Microscopy glass slides	Carl Roth, Karlsruhe, Germany
MicroSeal ® sealing sheet	Bio-Rad Laboratories, Hercules, USA
Overshoes, blue	Diaprax GmbH, Wesel, Germany
PVDF blotting membrane	Bio-Rad Laboratories, Hercules, USA
Reaction tubes (1,5mL, 2mL)	Sarstedt, Nümbrecht, Germany
Reaction tubes (5mL)	Eppendorf SE, Hamburg, Germany
Reaction tubes (15ml, 50mL)	Corning, New York, USA
Reagent reservoir (50mL)	Corning, New York, USA
Refill tips non-filtered (10µL, 200µL, 1000µL)	Starlab, Hamburg, Germany
Scalpel Feather Fig. 21	megro, Wesel, Germany
Serological pipettes (5mL, 10mL, 25mL)	Corning, New York, USA
Single-cap PCR tubes	Biozym, Hessisch Oldendorf, Germany
Stericup (0,45µm)	Merck, Darmstadt, Germany
Syringes (5mL, 10mL , 20mL)	BD, Heidelberg, Germany

2.7 Enzymes

Table 2.11: Enzymes

Name	Composition/supplier
Q5 High fidelity DNA polymerase	New England Biolabs (NEB), Frankfurt a.M., Germany
Recombinant shrimp alkaline phosphatase	New England Biolabs (NEB), Frankfurt a.M., Germany
Restriction enzymes	New England Biolabs (NEB), Frankfurt a.M., Germany
RNaseR	BioCat, Heidelberg, Germany
T4 DNA ligase	New England Biolabs (NEB), Frankfurt a.M., Germany
T7 RNA polymerase	Self made

2.8 Equipment

Table 2.12: Equipment

Name	Supplier
ÄKTApure chromatography system	GE Healthcare, Chicago, USA
Agarose gel chamber	VWR International, Darmstadt, Germany
Analytical scale LP-3102	VWR International, Darmstadt, Germany
Analytical fine scale LA-124i	VWR International, Darmstadt, Germany
Biological safety cabinet HeraSafe 2020	ThermoFisher Scientific, Waltham, USA
C1000 Touch Thermal Cycler	Bio-Rad Laboratories, Hercules, USA
Cell culture centrifuge Rotina 380R	Andreas Hettich GmbH, Tuttlingen, Germany
Centrifuge 5424	Eppendorf SE, Hamburg, Germany

Table 2.12: Continued Equipment

Name	Supplier
Centrifuge 5424 R	Eppendorf SE, Hamburg, Germany
Centrifuge Sorvall LYNX4000	ThermoFisher Scientific, Waltham, USA
CFX Connect™ real time PCR detection system	Bio-Rad Laboratories, Hercules, USA
CO_2 cell culture incubator IncuSafe	Sanyo, Moriguchi, Japan
CO_2 cell culture incubator C200	Labotect, Göttingen, Germany
Electrophoresis cell Mini-PROTEAN tetra vertical	Bio-Rad Laboratories, Hercules, USA
Electroporation device GenePulser Xcell	Bio-Rad Laboratories, Hercules, USA
ECL ChemoCam imager 3.2	INTAS Sciences, Göttingen, Germany
Flow cytometer LSRFortessa II	BD, Heidelberg, Germany
Freezer Liebherr premium	Liebherr, Kirchdorf a.d. Iller, Germany
Fridge Med Line	Liebherr, Kirchdorf a.d. Iller, Germany
Gel documentation system iDoc	INTAS Sciences, Göttingen, Germany
Heatblock/shaker ThermoMixer C	Eppendorf SE, Hamburg, Germany
Inverted microscope Primovert	Carl Zeiss, Jena, Germany
Liquid nitrogen tank	Tec-lab, Hünfelden, Germany
Luminometer Mithras LB943	Berthold Technologies, Bad Wildbad, Germany
Magnetic stirrer MR Hei-Standard	Heidolph Instruments, Schwabach, Germany
Microscope Nikon Eclipse Ti	Nikon, Minato, Japan
Microscope Nikon Eclipse Ts2	Nikon, Minato, Japan
Microwave oven	Clatronic, Kempen, Germany
Multiskan EX plate reader	ThermoFisher Scientific, Waltham, USA
PipetBoy acu2	Integra, Biebertal, Germany

Table 2.12: Continued Equipment

Name	Supplier
Pipette Research Plus 10µL, 20µL, 200µL, 1000µL	Eppendorf SE, Hamburg, Germany
Power supply PowerPac™	Bio-Rad Laboratories, Hercules, USA
Pump BVC Professional	VacuuBrand, Wertheim, Germany
Rotating mixer multiaxle	VWR International, Darmstadt, Germany
Spectrophotometer NanoDrop 1000	ThermoFisher Scientific, Waltham, USA
Tabletop pump Vacusip	Integra, Biebertal, Germany
Transfer system Trans-Blot turbo	Bio-Rad Laboratories, Hercules, USA
Ultracentrifuge Optima LE-80K	Beckman-Coulter, Brea, USA
UV transilluminator	Vilber Lourmat, Eberhardzell, Germany
Vortex Genie 2	Carl Roth, Karlsruhe, Germany

2.9 Kits

Table 2.13: Kits

Name	Purpose	Supplier
High capacity cDNA synthesis kit	Reverse transcription	Applied Biosystems, Waltham, USA
Mammalian calcium phosphate transfection kit	Transfection of HEK cells for lentivirus productin	TaKaRa Bio, Kusatsu, Japan
Monarch plasmid miniprep kit	Plasmid purification	New England Biolabs (NEB), Frankfurt a.M., Germany
Monarch total RNA miniprep kit	RNA extraction	New England Biolabs (NEB), Frankfurt a.M., Germany
Monarch gel extraction kit	DNA extraction from agarose gels	New England Biolabs (NEB), Frankfurt a.M., Germany

Table 2.13: Continued Kits

Name	Purpose	Supplier
Monarch DNA cleanup kit	Purification of PCR products	New England Biolabs (NEB), Frankfurt a.M., Germany
NucleoBond PC500 kit	Plasmid purification	Macherey-Nagel, Düren, Germany
QIAAmp viral RNA isolation kit	RNA extraction from viral supernatants	Qiagen, Hilden, Germany

2.10 Oligonucleotides

Table 2.14: Oligonucleotides for cloning

Name	Sequence
BatHepaci-E2-linker	ggatcaggagcacaccagcaactttccactgaagcgtatc
BatHepaci-E2-HA	gcccgcataatccggcacatcatacggataagcggtagcagtctcgacg
BatHepaci-E2-SbfI-fw	gtttacctgcaggatgggactggttttcttcttcttg
BatHepaci-E2-SpeI-rev	ggcggactagtgtcaacaccttggatgc
AMDV-env-HindIII-fw	ctaggcaagcttgactgggaaatacatcatcaagtc
AMDV-env-NotI-rev	ccatagcggccgcgaagaacaaagtagtgcctgtcc
AMDV-S-HindIII	aagcttcacaaccacacacgatg
AMDV-HA-S-fw	tatccgtatgatgtgccggattatgcggggtcaacattatccaatg
AMDV-HA-S-rev	catcgtgtgtggttgtg
AMDV-S-HA-fw	tatccgtatgatgtgccggattatgcgtagagatcaatcctgaaaaaactaaatg
AMDV-S-HA-rev	acttcctcccgtaatgtgtgaatagg
BgHBV-env-HindIII-fw	gtattaagcttgcggggaaccatattcctg
BgHBV-env-EcoRI-rev	caattgaattcctcgagagggtacctgac
BgHBV-S-HindIII	aagcttagcgaccccaacg

Table 2.14: Continued Oligonucleotides for cloning

Name	Sequence
BgHBV-HA-S-fw	tatccgtatgatgtgccggattatgcgacagggtttttctcagggtg
BgHBV-HA-S-rev	catctgtggcggtgacgttgg
BgHBV-S-HA-fw	tatccgtatgatgtgccggattatgcgtagaccccgagaaaacaaagtggtcag
BgHBV-S-HA-rev	acttcctgtggatccccagagaaagtag
CSKV-env-HindIII-fw	ctaggaagcttggaagtttcaccatctgc
CSKV-env-NotI-rev	gttggagcggccgccttcaactggagcagtg
CSKV-S-HindIII	aagcttgcaactcgacacttctaaac
CSKV-HA-S-fw	tatccgtatgatgtgccggattatgcggcaaaaacaccagagatatc
CSKV-HA-S-rev	catctcgtccgtctcggttg
CSKV-S-HA-fw	tatccgtatgatgtgccggattatgcgtagacatggacaaatctactcctc
CSKV-S-HA-rev	acttcccaattccccactcattgaataaac
DHBV-NheI-fw	cagctagtagctagcgtcgacgtggaactta
DHBV-NotI-rev	cagtatgcggccgctcatgcatgagatcc
DHBV-env-NheI-fw	gttactgctagccatgaatcaatagtagg
DHBV-env-NotI-rev	cagtatgcggccgccattcaccggagaag
DHBV-S-NheI	gctagcccagtgataaaaactcc
DHBV-HA-S-fw	tatccgtatgatgtgccggattatgcgtctggtaccttcgggggaatac
DHBV-HA-S-rev	cattttcttcttcaaggggg
DHBV-S-HA-fw	tatccgtatgatgtgccggattatgcgtaggaataagaataaactttgacaaaac
DHBV-S-HA-rev	acttccactcttgtaaaaaagagcag
HBV-env-HindIII	gtaccaagcttaaacaacacatagcgcc
HBV-env-NotI	gtattgcggccgcagtaaccccatctctttg
HBV-S-HindIII	aagcttcttctcgaggattgg
HBV-HA-S-fw	tatccgtatgatgtgccggattatgcggagaacatcacatcaggattc

Table 2.14: Continued Oligonucleotides for cloning

Name	Sequence
HBV-HA-S-rev	catgttcagcgcagggtcc
HBV-S-HA-fw	tatccgtatgatgtgccggattatgcgtagaccctaacaaaacaaagagatg
HBV-S-HA-rev	acttccaatgtatacccaaagacaaaag
HeHBV-env-HindIII	gattcagaagcttgcaccttgtcccgcaac
HeHBV-env-NotI	gattacagcggccgccggggaaggagtcat
HeHBV-S-HindIII	aagcttcccaaagctcaccaacaag
HeHBV-HA-S-fw	tatccgtatgatgtgccggattatgcgggagctaccttcgggggaatac
HeHBV-HA-S-rev	cattttcttcttgttggtgagc
HeHBV-S-HA-fw	tatccgtatgatgtgccggattatgcgtagggatcaactttgacaaaatgactc
HeHBV-S-HA-rev	acttcctcccgaattcttgaagaaaag
RRHBV-env-HindIII	ctttataggacaagcttatccttgg
RRHBV-env-NotI	cattaagcggccgcccaccattttgttttatcgg
RRHBV-S-HindIII	aagcttgaccctgtccggg
RRHBV-HA-S-fw	tatccgtatgatgtgccggattatgcgacaaccgaaaatgcatctcg
RRHBV-HA-S-rev	catgtttccccggacagggtc
RRHBV-S-HA-fw	tatccgtatgatgtgccggattatgcgtagagataaaccccgataaaacaaaatg
RRHBV-S-HA-rev	acttccccccccagatataccagaaag
SkHBV-env-NheI	cataagctagcggtaggggtgctatacaag
SkHBV-env-NotI	cttaagcggccgccctcgctggttcaggtg
SkHBV-S-HindIII	aagcttcaccactagctactc
SkHBV-HA-S-fw	tatccgtatgatgtgccggattatgcggcagaagactctgtcacgtc
SkHBV-HA-S-rev	catcttctgagttggtggaggc
SkHBV-S-HA-fw	tatccgtatgatgtgccggattatgcgtagatgtggacaaatctacacctgaacc
SkHBV-S-HA-rev	acttcctgatgatcccatagctttgtag

Table 2.14: Continued Oligonucleotides for cloning

Name	Sequence
SLHBV-S-HindIII	aagcttgacacctcaaccggag
SLHBV-S-NotI	ctcgagcggccgcgtac
SLHBV-HA-S-fw	tatccgtatgatgtgccggattatgcggcgacaaacgacttttctatg
SLHBV-HA-S-rev	catgttctgactctccggttg
TFHBV-env-HindIII	cgaaatcaagcttgaacgcctgttaggaccattg
TFHBV-env-NotI	gcttaatagcggccgccacaatttgtctggtgg
TFHBV-S-HindIII	aagcttgaagctggaagaaaagag
TFHBV-HA-S-fw	tatccgtatgatgtgccggattatgcgagcggcgctgtttctcccg
TFHBV-HA-S-rev	catgtttgcagttgtactcttttc
TFHBV-S-HA-fw	tatccgtatgatgtgccggattatgcgtagactttgacaaatctacactaacc
TFHBV-S-HA-rev	acttcctcctgaccccatattgttg
TMDV-env-HindIII	gtataagcttctattcatgggaggctcg
TMDV-env-NotI	cttaagcggccgccagtccacttagtcttttc
TMDV-S-HindIII	aagcttcttcgtccattggac
TMDV-HA-S-fw	tatccgtatgatgtgccggattatgcgtttggaccgctcggaggattc
TMDV-HA-S-rev	catattggcagccgctgtcc
TMDV-S-HA-fw	tatccgtatgatgtgccggattatgcgtagatgaggaaaagactaagtggactg
TMDV-S-HA-rev	acttccgttgtatccccaaagattg
WHV-env-HindIII	cttggactaagcttcatattcttgggaacacagac
WHV-env-NotI	cagattagcggccgccctgaactagtaattacatatcc
WHV-S-HindIII	aagcttcctgcactgtcacc
WHV-HA-S-fw	tatccgtatgatgtgccggattatgcgtcaccatcaagtctcctaggactc
WHV-HA-S-rev	catctccggtgacagtgcag
WHV-S-HA-fw	tatccgtatgatgtgccggattatgcgtagatgtcaataaaacaaaatggtg

Table 2.14: Continued Oligonucleotides for cloning

Name	Sequence
WHV-S-HA-rev	acttccaatgtatacccaaatcaagaaaaac

Table 2.15: Oligonucleotides for RT-qPCR

Name	Sequence
HCV-fw	tctgcggaaccggtgagta
HCV-rev	gggcatagagtgggtttatcca
HCV-probe	6-FAM-aaaggacccagtcttcccggcaatt-TAMRA
HDV-fw	gcgccggctgggcaac
HDV-rev	ttcctcttcgggtcggcatg
HDV-probe	6-FAM-cgcggtccgacctgggcatccg-BHQ1

2.11 Plasmids

Table 2.16: Plasmids

Name	Backbone	Gene of interest	Source
pCHT-HBV1.1	pCHT	1,1x HBV gtD	Kind gift from M. Nassal
pcDNA-eGFP	pcDNA3.1	eGFP	Addgene
pcDNA-gHDV	pcDNA3.1	HDV 1,1x genome	Kind gift from S. Urban
pcDNA-HDV-2xUAA	pcDNA3.1	HDV antigenome not producing L-HDAg	Kind gift from S. Urban
pcDNA-SHDAg	pcDNA3.1	HDV S-HDAg	Kind gift from S. Urban

Table 2.16: Continued Plasmids

Name	Backbone	Gene of interest	Source
pcDNA-nonhuman HBV	pcDNA3.1	Unitlength genome of non-human HBV	self-designed
pcDNA-nonhuman-HBV-env	pcDNA3.1	Non-human HBV env ORF	Self cloned
pcDNA-nonhuman-HBV-HA-env	pcDNA3.1	Non-human HBV env ORF, HA tag on N-terminus of S	Self cloned
pcDNA-nonhuman-HBV-env-HA	pcDNA3.1	Non-human HBV env ORF, HA tag on C-terminus of S	Self cloned
pcDNA-nonhuman-HBV-S	pcDNA3.1	Non-human HBV S protein	Self cloned
pcDNA-nonhuman-HBV-HA-S	pcDNA3.1	Non-human HBV S protein, HA tag on N-terminus	Self-cloned
pcDNA-nonhuman-HBV-S-HA	pcDNA3.1	Non-human HBV S protein, HA tag on C-terminus	Self-cloned
pCMVΔR8.91		HIV gag-pol	Addgene
pFK-Jc1	pFK	HCV Jc1 full length genome	Christopher Dächert
pFK-sgJFH1-5A-mCherry	pFK	JFH1 subgenomic replicon, NS5A tagged with mCherry	Own group
pJC126	pcDNA	HDV 1,1x antigenome	Kind gift from S. Urban
pLX304-HB2.7	pLX304	HBV S, M, L, X	Kind gift from S. Urban
pMD2.G	pMD2.G	VSV-G	Addgene
pWPI-C-NS2	pWPI	HCV Jc1 C-NS2	Own group

Table 2.16: Continued Plasmids

Name	Backbone	Gene of interest	Source
pWPI-CD81	pWPI	Human CD81	Own group
pWPI-E1E2	pWPI	HCV Jc1 E1E2	Own group
pWPI-NTCP	pWPI	Human NTCP	Kind gift from S. Urban
pWPI-prME	pWPI	DENV prME	Own group

2.12 Software

Table 2.17: Software

Name	Supplier
AlphaFold2	accessed via the Google ColabFold (ColabFold v1.5.2-patch: AlphaFold2 using MMseqs2), originally developed by DeepMind [87]
Bio-Rad CFX Maestro	Bio-Rad Laboratories, Hercules, USA
ChimeraX	Open source software, UCSF, San Francisco, USA (`www.cgl.ucsf.edu/chimerax`)
Fiji	Open source software (`www.imagej.net/software/fiji`) [169]
GraphPad Prism	Insight Partners, New York, USA
Ilastik	Open source software, EMBL, Heidelberg, Germany [12]
Inkscape	Open source, inkscape community (`www.inkscape.com`)
INTAS Chemostar	INTAS Sciences, Göttingen, Germany
Jalview	Open source software (`www.jalview.org`) [205]
Microsoft office	Microsoft, Redmond, USA
NIS Elements Advanced Research	Nikon, Minato, Japan

Table 2.17: Continued Software

Name	Supplier
Snap Gene	GSL Biotech LLC, Chicago, USA
Unicorn Versions 5.11 and 7.2	GE Healthcare, Chigaco, USA

2.13 Viruses and Bacteria

Table 2.18: Viruses and bacteria

Name	Description
HBV	Genotype D
HCV	Genotype 2a, strain Jc1
HDV	Genotype 1, with HBV gtD envelope
Escherichia coli (E.coli)	Strain DH5α

3 Methods

3.1 Cell Culture

3.1.1 Cultivation

Cells were maintained in the respective media (see table 2.8) at 37°C, 95% relative humidity and 5% CO_2. Passaging was done twice a week. Therefore, supernatant was removed and cells were washed once with PBS. Cells were detached by adding 0,025% Trypsin/EDTA solution and incubating for several minutes at culturing conditions. Afterwards, cells were resuspended in cultivating medium, diluted to the desired concentration and seeded on fresh culturing plates.

3.1.2 Freezing and thawing

For freezing, cells were detached as described for regular maintenance (see section 3.1.1) but transferred to a 50mL conical tube. After 5min centrifugation at 500g and room temperature, the supernatant was removed and the cell pellet was resuspended in FCS + 10% DMSO. The suspension was distributed in 1mL aliquots to cryo vials and frozen in an isopropanol freezing container lowering the temperature by approximately 1°C per minute to -80°C. For long term storage, frozen cells were transferred to liquid nitrogen. Cells were thawed quickly and resuspended in warm cultivating medium. Afterwards, cells were centrifuged for 5min at 500g and room temperature followed by resuspension of the pellet and plating cells in cultivating medium, or directly plated after thawing. One day after plating, the medium was exchanged to remove residual DMSO from the culture.

3.1.3 Counting

Cells were detached as described for regular maintenance (see section 3.1.1) and transferred to a 50mL conical tube. For counting, 10µL of the culture were counted in a Neubauer counting chamber.

3.1.4 DNA transfection

Plasmid transfection except for production of lentiviral particles was performed using TransIT-LT1 transfection reagent following the manufacturer's protocol.

In brief, one day before transfection, cells were seeded to reach 90% confluency at the day of transfection. Transfection reagent, plasmids and OptiMEM were slowly brought to room temperature. Approximately, 45min before transfection, the supernatant was removed and cells were covered with fresh cultivating medium. Transfection mixes were prepared by first diluting plasmid to the desired concentration in OptiMEM, then adding TransIT-LT1 transfection mix in a 3X excess to the amount of DNA (e.g. 1µg DNA in OptiMEM mixed with 3µL TransIT-LT1), and mixing by inverting the tube. Transfection mixes were incubated at room temperature for 20min to allow formation of lipoparticles and then added to the cells. Plates were gently shook in order to equally distribute the transfection mix and incubated at cultivating conditions. One day after transfection, the supernatant was removed, cells were washed 3x with PBS and covered with fresh cultivating medium.

3.1.5 Generation of stable cell lines

Cell lines stably overexpressing certain proteins of interest were generated by lentiviral transduction. HEK293T cells were seeded in 6cm dishes at a density of $1{,}2\text{x}10^6$ cells per dish one day before transfection. 30-45min before transfection, the medium was exchanged to 4mL cultivating medium. Plasmids encoding for VSV-G (pMD.G; 2,14µg), HIV gag-pol (pCMVΔR8.91; 6,42µg) and the protein of interest (pWPI-PI; 6,42µg) were diluted in water to a final volume of 438µL. Subsequently, 62µL $CaCl_2$ and 500µL 2X HBS were added and mixed by gentle pipetting. The entire volume was added dropwise to the cells and incubated at 37°C. One day after transfection, the medium was exchanged to 5mL cultivating medium and target cells were seeded to 6cm dishes for transduction. Supernatants of transfected HEK293T cells were harvested twice on d2 p.t. (morning and afternoon) and once on d3 p.t. (morning) and filtered through a 0,45µm pore size filter unit. Medium on target cells was removed and filtered supernatant was added to the cells. The afternoon after the third transduction, cells were washed twice with PBS and split to 10cm dishes. Selection was started during the first split with the required antibiotic concentration.

3.1.6 RNA electroporation

Cells were detached as described for regular maintenance (see section 3.1.1) and diluted to $1\text{x}10^7$ cells per mL in cultivating medium. After centrifugation at 500g and room temperature for 5min, the supernatant was discarded and the pellet washed in 35mL PBS. Cells were again pelleted at 500g and room temperature for 5min and then resuspended

in 200µL freshly prepared Cytomix per electroporation reaction. The cell suspension was mixed with 2,5-5µg in vitro transcribed RNA and transferred to a 0,2mm gap width electroporation cuvette. Electroporation was performed at 500µF and 166V for approximately 8-9ms. Afterwards, cells were resuspended in pre-warmed cultivating medium and seeded to a density of $1{,}7x10^6$ cells per well for timepoints earlier than d3 and $8x10^5$ cells per well for timepoints d3 and later.

In case of flHCV RNA electroporation, cells were allowed to attach for 4h and then transferred to BSL-3 conditions.

3.2 Viruses

Experiments including work with infectious full length HBV and HCV were performed under BSL-3 safety conditions. All work with HDV was performed under BSL-2 conditions including handling pseudotyped HDV.

3.2.1 Infection

Viral infection experiments were performed in infection medium consisting of cultivating medium supplemented with DMSO (1,5% for Huh7 based cell lines and 2,5% for HepG2 based cell lines). Virus stocks were diluted in infection medium to the desired MOI and PEG8000 was added to a final concentration of 4%. Infections were performed over night in half the cultivating volume (e.g. 250µL per 24 well plate). Afterwards, the inoculum was removed, cells were washed three times with PBS and covered with the full volume of infection medium.

3.2.2 Viral stock production HBV and HDV

Viral stocks of HBV and HDV were produced using the stable producer cell lines HepAD38 (HBV) and Huh7-END (HDV). Cells were expanded to 6x T175 flasks to reach the number of cells required to be seeded on two 5-layer multiflasks (growth area $875cm^2$) and two T25 control flasks. HepAD38 cells were kept under +2µM Doxycycline conditions until 14 days after seeding, before Doxycycline was removed to induce virus production. Supernatants from both cell lines were harvested every three to four days, filtered through a 0,22µm pore size filter unit and stored at 4°C. The total culturing time was 100 days and 14 days for HepAD38 and Huh7-END, respectively. All supernatants of Huh7-END and supernatants of HepAD38 showing the highest virus concentrations, as determined by HBsAg and HBeAg specific ELISA, were pooled for further processing. Viral particles were purified and concentrated at 4°C on a HiTrap 5mL HP heparin column using a fully automated ÄKTApure device as described by Seitz et. al. [174]. Briefly, the column was equilibrated with 3 column volumes (CV) 1X

TN buffer at 2mL/min. A total volume of 450mL cell culture supernatant was loaded to the column at 0,4mL/min, before the column was washed with 5 CV at 2mL/min. Viral particles were eluted over 5 CV at 2mL/min using a linearly increasing salt concentration ranging from 140mM to 2140mM NaCl in 1X TN buffer. Eluates were collected in 2,5mL fractions and the column was re-equilibrated with 5 CV at 2mL/min. During the entire procedure, UV absorption was measured at 254nm and 280nm. Collected fractions were immediately diluted with deionised water in order to reduce the salt concentration and thereby minimise particle damage. For further concentration of viral particles, fractions around the highest UV-peak were pooled and applied to Amicon Ultra-15 100k filter units by centrifugation at 3000g and 4°C for 3h. Concentrated viral particles were resuspended to 3mL 1X TN buffer + 10% FCS and stored at -80°C. Viral titers as indicated by genome equivalents per mL were determined by qPCR. For HBV particles, titer dertermination was kindly performed by Dr. Paul Schnitzler.

3.2.3 Concentration of viral supernatants

Supernatants harvested from transfected or stable cells producing viral particles (besides virus stocks) were concentrated by either PEG-precipitation or Amicon filter units. In both cases, cell culture supernatants were filtered through a 0,45µm pore size filter and then applied to the respective concentration procedure.

Amicon filter unit

Filtered supernatants were directly applied to Amicon Ultra filter units with a 100kDa weight cutoff and centrifuged for 20min at 4000g and 4°C. The flow-through was discarded and the filtrate was stored at -80°C.

PEG-precipitation

PEG8000 (40% (w/v) stock solution in PBS) was added to filtered cell culture supernatants in a final concentration of 6% and mixed by inverting the tube. After incubation over night at 4°C, particles were pelleted by centrifugation for 1h at 10000g and 4°C. Supernatants were discarded and the pellet was resuspended in 150µL OptiMEM or 1% FCS in 1X TN buffer and stored at -80°C.

3.3 Nucleic acids

3.3.1 *In vitro* transcription

Viral RNA used for electroporation was produced by *in vitro* transcription. HDV RNA was generated from a plasmid encoding an 1,1x overlength genome (gHDV) or antigenome (agHDV) and HCV RNA was produced from a plasmid encoding unit length RNA (flHCV) or subgenomic replicon RNA (sgHCV). In addition, an mRNA analogue of S-HDAg was synthesised. All plasmids were digested at a quantity of 10-20µg with suitable restriction enzymes (see tables 3.1 and 3.2) for 2h at 37°C. Afterwards, the DNA was run on a preparative agarose gel. The required fragments were excised and extracted from the gel using the Monarch gel extraction kit as described in section 3.3.7. *In vitro* transcription was performed using T7 polymerase in the reaction mix as described in tables 3.3, 3.5 and 3.4 over 4h at 37°C. After 2h incubation, another 2µL of T7 polymerase was added in order to increase efficiency. The DNA template was digested by 1,5U DNaseI over 1h at 37°C. In the case of S-HDAg mRNA production, 10µL poly(A)-polymerase buffer and 5U E.coli poly(A)-polymerase were added and incubated at 37°C for 30min. Samples were stored at -80°C or directly processed for RNA isolation by phenol-chloroform-extraction.

Table 3.1: Restriction enzymes used for preparation of HDV or HCV full length or subgenomic RNAs

Construct	**Enzyme**
gHDV	SacI, NotI
agHDV	MluI, MscI
S-HDAg mRNA	SacI, NotI
flHCV	SbfI, MluI
sgHCV	AfeI

Table 3.2: Template preparation for *in vitro* transcription. Volumes given are required for one reaction.

Reagent	**Amount**
Restriction enzyme	1µL
Buffer CutSmart	10µL
DNA template	10-20µg
Nuclease free H_2O	ad 100µL

Table 3.3: Reagents for *in vitro* transcription of full length HDV RNAs. Volumes given are required for one reaction.

Reagent	**Amount**
10X Polymerase buffer	10µL
rNTPs (25mM each)	12,5µL
RNasin (40U/µL)	2,5µL
T7 polymerase	2µL
RNA template	60µL
Nuclease free H_2O	ad 100µL

Table 3.4: Reagents for *in vitro* transcription of S-HDAg mRNA analogue. Volumes given are required for one reaction.

Reagent	**Amount**
10X Polymerase buffer	8,5µL
rNTPs (25mM ATP, CTP, UTP; 12,5mM GTP)	12,5µL
ARCA cap analogue	20µL
RNasin (40U/µL)	2,5µL
T7 polymerase	2µL
RNA template	40µL

Table 3.5: Reagents for *in vitro* transcription of HCV RNAs. Volumes given are required for one reaction.

Reagent	**Amount**
5X RRL buffer	23µL
rNTPs (25mM each)	12,5µL
RNasin (40U/µL)	2,5µL
T7 polymerase	2µL
RNA template	60µL
Nuclease free H_2O	ad 100µL

3.3.2 Phenol-chloroform-extraction

RNA produced by *in vitro* transcription was mixed with RNase free water, phenol (water saturated, pH<5) and sodium acetate (2M, pH4,5) according to table 3.6.

Table 3.6: Reagents for phenol-chloroform extraction. Volumes given are required for one reaction.

Reagent	Amount
IVT RNA	100µL
RNase free water	440µL
Sodium acetate (2M, pH 4,5)	60µL
Phenol (water saturated pH<5)	400µL

The mixture was vortexed for 5s, incubated on ice for 10min and centrifuged for 10min at 4°C and 12000g. The upper phase was transferred to a clean 1,5mL tube and mixed with the same volume of chloroform. After vortexing for another 5s, the samples were centrifuged for 3min at room temperature and 20000g. The upper phase was transferred to a clean 1,5mL tube and the RNA was precipitated by mixing with 0,7 volumes of isopropanol and centrifugation for 20min at room temperature and 20000g. The supernatant was discarded and the pellet was resuspended in 300µL freshly prepared 70% ethanol. After centrifugation for 3min at room temperature and 20000g, the supernatant was discarded and the pellet was air-dried for 10min. The RNA was resuspended in 50µL RNase free water and dissolved by incubation at 37°C and 450rpm for 5min.

RNA concentration was assessed spectrophotometrically using the NanoDrop1000 device and RNA integrity was checked by agarose gel electrophoresis in 1X TBE buffer.

3.3.3 RNA isolation from cells

Isolation was performed using the Monarch total RNA miniprep kit according to manufacturer's instructions. If not stated otherwise, centrifugation was performed at 16000g and room temperature for 30s. In brief, medium was removed and cells were washed once with PBS. Lysis was performed by adding 300µL Monarch RNA lysisbuffer and freezing the lysate at -80°C. Prior to RNA isolation, lysates were thawed at room temperature. The lysate was applied to a gDNA removal column and centrifuged. The flowthrough was mixed with the same volume of 95% ethanol, applied to an RNA isolation column and centrifuged. The flowthrough was discarded and the column washed once with 500µL Monarch wash buffer. On-column DNaseI digest was performed by

adding 5µL DNaseI in 75µL DNaseI reaction buffer to the column and incubating 15min at room temperature. Afterwards, 300µL Monarch RNA prime buffer was applied to the column and centrifuged. The flowthrough was discarded and the column washed once with 500µL Monarch wash buffer. After centrifugation, the column was washed again with 500µL Monarch wash buffer. Centrifugation was performed for 2min. Columns were transferred to a fresh 1,5mL tube and RNA was eluted in 50µL RNase free water by centrifugation. RNA concentration was determined by spectrophotometry using the NanoDrop1000 device and software. Isolated RNA was stored at -80°C.

3.3.4 RNA isolation from viral supernatants

Isolation from viral supernatants was performed using the QiaAmp viral RNA isolation kit according to manufacturer's instructions. Prior to RNA isolation, supernatants harvested from cells after plasmid transfection were incubated with RQ1 DNase for 1h at 37°C. If not stated otherwise, centrifugation was performed at 11000g and room temperature for 1min. In brief, viral supernatants were brought to 140µL by adding sterile PBS. Diluted supernatants were mixed with 560µL buffer AVL containing 5,6µL carrier RNA and pulse-vortexed for 15s. After incubation at room temperature for 10min, 560µL 95% ethanol was added and pulse-vortexed for 15s. The mixture was applied to RNA isolation columns in 630µL steps and centrifuged. Columns were washed once with wash buffer AW1 and centrifuged. A second wash was performed by adding 500µL wash buffer AW2 and centrifugation for 3min at 20000g. The column was dried by centrifugation at 20000g and transferred to a fresh 1,5mL tube. Elution buffer AVE was added at a quantity of 50µL and incubated for 1min at room temperature. RNA was eluted by centrifugation and stored at -80°C.

3.3.5 Plasmid DNA extraction

Circular plasmid DNA was extracted from 5mL bacterial cultures using the Monarch plasmid miniprep kit or from 350mL bacterial cultures using the NucleoBond PC500 kit. Both extractions were performed according to manufacturer's instructions.

Using the Monarch plasmid miniprep kit, centrifugations were carried out at 16000g and room temperature for 1min, if not stated otherwise. Cells were precipitated from 5mL bacterial suspension over 30s centrifugation. The supernatant was discarded and cells were resuspended in 200µL buffer B1. For lysis, 200µL buffer B2 was added and mixed well by inverting the tube. After 1min incubation at room temperature, 400µL buffer B3 was added and mixed by inverting the tube. The suspension was cleared by centrifugation for 10min and 800µL supernatant was applied to the column by centrifugation. The flowthrough was discarded and the column washed once with 200µL wash buffer 1 and once with wash buffer 2. Elution was performed in 50µL ultrapure water into 1,5mL

reaction tubes after incubation for 1min at room temperature. DNA concentration was determined spectrophotometrically using the NanoDrop1000 device.

From larger 350mL bacterial cultures, 1mL was mixed 1:1 with 50% glycerol and stored at -80°C for cryopreservation. The volumes given during the procedure refer to the high copy protocol, numbers given in brackets state deviations if the low copy protocol was followed. The remaining culture was centrifuged at 6000g and 4°C for 15min. The supernatant was discarded and the pellet resuspended in 12mL (24mL) buffer S1. For lysis, 12mL (24mL) buffer S2 was added and mixed by inverting the tube. After incubation at room temperature for 3,5min, 12mL (24mL) buffer S3 was added and mixed by inverting the tube. The suspension was incubated on ice for 5min, while the column was equilibrated with 6mL buffer N2. The lysate was applied to the column through a folded filter, the flowthrough was discarded. The column was washed once with 32mL (twice with 18mL) buffer N3. Elution was performed in 15mL buffer N5 into 50mL conical tubes. For precipitation, the eluate was mixed with 11mL isopropanol by gently inverting the tube and centrifuged at 4500g and 4°C for 30min. The supernatant was discarded and the pellet transferred to a fresh 1,5mL tube and mixed with 1mL 70% ethanol. After centrifugation at 4500g and room temperature for 10min, the supernatant was discarded and the pellet was allowed to dry at room temperature for 15min. Plasmid DNA was resuspended in 80-100µL ultrapure water and incubated over night at 4°C. DNA concentration was determined spectrophotometrically using the NanoDrop1000 device and adjusted with ultrapure water to 1µg/µL, if necessary.

3.3.6 Cloning

Generation of new plasmids was performed using PCR amplification of desired fragments and restriction cloning. Restriction enzymes were purchased from NEB and used in buffers and at temperatures given by the manufacturer. After restriction digest, the plasmid backbone was dephosphorylated by adding 1µL recombinant shrimp alkaline phosphatase (rSAP) to the digest mixture followed by incubation at 37°C for 30min. Insert and vector fragments were purified by preparative agarose gel electrophoresis and gel extraction (see 3.3.7). DNA concentration was determined using the NanoDrop1000 device. Ligation was performed in a reaction volume of 10µL using 400U/reaction T4 Ligase and 1X Ligase buffer. Incubation was performed overnight at 13°C. Afterwards, 1-5µL of the ligation mixture was transformed into bacterial cells as described in section 3.4.1.

3.3.7 Preparative agarose gelelectrophoresis

DNA was mixed with 6X loading dye and run on 1% agarose in 1X TAE buffer. Desired fragments were cut out and weighed. Gel extraction was performed using the Monarch gel extraction kit according to manufacturer's instructions. Briefly, dissolution of the

gel was performed by adding four volumes of dissolve buffer and incubation at 50°C and 650rpm for approximately 10min. The DNA was bound to the column by adding a maximum of 800µL per run on the column and centrifuged for 1min at 16000g. The column was washed twice with 200µL wash buffer (16000g, 1min) and eluted in 20µL ultrapure water after incubation at room temperature for 1min.

3.3.8 Site directed mutagenesis

In order to add tags or insert point mutations, linear DNA fragments were amplified by polymerase chain reaction (PCR) using the Q5 high fidelity polymerase. Primers were designed in a "tail-to-tail" binding orientation allowing amplification of the whole plasmid sequence to linear DNA molecules. One of the primers carries the desired mutation or overhang nucleotides in the 3'-end, while the other primer binds with its entire sequence to the template. The mastermix for one reaction is depicted in table 3.7 and amplification was performed according to table 3.8.

Table 3.7: Reagents for PCR mastermix. Volumes given are required for one reaction.

Reagent	**Amount**
5X Polymerase buffer	5,00µL
5X GC enhancer	5,00µL
10mM dNTP	0,50µL
10µM Primer fw	1,25µL
10µL Primer rev	1,25µL
Template DNA	2ng
Q5 Polymerase	0,25µL
H2O, nuclease free	ad 25µL

Table 3.8: Conditions for PCR amplification.

Step	**Action**	**Duration**
1	98°C	30s
2	98°C	10s
3	56°C	10s
4	72°C	40s/kbp
5	Repeat from step 2	35 cycles
6	72°C	120s

Table 3.8: Continued Conditions for PCR amplification.

Step	Action	Duration
7	4°C	infinite

PCR products resulting from whole plasmid amplifcation were analysed on a preparative agarose gel and extracted fragments were phosphorylated using 10U of T4 phosphonucleotidkinase (PNK) in a total reaction volume of 20µL supplemented with T4 Ligase buffer. After incubation at 37°C for 30min, PNK was heat inactivated by incubation at 65°C for 20min and the ligation mix was prepared. In order to deliver fresh ATP, new 10X T4 ligase buffer was added together with 400U T4 ligase. Ligation was performed over night at 13°C in a total reaction volume of 25µL and then transformed into competent bacteria as described in section 3.4.1.

3.3.9 Reverse transcription and quantification of RNA

In order to quantify intracellular or extracellular RNA by quantitative PCR (qPCR), RNA was reverse transcribed using the high capacity cDNA synthesis kit. For detecting intracellular RNA, samples were diluted to 16ng/µL in a total volume of 6µL. Per reaction, 6µL mastermix (see table 3.9) were added and samples were incubated as follows in table 3.10.

Table 3.9: Reagents for reverse transcription mastermix. Volumes given are required for one reaction.

Reagent	Amount
10X RT buffer	1,20µL
10X Primer	1,20µL
25X dNTP	0,48µL
RNase Inhibitor (40U/mL)	0,60µL
RT	0,60µL

Table 3.10: Conditions for reverse transcription.

Step	Action	Duration
1	25°C	10min
2	37°C	2h

Table 3.10: Continued Conditions for reverse transcription.

Step	Action	Duration
3	85°C	5min
4	4°C	infinite

Samples were then diluted to 5ng/µL with nuclease free water and analysed by qPCR using 3µL cDNA per reaction and the iTaq universal probes supermix. The mastermix for one reaction is depicted in table 3.11, the amplification was performed as follows in table 3.12.

Table 3.11: Reagents for qPCR mastermix. Volumes given are required for one reaction.

Reagent	Amount
2X iTaq Universal Probes Supermix	7,5µL
100µM Primer fw	0,06µL
100µM Primer rev	0,06µL
100µM Probe	0,03µL
cDNA template	3µL
Nuclease free H2O	4,35µL

Table 3.12: Conditions for qPCR amplification.

Step	Action	Duration
1	95°C	3min
2	95°C	15s
3	60°C	1min
4	Repeat from step 2	45 cycles

Quantification of viral genome copies was performed using a standard curve ranging from 10^2 – 10^8 copies per qPCR reaction. The standard curve was produced from *in vitro* transcribed RNA and processed in parallel to the samples.

3.3.10 Sequencing

Determination of DNA sequences was performed using the Eurofins light run DNA sequencing service. Samples were diluted to 100ng/µL and mixed in a ratio of 1:1 with 10µM primer using one sequencing primer per tube and sent to Eurofins. Determined sequences were analysed using the SnapGene software package.

3.4 Bacterial Work

3.4.1 Plasmid amplification

Amplification of circular plasmid DNA was performed after heat shock transformation in the E.coli strain DH5α. Briefly, bacterial cells were thawed on ice and 50µL of the suspension were mixed with 1µL plasmid (100ng/µL or less). The mixture was incubated on ice for 30min. Heat shock was performed by incubation at 42°C for 45s followed by immediate incubation on ice for 2min. Cells were mixed with 300µL LB medium without antibiotic and incubated at 37°C and 450rpm for 1h. Afterwards, cells were pelleted at full speed for 20s. 250µL supernatant was discarded, cells were resuspended in the remaining volume, and plated on LB plates containing 1mg/mL Ampicillin (LB-Amp). Plates were incubated over night at 37°C. Single colonies were picked and incubated in 5mL or 350mL LB-Amp over night at 37°C and 200rpm.

3.5 Protein Work

3.5.1 Flow cytometry

Expression of reporter proteins was investigated using flow cytometry. Cells were trypsinised from 6-well plates as for regular maintenance (see section 3.1.1) and transferred to a 2mL tube. After centrifugation for 8min at 1000g, the supernatant was discarded and cells were resuspended in PBS + 1% FCS. If cells needed to be fixed in order to inactivate virus, they were pelleted for 3min at 11000g and resuspended in 100µL Cytofix/Cytoperm solution and incubated in the dark for 20min at 4°C. Cells were pelleted again for 3min at 11000g, washed once with PBS and once with PBS + 1% FCS and finally resuspended in 1mL PBS + 1% FCS.
Measurement was performed a the LSRFortessa II gating for respective fluorescent proteins.

3.5.2 Immunofluorescence

Cells for investigation by immunofluorescence (IF) were seeded in 24 well plates on glass coverslips. At desired time points, cells were washed once with 500µL PBS and fixed with 500µL 4% PFA in PBS for 10min at room temperature. PFA was removed, cells were washed three times with PBS and stored at 4°C, covered in PBS until the staining was performed.
In order to reach intracellular targets, cells were permeabilised with 250µL 0,5% TritonX-100 in PBS over 10min at room temperature. After washing three times with PBS, cells were transferred to a tray covered with parafilm, and blocked with 100µL 3% BSA in PBS for 1h at room temperature. Incubation with the primary antibody (dilutions see table 2.2) was performed in 0,5% BSA in PBS over night at 4°C in a humid chamber. The primary antibody was discarded and cells were washed three times with PBS. Secondary antibody incubation (dilutions see table 2.3) was performed in 0,5% BSA in PBS for 1h at room temperature and covered from light. Staining for DNA in the nuclei was performed with 4',6-Diamidin-2-phenylindol (DAPI, 1:5000) in parallel to the secondary antibody incubation. Afterwards, cells were washed three times with PBS and dipped once in deinonised water. Excess liquid was removed using a tissue and coverslips were mounted, with the cells facing the object trays, using 6µL FluoromountG solution. Samples were allowed to dry over night at room temperature and then investigated using the Nikon Eclipse Ti fluorescence microscope. Image analysis was performed using Fiji and Ilastik software.

3.5.3 Luciferase assay

Detection of firefly luciferase activity was performed in order to detect replication of a luciferase tagged HCV replicon. After electroporation of *in vitro* transcribed RNA as described in section 3.1.6, cells were harvested at different time points for investigating the luciferase activity. The supernatant was discarded and cells were washed once with PBS. Lysis was performed by adding 100µL luciferase lysis buffer supplemented with 1mM DTT per 24-Well and freezing at -80°C. Luciferase substrates were prepared during thawing of the plates as described in table 3.13.

Table 3.13: Reagents for luciferase substrate solution. Volumes given are required for 25mL.

Reagent	**Amount**
Luciferase assay buffer	22,5mL
D-Luciferin	2mL
ATP (100mM)	500µL
DTT (1M)	25µL

After washing and priming the luminometer, measurement was performed by injecting 4x 100µL substrate solution per well, shaking and measuring luciferin counts.

3.5.4 Structure prediction

Protein structure prediction was performed using AlphaFold2 with MMSeq2 accessed via Google ColabFold (see section 2.12). Protein sequences, which were translated from the plasmid nucleotide sequence using the web based Expasy translate tool [183], were used as input files. Prediction was performed without amber relaxation and run until five ranked models were obtained. If not stated otherwise, rank 1 model was used for visualisation in the ChimeraX software.

3.5.5 Western blot

Cells were washed once with PBS and lysed in 1X Laemmli buffer. Samples were incubated at 95°C for 5min or 65°C for 30min (for HBsAg specific samples) and stored at -20°C. Proteins were separated on 12% acrylamide-bisacrylamide gels and transferred to methanol activated PVDF membranes using the semi-dry transfer method at 0,1V and 25mA for 1h. Afterwards, membranes were incubated shortly in 0,1% Tween20 in PBS (PBS-T) to remove remaining methanol and then blocked in 5% BSA or skim milk in PBS-T for 1h at room temperature. Primary antibody incubation (dilutions see table 2.4) was performed in 5% BSA or skim milk in PBS-T over night at 4°C. Antibodies were re-used up to 6 times and in the meanwhile stored at -20°C. Membranes were washed three times with PBS-T (20min per washing step) and HRP-coupled secondary antibody (dilutions see table 2.5) incubation was performed in 5% BSA or skim milk in PBS-T over 1h at room temperature. Membranes were washed three times in PBS-T and proteins were detected at the INTAS Western Blot Imager after adding ECL peroxide and luminol/enhancer solution in a ratio of 1:1. Image analysis was performed using Fiji software.

3.5.6 Quantification of secreted viral antigens

Secreted HBsAg and HBeAg in cell culture supernatants were analysed at the analytic center of the University Hospital Heidelberg. Detection was performed using the ARCHITECT chemoluminescent microparticle immunoassay (Abbott, Chicgao, USA) for HBsAg and the ADVIA Centaur XPTM automated chemoluminescence system (Siemens, Berlin, Germany) for HBeAg.

Extracellular HDAg was detected using a home-made enzyme linked immunosorbant assay (ELISA) in 96-well half-area plates. Plates were coated over night at 4°C with anti-HDAg (FD3A7, rabbit) 1:2000 in 50µL coating buffer per well. The next day, the coating solution was discarded and wells were washed three times with 150µL washing buffer.

Wells were blocked over 1h at RT with 100µL blocking buffer. After discarding the blocking buffer and washing once with 150µL washing buffer, wells were incubated over 1h at 37°C with 100µL sample or controls diluted in dilution buffer. Infectious material was inactivated with 1% TritonX-100 before applying to the plate. Dilution buffer only was used as negative control, wheras inactivated HDV virus stock with an amount corresponding to $1x10^7$ viral copies determined by RT-qPCR served as positive control. The supernatants were discarded and the plate washed five times with 150µL washing buffer. Incubation with anti-HDAg secondary antibody coupled to HRP (FD3A7, mouse) was performed 1:2000 in dilution buffer over 1h at 37°C. After discarding the secondary antibody, the plate was washed five times with 150µL washing buffer. TMB substrate solution A and B were mixed 1:1 and incubated with 50µL over 10min at RT. Reaction was stopped by addition of 25µL 2N sulfuric acid and absorbance was measured at 450nm and 570nm for background correction.

3.6 Statistical analysis

Statistical analysis was performed using the GraphPad Prism software package version 10. Two-way ANOVA followed by multiple comparison testing was applied to determine statistical significance and asterisks were used to depict significance levels as follows: *: p<0,05; **: p<0,01; ***: p<0,0001; ns: not significant

4 Results

To investigate the potential envelopment and spread of HDV by different helper viruses, my initial objective was to develop systems that would allow me to study the role of HCV for HDV transmission based on RNA transfection or viral infection. In a second step, I focused on assessing the ability of VSV-G protein to provide an envelope for HDV. Additionally, I explored possible reasons why HDV transmission without an HBV envelope might not occur. Finally, I expanded the knowledge about potential alternative hepadnaviral helper viruses by investigating their SVP production and envelopment capacity for HDV.

4.1 Envelopment of HDV by human non-HBV viruses

4.1.1 Establishment of a co-replication system for HDV and HCV

In order to investigate HDV and HCV co-replication, it is crucial to deliver both viral RNAs simultaneously into the same cell. For HCV, transfection of *in vitro* transcribed RNA is well established. In contrast, HDV research is often based on plasmid transfection of an 1,1x overlength antigenomic sequence (agHDV), which is sufficient to initiate replication in several cells. However, in natural infection, genomic RNA (gHDV) is delivered together with S-HDAg, which has been shown to promote viral replication [96, 58]. Therefore, I aimed to initiate HDV replication by providing S-HDAg using the stably S-HDAg producing cell line Huh7-S. Furthermore, I examined the replication efficiency of RNA delivered in agHDV and gHDV orientation. However, stable S-HDAg expression of initially used Huh7-S cells could interfere with IF based detection of HDAg after transfection. To overcome this issue, I evaluated provision of S-HDAg by co-transfection of an mRNA analogue instead.

As seen in Fig. 4.1A, initiation of viral RNA replication was most efficient when gHDV was present, either transfected alone or together with agHDV. Transfection of agHDV resulted in clearly lower amounts of intracellular RNA compared to gHDV, but showed similar kinetics. I both cases, intracellular RNA levels reached a plateau around d6p.t. The detection of intracellular protein, which was primarily influenced by the stable expression of S-HDAg in Huh7-S cells, resulted in approximately 70% HDAg positive cells in Mock transfected cells (see Fig. 4.1B and C). Similar levels were observed in cells transfected only with agHDV. However, upon transfection with gHDV, this number

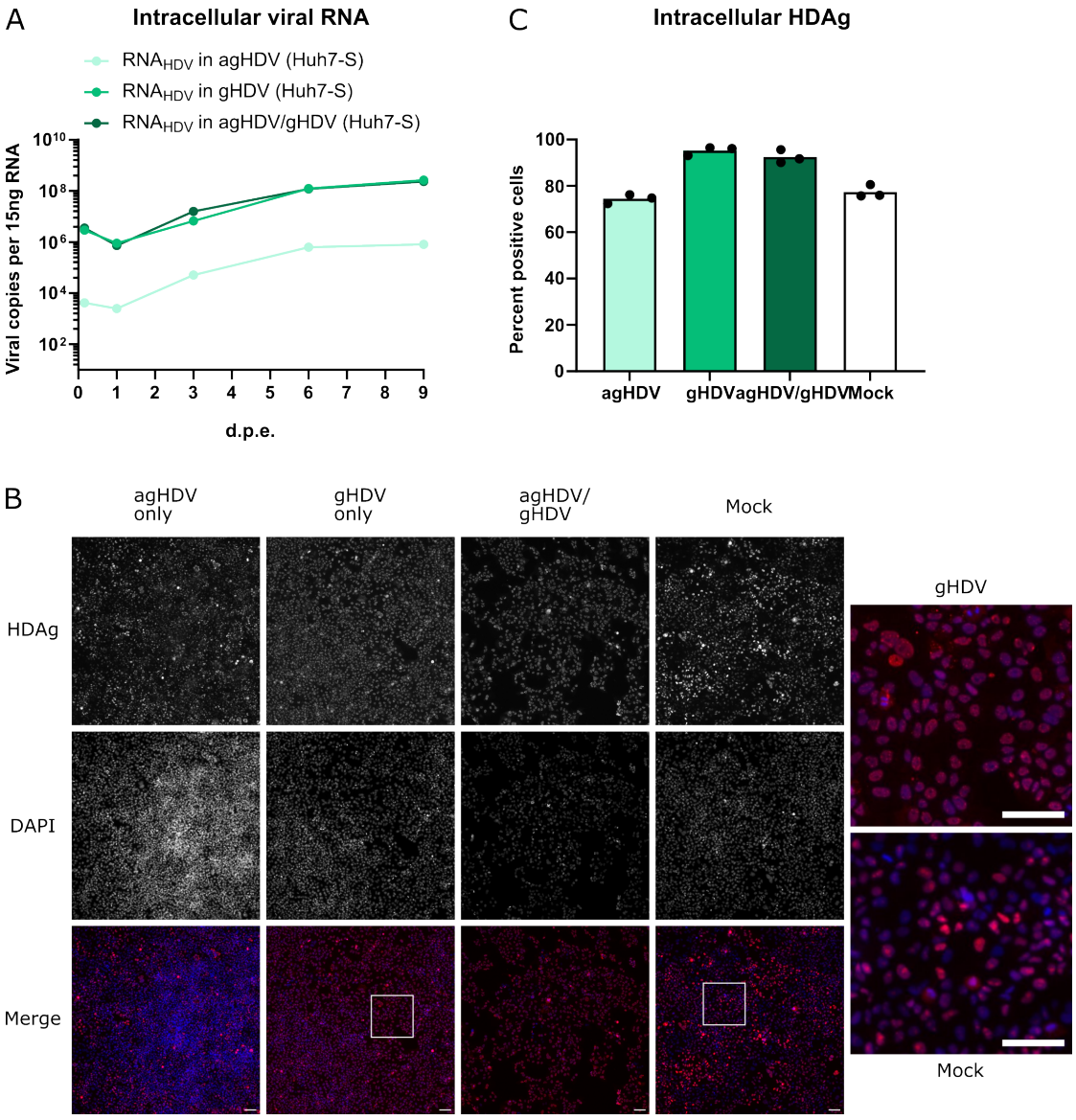

Figure 4.1: Replication of genomic HDV RNA in Huh7 cells.
Huh7-S cells were transfected with 2,5µg *in vitro* transcribed RNA for agHDV, gHDV or agHDV + gHDV. A) Intracellular viral RNA was quantified by RT-qPCR between 4h-d9. B, C) Intracellular HDAg was determined by IF at d3 and quantified. The number of positive cells was determined by analysing the staining of HDAg and DAPI. Dots represent the values of three technical replicates. Scalebar: 100µm, N=1

increased to over 90% of the cells becoming positive for HDAg. Considering the higher viral replication and the similarity of gHDV to the naturally delivered RNA during infection, the following experiments were performed using gHDV transfection.

In a next step, I aimed to investigate the provision of S-HDAg by an mRNA analogue to improve detection of HDAg by IF. Additionally, I investigated co-replication of gHDV and HCV. To focus exclusively on the aspect of replication and potential interference of HDV and HCV at this point of the replication cycle, I made use of a subgenomic HCV replicon lacking the structural proteins (sgHCV) [107].
To measure intracellular viral RNA copies and investigate intracellular viral protein, I used Huh7-wt (co-transfected with S-HDAg mRNA analogue) and Huh7-S cells. The results, as shown in Fig. 4.2, indicate that there is no significant difference in HDV replication between Huh7-wt and Huh7-S cells. The initial drop of HDV RNA copy numbers was more pronounced in Huh7-wt cells, but it did not reach statistical significance. Analysis of intracellular protein expression in Huh7-wt cells confirmed a broad expression of S-HDAg in almost all cells, which is comparable to what has already been observed in Huh7-S cells (see Fig. 4.1). Therefore, S-HDAg mRNA analogue was co-transfected in all following experiments.

Comparing the replication efficiency of sgHCV and gHDV, similar RNA levels could be observed for both viruses in both settings (co-transfection and mono-transfection). Total levels of HCV RNA were slightly lower than for HDV. Analysis of intracellular protein expression of HDAg and HCV NS5A as surrogate for viral replication clearly showed up to 50% HDAg/NS5A positive cells, indicating co-replication in the same cell.

In order to investigate potential envelopment and spread of HDV by HCV envelope proteins, co-transfection of both viral RNAs was repeated using the full length RNA of HCV (flHCV). This RNA encodes for all HCV proteins and is therefore suitable for producing progeny viruses.
Viral replication was assessed by determining intracellular RNA copies, as well as intracellular HDAg and HCV NS5A. As for the subgenomic replicon before, there were no significant differences observed in the replication of both HDV and flHCV. Similarly, HCV RNA levels were slightly lower than HDV RNA levels (see Fig. 4.3A). Analysis of intracellular viral protein expression further confirmed the co-replication of HDV and HCV in the same cell. Both viral proteins, HDAg and NS5A, remained in their respective localisation: HDAg intranuclear and NS5A in the cytoplasm (see Fig. 4.3B). The number of cells showing expression of HDAg or NS5A did not significantly differ between single and co-transfected cells. The number of HDAg/NS5A positive cells was with approximately 20% lower compared to sgHCV/gHDV transfected cells, likely resulted by the lower number of HDAg positive cells (see Figs. 4.3C and 4.2).

Supernatants of transfected cells were harvested, concentrated and subsequently used to inoculate Huh7-CD81-NTCP cells. These cells express the relevant receptors for infection of both HCV and HBV-enveloped HDV and would allow for detection of possible HCV-enveloped HDV. As determined by RT-qPCR at d6p.i., HCV but not HDV RNA could

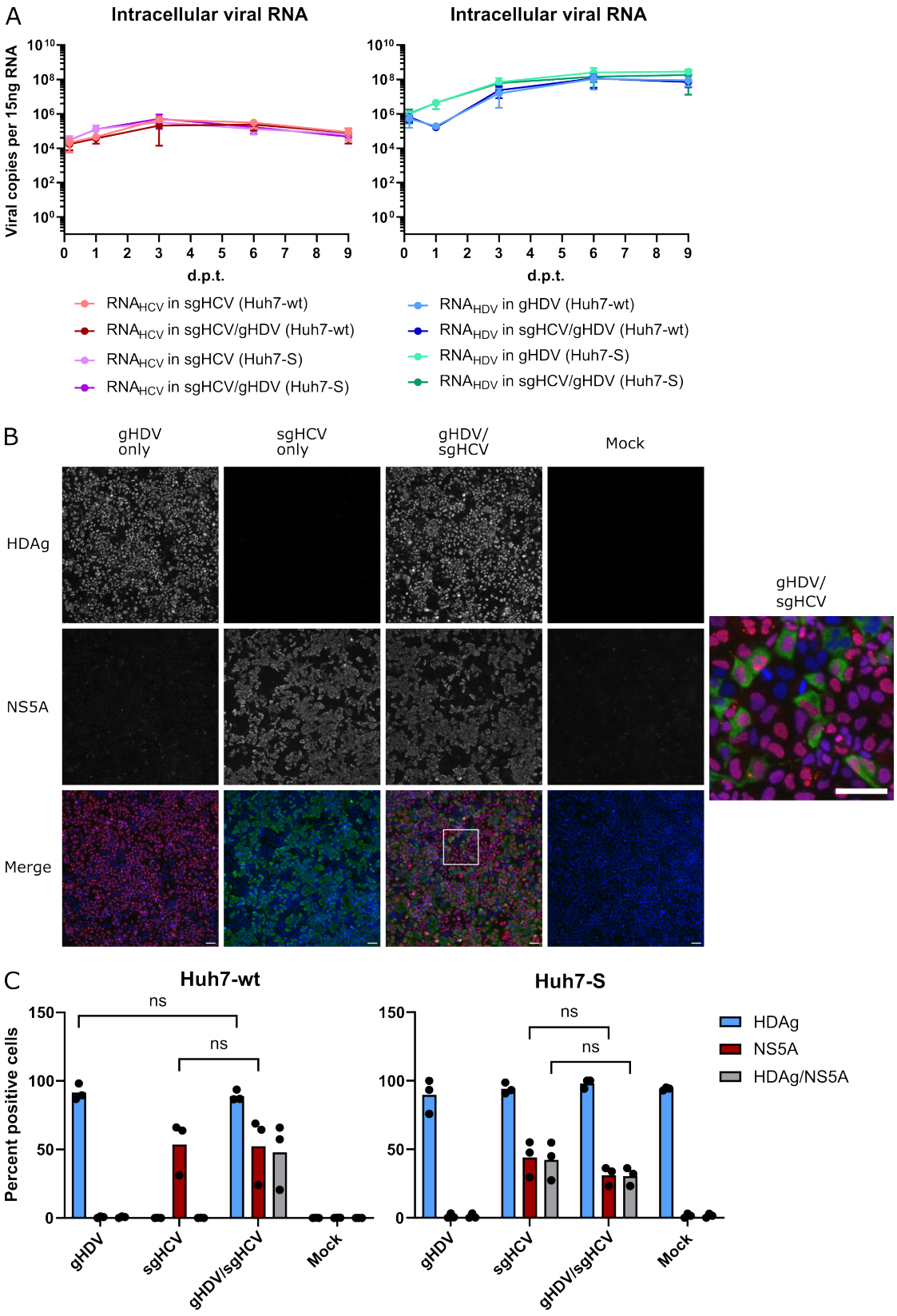

Figure 4.2: Figure legend on the next page

Figure 4.2: Robust subgenomic virus replication in co-transfected cells.
Huh7-wt or Huh7-S cells were transfected with 2,5µg *in vitro* transcribed RNA for sgHCV, gHDV or sgHCV/gHDV. In the case of Huh7-wt cells, gHDV was transfected in combination with 1,5µg S-HDAg mRNA analogue. A) Intracellular viral RNA was quantified by RT-qPCR between 4h-d9p.t. B) Intracellular viral protein (HDAg and NS5A, respectively) was determined by IF at d3 and is representatively shown for Huh7-wt cells. C) Quantification of intracellular viral protein detected in IF. The number of positive cells was determined by analysing the staining of HDAg, HCV NS5A and DAPI. Ordinary two-way ANOVA with Tukey's multiple comparison test, ns = not significant. Scalebar: 100µm, N=3

be detected in these target cells. Additionally, the presence of HDV in the originally transfected cells did not impair the transmission efficiency of HCV (see Fig 4.4).

4.1.2 Establishment of a co-infection system for HDV and HCV

After observing efficient co-replication of HDV and HCV in transfected cells, but no production of HCV-enveloped HDV particles, I aimed for investigating HCV-mediated transmission of HDV in a co-infection system. This system was considered more relevant, as it covers all steps of the viral replication cycle, including entry. In addition, it might provide insights into potential interference mechanisms during early steps of the viral replication cycle.

As shown in Fig. 4.5, HDV and HCV exhibited co-replication after co-infection. Total RNA levels are comparable between both viruses and between mono- and co-infection. Analysis of intracellular HDAg and NS5A revealed 1,9% double infected cells at d6p.i. (see. Fig 4.5B), displaying the characteristic staining pattern of intranuclear HDAg and cytoplasmatic NS5A. Co-localisation of both proteins was not observed, confirming the data obtained from co-transfection experiments (see Fig. 4.3). Interestingly, the percentage of HDAg or NS5A positive cells did not significantly differ between mono- and co-infection. However, the percentage of HDAg/NS5A positive cells after co-infection was significantly lower than expected based on the calculated co-infection coefficient (CIC). The CIC, calculated using the formula described by B. Erbes [44], indicates a potential viral interference during co-infection. The formula for CIC is described as $CIC = \frac{p(HDV/HCV)}{p\exp(HDV/HCV)}$, where p(HDV/HCV) equals the percentage of HDAg/NS5A double positive cells in co-infection and p_{exp}(HDV/HCV) equals percentages of double positive cells estimated from multiplication of HDAg and NS5A single positive cells in single infection. To this end, CIC = 1 would indicate no interference between both viruses, whereas CIC <1 would indicate a co-infection exclusion and CIC >1 a co-infection enhancement. As seen in Fig. 4.5D, CIC <1, indicating a potential viral interference during co-infection.

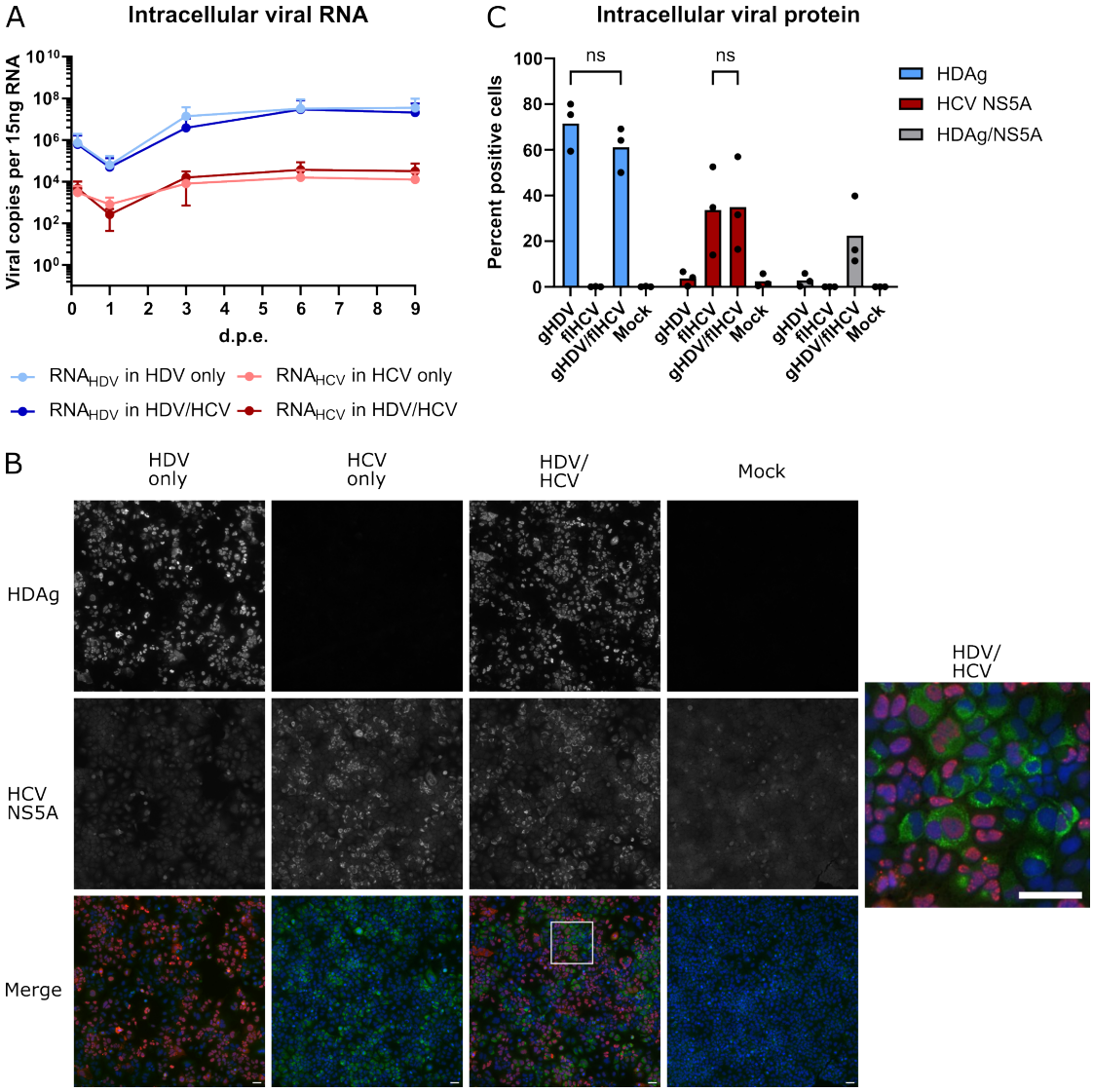

Figure 4.3: Robust co-replication of HDV and HCV in co-transfected cells. Huh7 cells were transfected with 2,5µg *in vitro* transcribed RNA for gHDV/S-HDAg, flHCV or gHDV/S-HDAg+flHCV. The S-HDAg mRNA analogue was transfected at 1,5µg. A) Intracellular viral RNA was detected by RT-qPCR between 4h-d9p.t. and B) intracellular viral protein (HDAg and NS5A, respectively) by IF at d3p.t. Scalebar: 100µm C) Quantification of intracellular viral protein determined by IF at d3. The number of positive cells was determined by analysing the staining for HDAg, HCV NS5A and DAPI. Ordinary two-way ANOVA with Tukey's multiple comparison test: ns = not significant, N=3

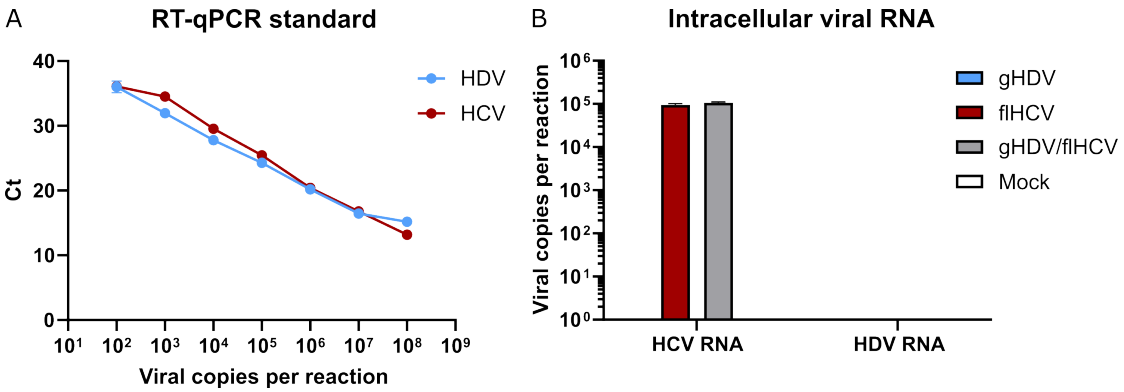

Figure 4.4: No production of infectious HDV particles from co-transfected cells.
Supernatants of co-transfected cells (see Fig. 4.3) were harvested, pooled and concentrated using Amicon Ultra-15 100kDa cutoff filter units. The entire volume was used for infection of Huh7-CD81-NTCP cells. Cells were harvested at d6p.i. and intracellular viral RNA was assessed by RT-qPCR. A) Viral copy number per reaction was determined using a standard curve of *in vitro* transcribed RNA measured in RT-qPCR. B) Viral copy number in infected cells was determined on 15ng RNA input by RT-qPCR using this standard curve. Data of one representative experiment is shown. Error bars indicate the deviation between technical replicates.

In order to check for infectious particles, supernatants harvested from d3-9p.i. were concentrated through Amicon Ultra-15 100k filter units and used to inoculate Huh7-CD81-NTCP cells. Qualitative analysis by IF staining for intracellular production of NS5A and HDAg showed efficient transmission of HCV to new cells (see Fig. 4.6). In contrast, as expected from co-transfection experiments, HDV could not be transmitted, neither from single infection nor from HCV co-infection. Notably, HCV particle production seemed to be unaffected by HDV co-infection, although direct intracellular effects would be difficult to observe due to the low number of co-infected cells compared to HCV only infected ones.

4.1.3 Establishment of a co-transfection system for HDV and other envelope proteins

Perez-Vargas et. al. demonstrated transmission of HDV through several non-HBV envelope proteins, including HCV and VSV-G [150]. As previously mentioned, transmission of HDV by HCV could not be observed, neither after RNA transfection nor viral infection. Nevertheless, the aforementioned publication was initially based on plasmid transfection experiments. To ensure better comparability to published results, experiments in this section were also conducted using plasmid transfection.

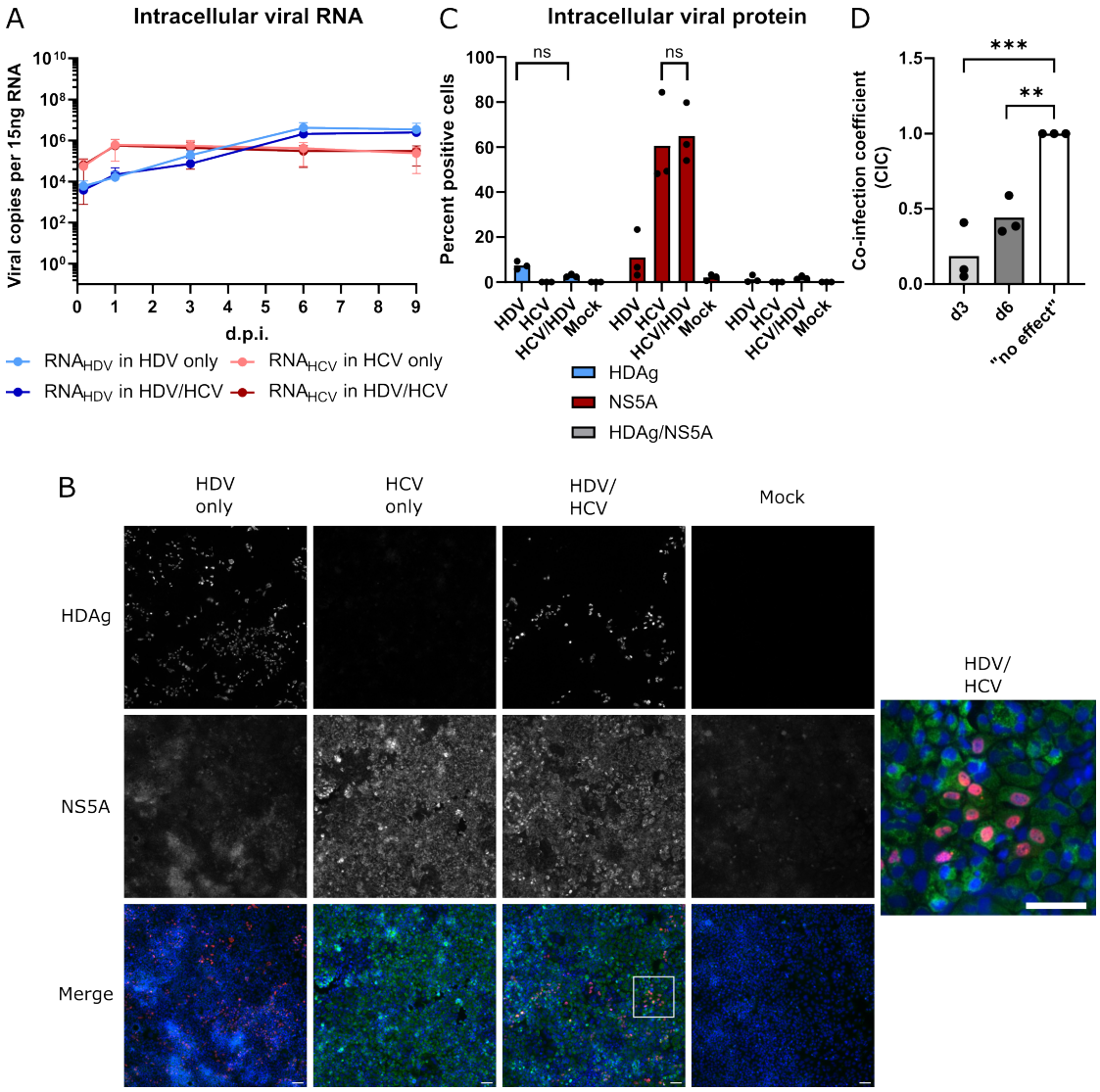

Figure 4.5: Robust co-replication of HDV and HCV in co-infected cells. Huh7 cells were infected with HDV gt1 (enveloped by HBV gtD envelope proteins, MOI10 GE/cell), HCV (Jc1, MOI1) or HDV/HCV (MOI10/1). A) Intracellular viral RNA was quantified by RT-qPCR between 4h-d9p.i. and B) intracellular viral protein (HDAg and NS5A, respectively) by IF at d3 and d6p.i. Images of one representative experiment are shown for d6.p.i. Scalebar: 100µm. Additionally, a zoom in to HDV/HCV co-infected cells is shown. C) Quantification of d6.p.i IF pictures with regard to intracellular HDAg and NS5A; Ordinary two-way ANOVA with Tukey's multiple comparison test: ns = not significant. D) Calculation of co-infection coefficient (CIC) by $CIC = (p(HDV/HCV))/p_{\exp}(HDV/HCV)$, Ordinary one-way ANOVA with Dunnett's multiple comparison test: *** p<0,001; ** p<0,01; N=3

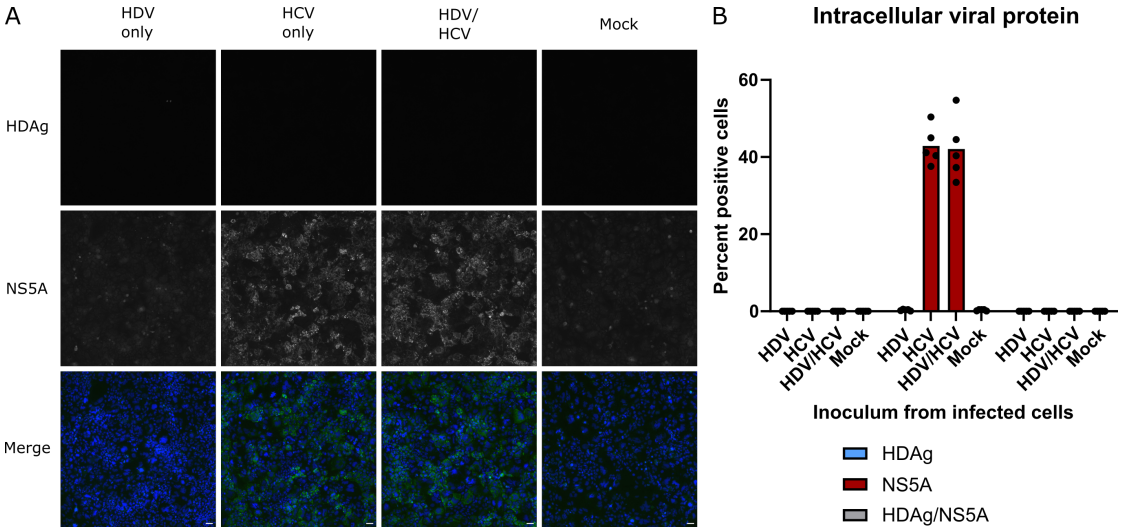

Figure 4.6: No production of infectious HCV enveloped HDV particles after co-infection.
Supernatants from Huh7-CD81-NTCP co-infected cells were harvested between d3-9p.i.and concentrated by Amicon Ultra-15 100k filter units. A) Naïve Huh7-CD81-NTCP cells were inoculated with 50% volume of the concentrated supernatant and analysed for intracellular HDAg and NS5A expression at d6p.i. by IF. Images of one representative experiment are shown and B) quantified. Dots in the graph represent quantification of different areas on the same slide. Scalebar: 100µm

Two different constructs were used to provide HCV envelope proteins: E1E2 (containing both glycoproteins) and C-NS2 (containing core, E1E2, and NS2). The C-NS2 construct has previously been shown to envelop and transmit sgHCV in an HCV-transcomplement system [107]. Co-transfection was performed using the established plasmid for 1,1x overlength HDV antigenome and constructs for envelope proteins of different viruses: HBV (HB2.7), HCV (E1E2 or C-NS2), VSV-G, or GFP as negative control. Due to the high cytotoxicity of VSV-G caused by rapid cellular membrane fusion, co-transfection with VSV-G was performed in a ratio of 1:1 (HDV:VSV-G), while the other constructs were co-transfected in a ratio of 1:4 (HDV:env). Intracellular viral RNA was analysed by RT-qPCR after DNaseI treatment to remove residual plasmid, and intracellular protein (HDAg and HBsAg, E2, or VSV-G) was investigated by IF.

HDV was able to replicate in transfected cells after co-transfection with any of the used envelope proteins or GFP (see Fig. 4.7A). Intracellular staining showed co-expression of HDAg and envelope proteins in the same cells, indicating the prerequisite for envelopment and excretion (see Fig. 4.7B).
Supernatants from transfected cells were harvested, concentrated through PEG-precipitation, and used to inoculate Huh7-CD81-NTCP cells. VSV-G pseudotyped particles use LDL-R as receptor [52], that is widely expressed on different cell types, and therefore do not rely on overexpression of an additional receptor molecule. The transmission efficiency of HDV by different envelope proteins was determined by intracellular HDAg expression as surrogate for established virus replication.

Fig. 4.8 shows intracellular HDAg expression in inoculated cells with supernatants from HDV/HB2.7 and, to a lesser extend, HDV/VSV-G. Although there was a clear tendency towards lower packaging efficiency of HDV by VSV-G compared to HBsAg, the differences did not reach statistical significance. The efficiency in both cases was relatively low, but consistent among replicates. Envelopment of HDV could not be observed by any of the HCV envelope constructs, confirming the data from previous RNA transfection and virus infection experiments.

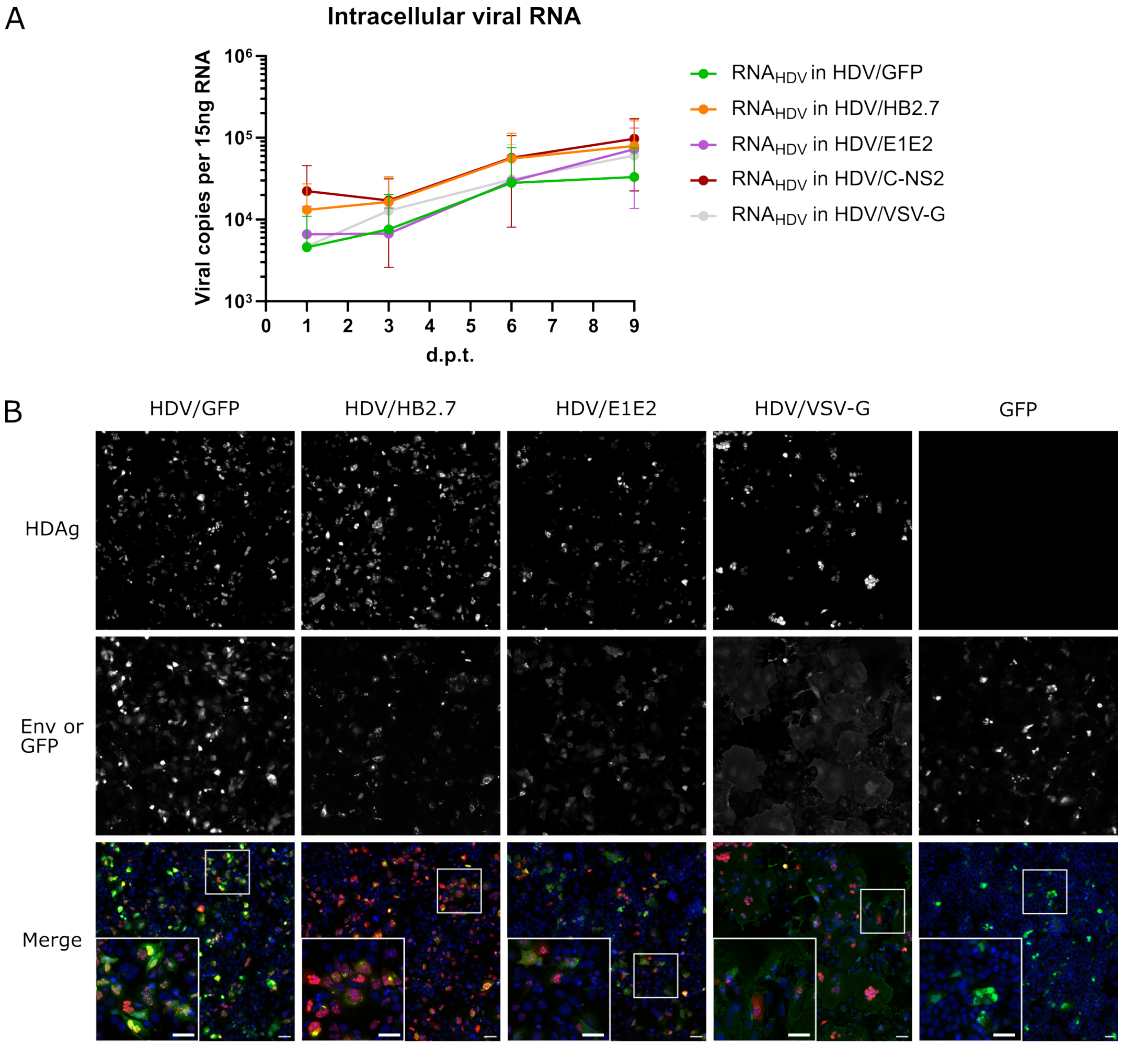

Figure 4.7: Replication of HDV after co-transfection with different envelope proteins.
Huh7-wt cells were transfected with plasmids encoding for the HDV antigenome (HDV) and envelope proteins (env) of different potential helper viruses: HBV (HB2.7), HCV (E1E2 or C-NS2), and VSV (VSV-G). The total amount of plasmid transfected equaled 420ng per 24-well. For HBV and HCV envelope proteins, the ratio between genome and envelope equaled 1:4. VSV-G was co-transfected in a ratio of 1:1 due to high cell toxicity. Cells were analysed for A) intracellular viral genome copies between d1-d9p.t. by RT-qPCR and for B) intracellular viral protein at d3p.t. by IF. As expression of C-NS2 lead to comparable results as E1E2, images are only shown for E1E2. Scalebar: 100µm, N = 3

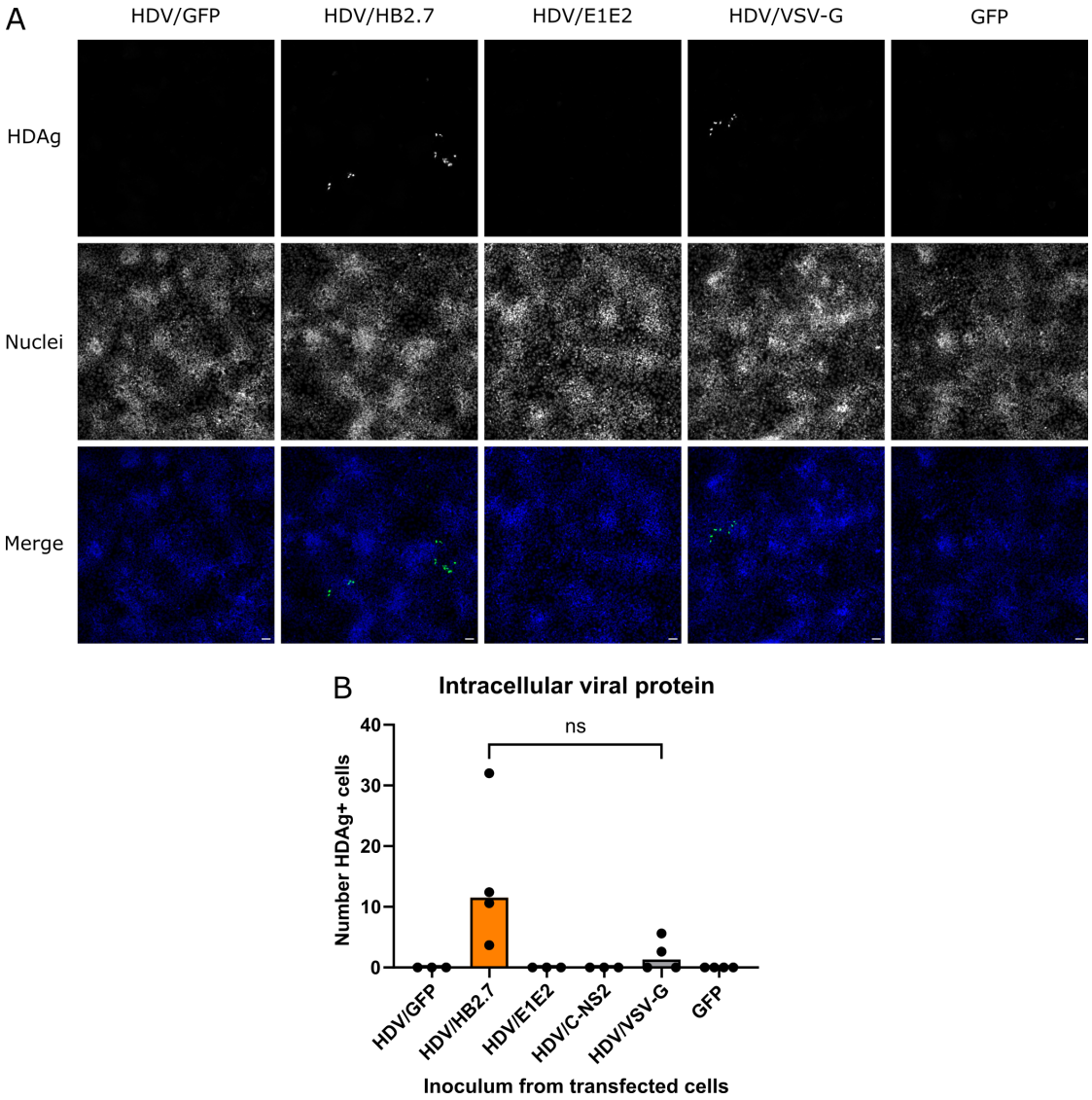

Figure 4.8: VSV-G can mediate HDV transmission with low efficiency. Supernatants of Huh7-wt cells transfected with HDV and different envelope proteins (as described for Fig. 4.7) were harvested, concentrated by PEG-precipitation and used to incoculate Huh7-CD81-NTCP cells. A) Intracellular HDAg was determined at d6p.i. by IF and B) quantified. The number of HDAg positive cells was determined analysing the staining of HDAg and DAPI and is stated per well. Every well was imaged at five different spots to cover almost the entire area. Images of one representative experiment are shown, Scalebar: 100µm, Ordinary one-way ANOVA with Tukey's multiple comparison test, ns=not significant, N=3-4

4.2 Possible reasons why HDV cannot use the envelope of non-HBV viruses

The lacking evidence supporting a transmission of HDV through HCV in the experimental conditions used above suggests the presence of a mechanism, either active or passive, that prevents this process. This section explores and discusses potential factors that might be responsible for inhibiting the utilisation of non-HBV envelope proteins by HDV.

4.2.1 Absence of a super-infection exclusion mechanism in HDV/HCV infected cells

Certain viruses actively prevent infection of an already infected cell by a mechanism called super-infection exclusion. This phenomenon has been observed in various instances, such as HIV [3], but also duck HBV (DHBV) [202] and HCV [195]. Additional evidence suggests, that also the human HBV exhibits a super-infection exclusion, which is dependent on the expression of HBsAg [111].

In order to investigate super-infections of HDV on an established HCV infection and vice versa, Huh7-CD81-NTCP cells were transfected with *in vitro* transcribed RNA for HCV or HDV and subsequently infected with HDV and HCV, respectively at d1p.t. The replication and infection efficiency were assessed by analysing intracellular viral RNA and protein.

Intracellular viral RNA copies of HDV or HCV did not differ between single transfection or infection and the super-infection setting (see Fig. 4.9A). Furthermore, the super-infection coefficient (SIC) was calculated as described for CIC to determine the presence of a super-infection exclusion (see section 4.1.3). To this end, a SIC value of 1 indicates no super-infection exclusion mechanism, while $SIC > 1$ suggests a super-infection exclusion and $SIC < 1$ a super-infection enhancement. This analysis revealed that $SIC \approx 1$, especially for HDV super-infection, indicating that neither HDV nor HCV had a significant influence on super-infection (see Fig. 4.9E).

4.2.2 Dependency of envelopment on L-HDAg

The envelopment of HDV by its natural helper virus HBV relies on the expression and farnesylation of L-HDAg. Once bound to the HDV RNA, L-HDAg localises the RNP to membranes, where HBsAg is expressed. Interaction between HBsAg and L-HDAg is mediated by the so called tryptophan-rich domain (Trp-rich domain, TRD) in the cytosolic loop between transmembrane helices III and IV of HBsAg [110]. This interaction leads to incorporation of the HDV RNP into HBsAg enveloped particles (see section 1.1.3). Interestingly, newly identified Delta-like agents are thought to utilise an HBV-independent

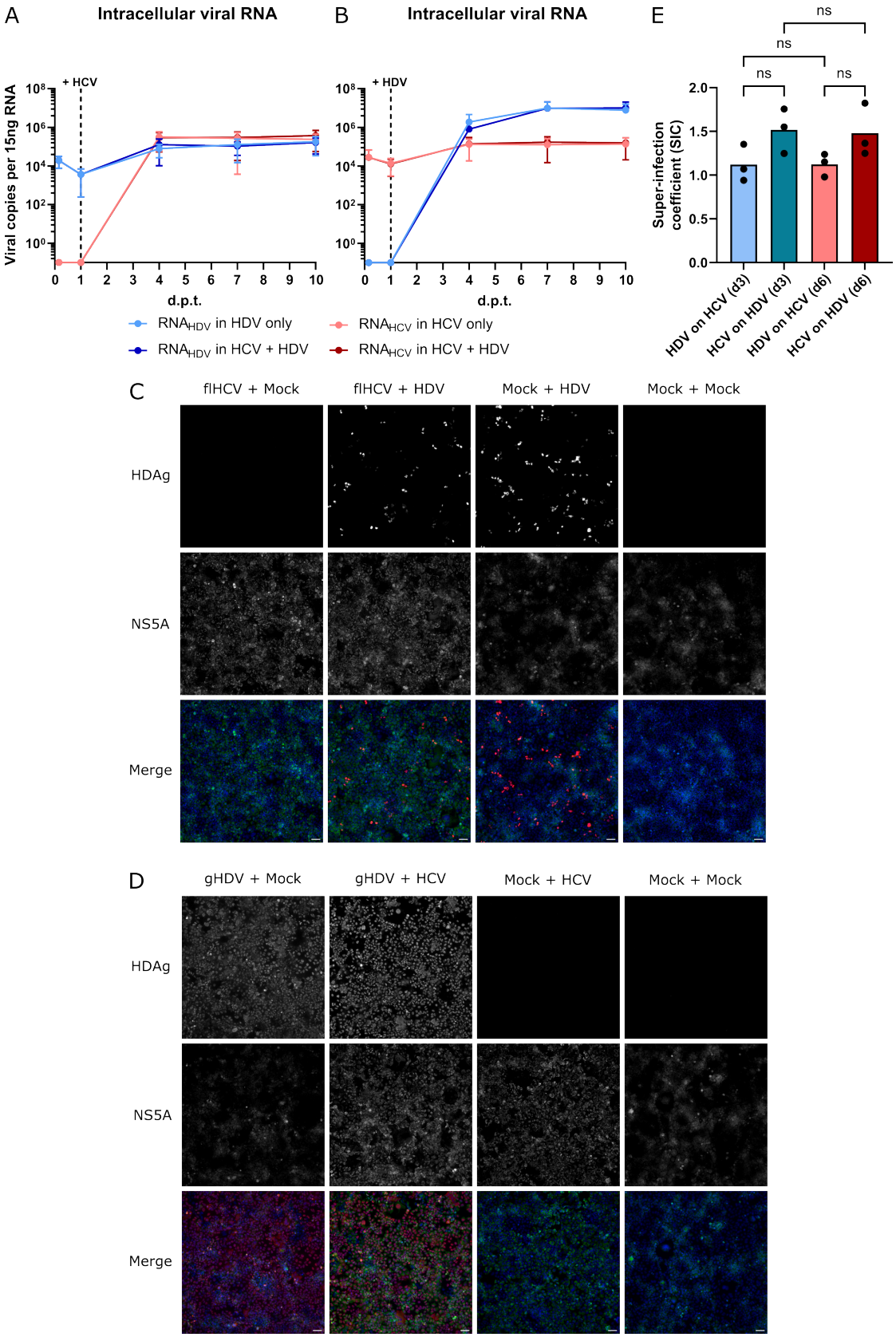

Figure 4.9: Figure legend shown on next page

Figure 4.9: Absence of a super-infection exclusion mechanism for HDV and HCV.
Huh7-CD81-NTCP cells were transfected with 2,5µg *in vitro* transcribed RNA for A, C) flHCV or B, D) gHDV/S-HDAg and subsequently infected with A,C) HDV (MOI10) or B,D) HCV (MOI1). A, B)Intracellular viral RNA was quantified by RT-qPCR between 4h-d10p.t. and C, D) intracellular viral protein detected by IF at d3 and d6p.t. Representative images for d3 are shown and were quantified E) Super-infection coefficient (SIC) was calculated as for CIC (see Fig. 4.5 and described by B. Erbes [44]). Ordinary two-way ANOVA with Tukey's multiple comparison test, ns = not significant. Scalebar: 100µm, N=3

spreading mechanism [24]. Of relevance for my work is the bat Delta-like agent (BHDV), as it has been found in rodents and bats through analysis of NCBI sequence read archives (Stefan Seitz, unpublished data). In both hosts, the same hepacivirus was detected together with BHDV in the same sequencing run, suggesting the possibility that BHDV might have spread from one host to another using the hepacivirus envelope (see section 1.2.3).

In order to investigate potential differences that might allow one Delta-like agent to utilise hepacivirus envelope proteins, while restricting the other virus, I performed sequence alignment of HDV and BHDV nucleotide and protein sequences.
By comparing the sequences of HDV and BHDV ORFs and proteins (see Fig. 4.10), it becomes evident, that they share several similarities, including the length of 645 and 648 nucleotides, respectively. Both possess an amber stop codon (UAG) that can be edited by the cellular deaminase ADAR1. Editing leads to the conversion of guanosine to inosine mediating a mismatch basepairing to tyrosine. This subsequently results in the introduction of an UAA codon in the newly produced genome that encodes for tryptophan instead. In the case of HDV, editing results in elongation of HDAg by 19 amino acids (AA), which is further farnesylated at C211. On the other hand, BHDV HDAg could potentially produce a 20 AA extended protein, that, in contrast to L-HDAg, lacks a cysteine residue for farnesylation.

The absence of a cysteine and farnesylation site in the BHDAg sequence is a clear distinction between the two viruses. The putative HBV-independent transmission might therefore be induced or at least not hindered by the absence of this farnesylation. On the other hand, the human HDV might be forced to use HBV-mediated transmission due to the farnesylated L-HDAg directing the RNP to the site of HBsAg production. Consequently, HCV envelope proteins might not be accessible to HDV carrying a farnesylated L-HDAg, thereby explaining the absence of HCV-enveloped HDV particles. In order to test this hypothesis, I investigated the envelopment efficiency of HDV by HCV in the presence of the farnesyltransferase inhibitor Lonafarnib (LFB) resulting in non-farnesylated HDAg.
Viral replication was assessed by detecting intracellular viral RNA copies in an RNA co-

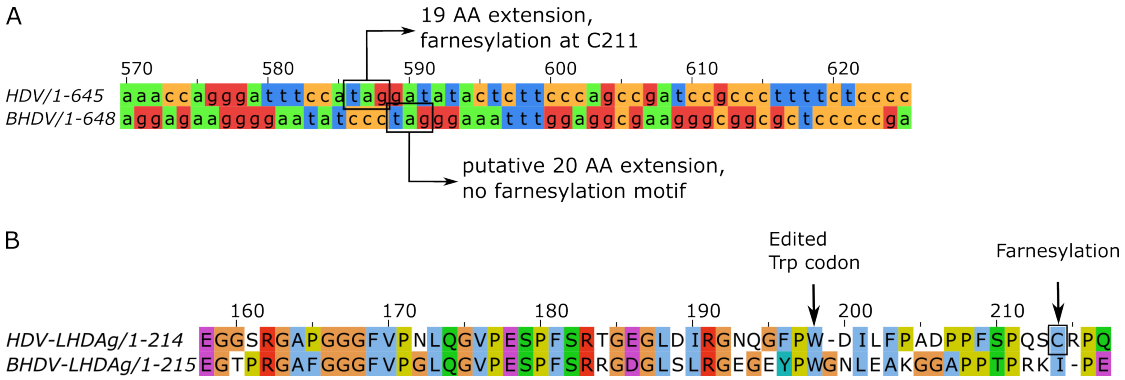

Figure 4.10: HDV and BHDV sequences contain an amber stop codon but proteins differ in farnesylation capacity.
A) Nucleotide sequence comparison of human HDV and BHDV (identified in *Peropteryx macrotis*) reveals presence of an amber stop codon (UAG) that could be edited to a Trp-codon (UAA). In HDV, editing leads to an extension of HDAg by 19 AA. Editing in BHDV might lead to a 20 AA extension. B) Protein alignment of HDV and BHDV L-HDAg was performed using Muscle. Amino acid numbering refers to the positions in the alignment. L-HDAg is farnesylated at the cystein residue C211 mediating its membrane localisation. Putative BHDV L-HDAg does not possess a cystein and therefore lacks the farnesylation motif. The tryptophan resulting from editing in both viruses as well as the farnesylated cystein in L-HDAg are marked with arrows.

transfection setup as described in section 4.1.1. As a positive control, gHDV transfection was performed in Huh7-HB2.7 cells stably expressing HBsAg.

Fig. 4.11 shows robust co-replication of HDV and HCV in both cell lines. Both viruses replicated to similar levels in mono- and co-transfected cells, while LFB treatment did not have an effect neither on replication efficiency nor cell viability. Supernatants of transfected cells were harvested, concentrated on Amicon filter units, and used to inoculate Huh7-CD81-NTCP cells. Determination of intracellular HDAg served as a surrogate for HDV replication in infected cells.

These results clearly demonstrated that HDV transmission occurred only in the presence of HBV envelope proteins under non-treated conditions (see Fig. 4.12). As expected, LFB treatment completely abrogated HDV transmission by HBsAg. Interestingly, HCV transmission appeared to be more efficient under LFB treatment. However, it did not improve transmission of HDV by HCV envelope proteins.

Since inhibiting the farnesylation of L-HDAg did not render HDV susceptible to HCV-mediated transmission, I further investigated the role of L-HDAg itself. It is possible that BHDV does not make use of the genome editing and keeps the small protein version, even though a potential editing site is available. Conversely, the presence of the additional 19 AA in the human L-HDAg might create steric hindrance for the interaction with HCV envelope proteins. By introducing a stop codon that cannot be edited by ADAR1,

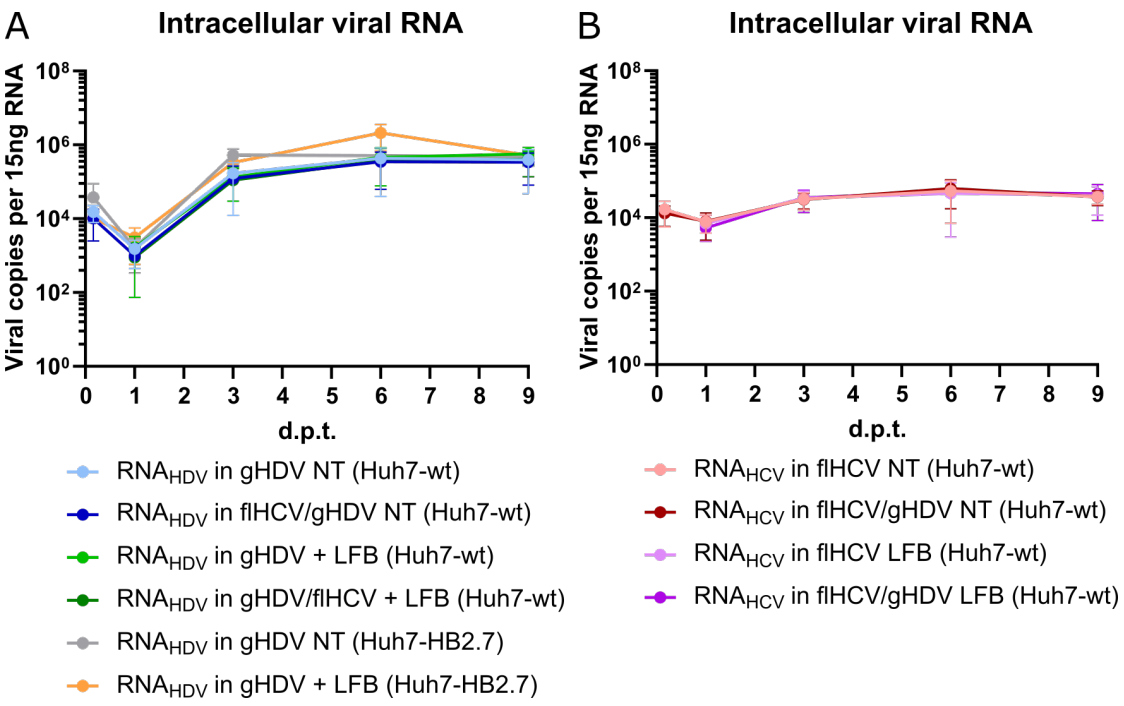

Figure 4.11: HDV is replication competent under Lonafarnib (LFB) treatment.
Huh7-wt cells were transfected with 2,5µg *in vitro* transcribed RNA of gHDV and/or flHCV. Huh7-HB2.7 cells were transfected with gHDV or L(-)gHDV. From 4h after transfection onwards, cells were constantly treated with 500nM Lonafarnib or left untreated. Cells were harvested between 4h-d9p.t. and intracellular viral copy numbers for A) HDV and B) HCV were determined by RT-qPCR. N=3

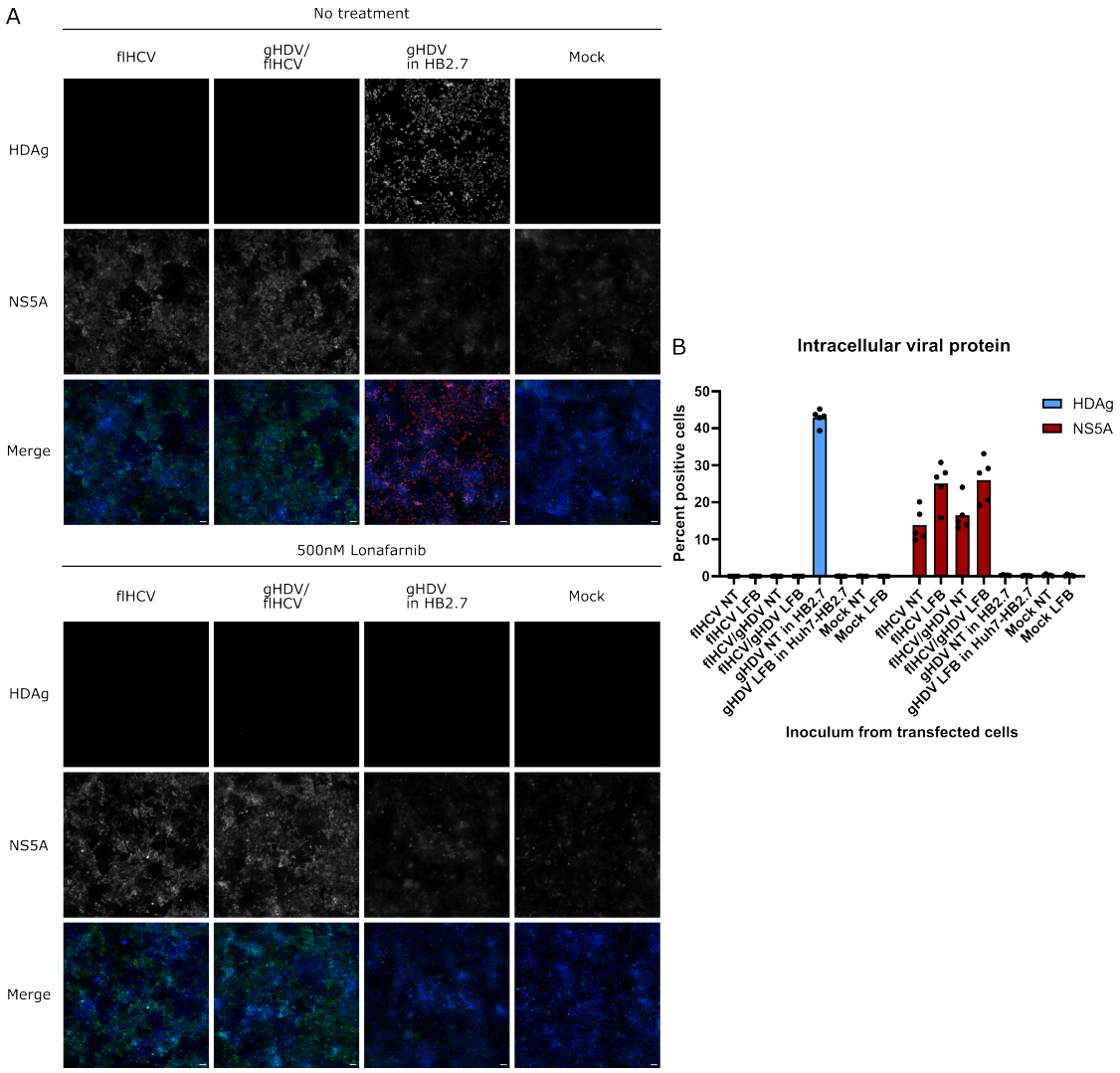

Figure 4.12: HCV does not mediate HDV envelopment under Lonafarnib (LFB) treatment.
Supernatants from transfected Huh7-wt cells were harvested between d3-d9, concentrated on Amicon Ultra-15 100k filter units and used for inoculation of Huh7-CD81-NTCP cells. Cells were harvested at d6p.i. and intracellular viral protein was determined by IF. A) Images and B) quantification of one representative experiment are shown. Dots in the graph represent quantification at different areas on the same slide. Scalebar: 100µm

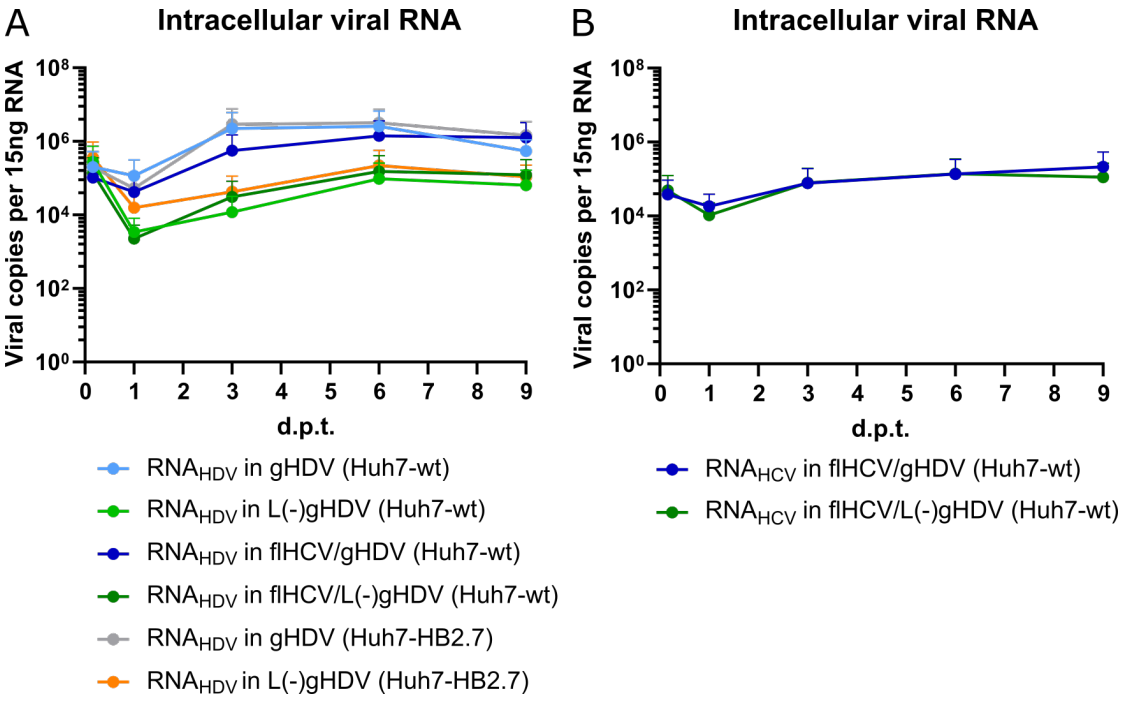

Figure 4.13: HDV with and without L-HDAg is replication competent.
Huh7-wt cells were transfected with 2,5µg *in vitro* transcribed RNA of L(-)gHDV or gHDV alone or together with flHCV. Huh7-HB2.7 cells were transfected with L(-)gHDV or gHDV. Cells were harvested between 4h-d9 p.t. and intracellular viral copy numbers for A) HDV and B) HCV were determined by RT-qPCR. N=3

the production of L-HDAg can be inhibited in the human HDV. Using this mutant in RNA transfection together with flHCV, I investigated its envelopment by HCV envelope proteins, while transfection into Huh7-HB2.7 cells served as positive control.
The mutant virus replicated in Huh7-wt and Huh7-HB2.7 cells, with slightly lower levels of total viral RNA compared to the wildtype virus. Intracellular HDV and HCV RNA levels did not differ between mono- and co-transfection settings, as for the wildtype virus (see Fig. 4.13). After concentrating the harvested supernatants, Huh7-CD81-NTCP cells were inoculated and intracellular HDAg was determined at d6p.i. (see Fig. 4.14). As expected, gHDV showed efficient transmission with HBsAg, whereas transmission was blocked for L(-)gHDV. HCV could be transmitted to new target cells in the same efficiency while gHDV or L(-)gHDV were present. In contrast, transmission of HDV by HCV was not observed, neither for L(-)gHDV nor the wildtype virus.

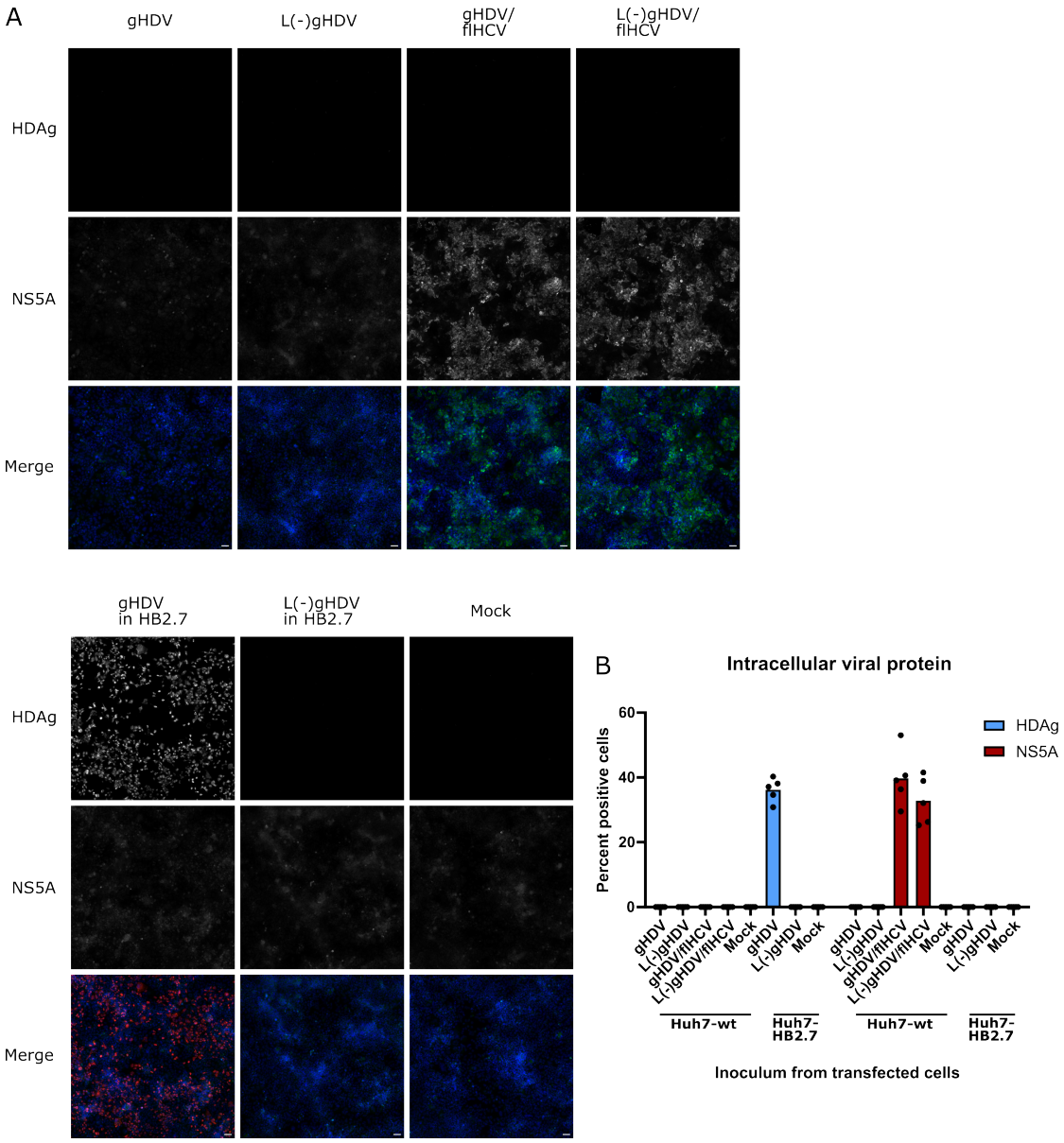

Figure 4.14: Only HBV envelope proteins render HDV particles infectious. Huh7-wt and Huh7-HB2.7 cells were transfected as described for Fig. 4.13. Supernatants were harvested between d3-9p.t., concentrated by Amicon Ultra15-100k filter units and used to inoculate Huh7-CD81-NTCP cells. Cells were harvested for IF at d6 p.i. A) Images and B) quantification of one representative experiment are shown. Dots in the graph represent quantification of different areas on the same slide. Scale bar: 100µm

4.2.3 Investigating the envelopment potential through protein interaction using structure comparison

As inhibiting the farnesyltransferase or deleting L-HDAg did not mediate transmission of human HDV by HCV envelope proteins, I employed AlphaFold2 protein structure prediction to investigate, whether sites required for HDV packaging in the HBV envelope proteins are present and accessible in non-HBV envelope proteins.

The envelopment of HDV by HBsAg is mediated by interaction of L-HDAg and the TRD in HBsAg. As described in section 1.1.3, the TRD is located between transmembrane helix III and IV, thereby facing the particle inner side. Residues 196, 199, and 201 are the tryptophan residues required for envelopment of HDV [92]. The predicted structures of HCV E1E2 and VSV-G (see Fig. 4.15) were analysed to determine the presence and accumulation of tryptophan residues (shown in red) that could form a TRD. Furthermore, accessibility of potential tryptophan residues was assessed by investigating the localisation of transmembrane domains (shown in orange) to estimate whether tryptophan residues are on the inner or outer side of the particle. The predicted structure of HBsAg served as control for comparisons.

Both HCV E1E2 and VSV-G possess single tryptophan residues in the protein sequence. Accumulation of at least two tryptophan residues was observed for both proteins (marked with arrows). E2 has three tryptophan residues in close proximity, while VSV-G has two. Transmembrane domains in E1E2 are localised at the last AA of E1 and E2 [31, 36], and for VSV-G in the C-terminal end at positions 465-490 [30]. All three proteins possess a single transmembrane domain as membrane anchor, while the major part of the protein locates on the particle outer side. The observed accumulations of tryptophan residues in E1E2 and VSV-G are situated within or near the described transmembrane domain on the outer side of the particle, indicating that they are likely not accessible. In contrast, the TRD in HBsAg is located between transmembrane domains and on the particle inner side rendering it accessible for interaction with L-HDAg.
Due to the distinct origin of these proteins, performing a sequence alignment was not feasible. However, comparing the local amino acid sequences around the potential TRDs (see Fig. 4.15C) did not reveal a re-occurring motif in all three proteins that could indicate an interaction despite the lack of an accessible TRD.

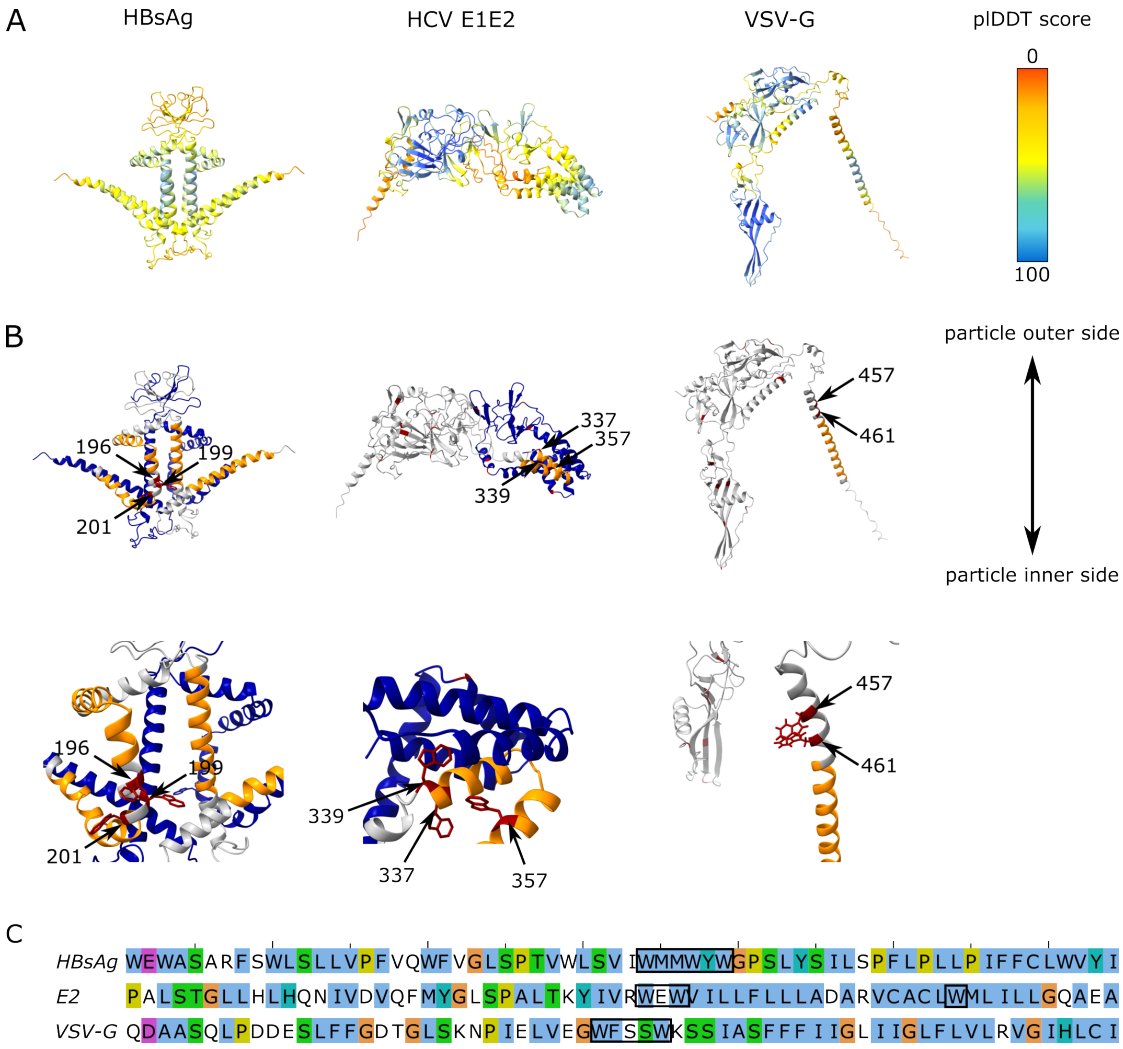

Figure 4.15: Protein structure analysis of HBsAg, HCV E1E2 (Jc1) and VSV-G suggests accessible tryptophan enrichment only for HBsAg.
Structure prediction was performed using AlphaFold2. A) shows the prediction confidence using the plDDT score. B) HBsAg is known to form homodimers, with single proteins of each monomer coloured in either grey or blue. E1E2 form heterodimers showing E1 in blue and E2 in grey. VSV-G is a monomer and coloured in grey. Transmembrane domains are shown in orange and tryptophan residues in red. In case of HBsAg, transmembrane domains and Trp residues are coloured for one monomer only for better visibility. Each HBsAg monomer possesses four transmembrane domains, the Trp residues mediating HDV envelopment (Trp 196, 199, 201) are located between domains III and IV and marked with arrows. HCV E1, E2 and VSV-G possess only one transmembrane domain that anchors the proteins on the outer side of the virus particle. Accumulating tryptophan residues are marked with arrows. The upper row shows the entire proteins and the lower row a zoom in to the potential tryptophan rich domains. Views were rotated if necessary for better visibility of tryptophan residues. C) shows a comparison of un-aligned sequences surrounding potential tryptophan rich domains. Black boxes indicate tryptophan enrichments.

4.3 Envelopment of HDV by non-human hepadnaviruses

4.3.1 Sequence comparison of S-ORFs

In recent years, several non-human hepadnaviruses have been identified, some of which share significant sequence similarities with HBV (see section 1.2.1). These non-human hepadnaviruses might also have the potential to provide an envelope for HDV, as demonstrated in the animal model of the woodchuck hepatitis virus (WHV) [141]. In order to investigate the helper potential for other non-human hepadnaviruses, I performed S-ORF sequence alignment of several viruses retrieved from NCBI sequence read archives (sequences obtained from Stefan Seitz, unpublished data). The alignment included representatives from all hepadnavirus genera. A phylogenetic tree highlighting the investigated viruses is shown in section 1.2.1, Fig. 1.8. A brief overview of the virus name, its genus and host species is given in table 4.1 .

Table 4.1: Investigated hepadnaviruses

Virus name	**Genus**	**Host species**
HBV	Orthohepadnavirus	human
RRHBV	Orthohepadnavirus	rice rat
WHV	Orthohepadnavirus	woodchuck
AMDV	Metahepadnavirus	astatotilapia
BgHBV	Metahepadnavirus	bluegill
TMDV	Metahepadnavirus	mexican tetra
CSKV	Parahepadnavirus	coho salmon
DHBV	Avihepadnavirus	duck
HeHBV	Avihepadnavirus	heron
SkHBV	Herpetohepadnavirus	skink
SLHBV	Herpetohepadnavirus	spiny lizard
TFHBV	Herpetohepadnavirus	tibetan frog

A partial sequence alignment focusing on the TRD is shown in Fig. 4.16, the entire alignment is shown in the appendix in Fig. 4.17. In both figures, it could be observed that several animal hepadnaviruses belonging to the clades of Orthohepadnaviruses (RRHBV,

WHV) and Metahepadnaviruses (AMDV, BgHBV, TMDV) possess an accumulation of tryptophan residues in the same region as HBV. In contrast, viruses belonging to the clades of Parahepadnaviruses (CSKV), Avihepadnaviruses (DHBV, HeHBV), or Herpetohepadnaviruses (SkHBV, SLHBV, TFHBV) do not possess a conserved TRD. The structure prediction by AlphaFold2 (see Fig. 4.18) revealed similar structures for most viruses within the same clade, except for BgHBV, which belongs to the clade of Metahepadnaviruses, but shows a very different structure compared to AMDV or TMDV.
In addition, viruses carrying an extended a-determinant (Orthohepadnaviruses and Metahepadnaviruses) exhibit a profound loop structure on the outer side of the particle. Of note, the local distance difference test score as a measurement for prediction confidence indicated intermediate to low overall confidence.
The presence and orientation of tryptophans in the identified TRD, similar to the HBV S protein, suggests that envelopment of HDV by animal hepadnaviruses possessing a TRD (HBV, RRHBV, WHV, AMDV, BgHBV, TMDV) might be possible.

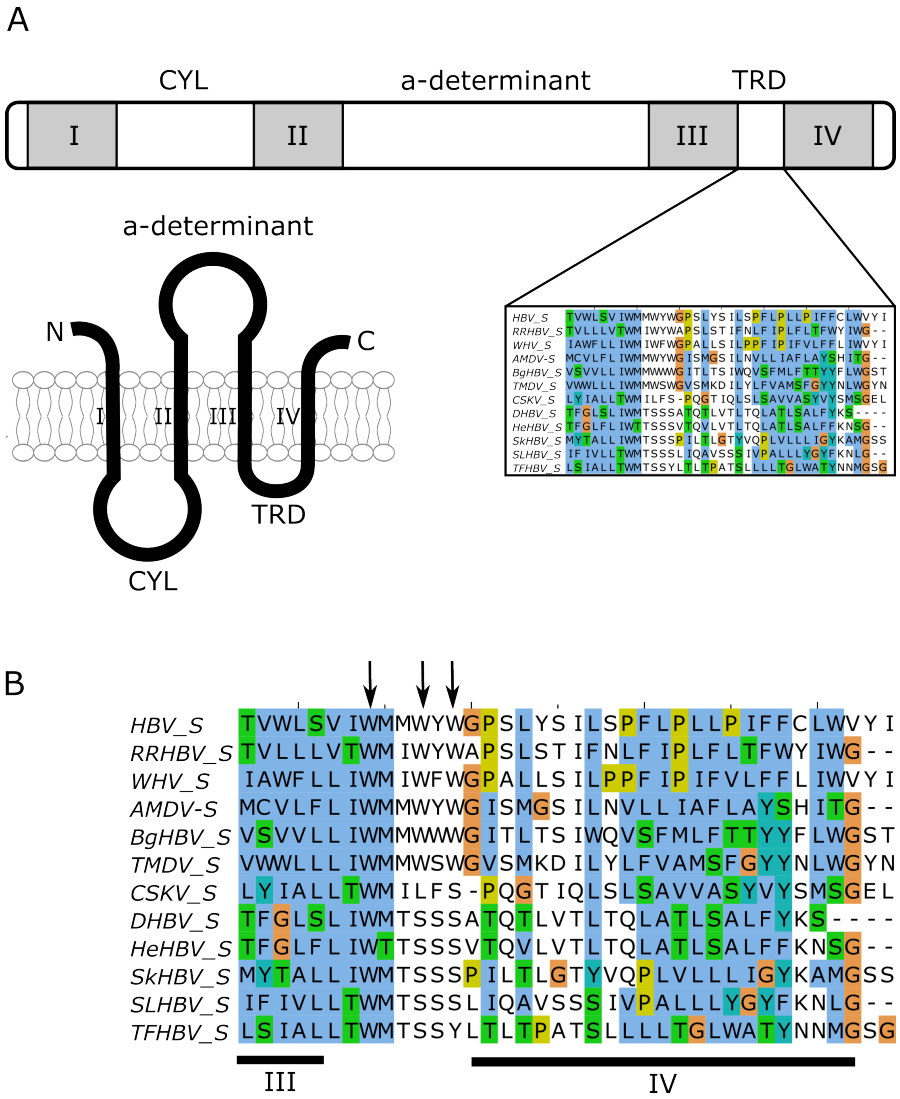

Figure 4.16: Partial Sequence alignment of selected hepadnavirus S-ORFs (tryptophan-rich domain).
A) depicts the topology of the HBV S protein as proposed in literature [110]. Marked with Roman numbers are the transmembrane domains I-IV. In addition, the cytosolic loop (CYL), the a-determinant and the tryptophan rich domain (TRD) are indicated. B) shows a section of the sequence alignment of selected hepadnavirus S-ORFs. Sequences were aligned using Muscle, and amino acids were colored using the Clustal color scheme. Tryptophan residues essential for human HBsAg-HDAg interaction are marked with arrows. These residues are conserved in Metahepadnaviruses (BgHBV, AMDV, TMDV) and Orthohepadnaviruses (RRHBV, HBV, WHV) but not Parahepadnaviruses (CSKV), Avihepadnaviruses (DHBV, HeHBV) and Herpetohepadnaviruses (SkHBV, SLHBV, TFHBV). Host species: BgHBV=bluegill; AMDV=astatotilapia; TMDV=mexican tetra; RRHBV=rice rat; HBV=human; WHV=woodchuck; CSKV=coho salmon; TFHBV=tibetan frog; SLHBV=spiny lizard; SkHBV=skink; DHBV=duck; HeHBV=heron

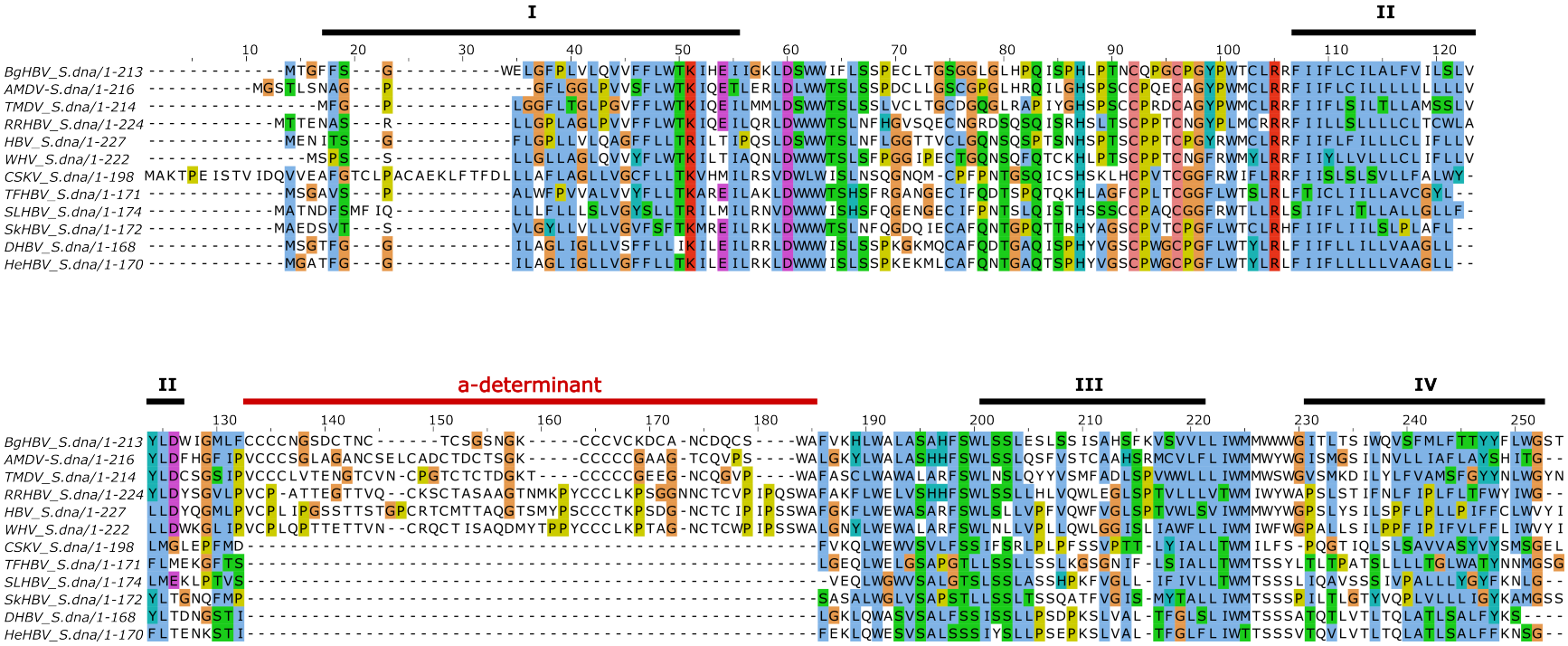

Figure 4.17: Sequence alignment of hepadnaviral S protein. Sequence alignment was performed using Muscle, and amino acids were colored using the Clustal color scheme. Numbers above the sequences refer to the alignment. Transmembrane domains of HBV are marked with black bars, the a-determinant is marked with a red bar.

4.3.2 Production of tagged SVPs

To investigate the capacity of these animal hepadnaviruses to envelop HDV, I first aimed for SVP production. To achieve this, the S-ORFs were cloned into pcDNA3.1 vectors for transfection into mammalian cells. Previous research has demonstrated that HDV can be packaged into self-assembling particles composed solely of the HBV S protein [180]. Additionally, it has been observed that overexpression of the L protein can inhibit the secretion of SVPs [151]. Therefore, the cloned constructs exclusively contained the S protein. In addition, an HA-tag was introduced at either the N- or C-terminus to facilitate the detection of expressed proteins. Subsequently, plasmids were transfected into Huh7-wt cells, and the intracellular production of tagged constructs was investigated by western blot and IF (see Figs. 4.19, 4.20 & 4.21). Negative controls included the transfection of untagged GFP and no transfection (No TF).

Tagged S proteins of all selected hepadnavirus were detected intracellularly (see Figs. 4.19, 4.20 & 4.21). However, there were differences in the expression level, depending also on the tag position. For Orthohepadnaviruses (HBV, RRHBV, WHV), successful protein expression detected by western blot was only achieved with the N-terminally tagged version. Additionally, HBV and RRHBV exhibited the expected double band pattern corresponding to the glycosylated and non-glycosylated form of S. In contrast, for other genera, the tag position did not seem to significantly impact protein expression. However, there were differences in band intensity, such in the case of TFHBV, where the C-terminal tag resulted in notably higher expression levels compared to the N-terminally tagged S. For DHBV and TFHBV, an additional band was observed when the C-terminal tag was used. Protein expression of BgHBV was too low to be detected by western blot, but HA-specific signal could be detected through IF (see Fig. 4.20 & 4.21). Interestingly, C-terminally tagged Orthohepadnavirus S proteins also became visible in IF. The IF staining for HA tag revealed a widely dispersed cytoplasmic localisation with certain areas within the cell exhibiting a higher signal intensity.

Following the confirmation of expression for all constructs, I aimed for detection of secreted particles. To achieve this, supernatants were harvested and concentrated using PEG-precipitation. The concentrated supernatants were then subjected to western blot analysis to determine the presence of tagged S proteins. Fig. 4.22 illustrates that particles were secreted for Ortho-, Avi- and Herpetohepadnaviruses. As expected, HBV and WHV particles were only detected when N-terminal tagging was employed. RRHBV was detected in both the N- and C-terminally tagged versions. Avihepadnaviruses exhibited an HA-specific signal for both N- and C-terminally tagged proteins as well. It is worth noting that for this genus, the N-terminally tagged protein was detected at a slightly smaller size compared to the C-terminally tagged version. Interestingly, both versions appeared at a comparable size intracellularly. Herpetohepadnaviruses (SkHBV, SLHBV, TFHBV) were exclusively secreted with a C-terminal tag. A faint band was observed for TMDV S in the C-terminally tagged version, but not for any other Metahepadnavirus or CSKV as Parahepadnavirus.

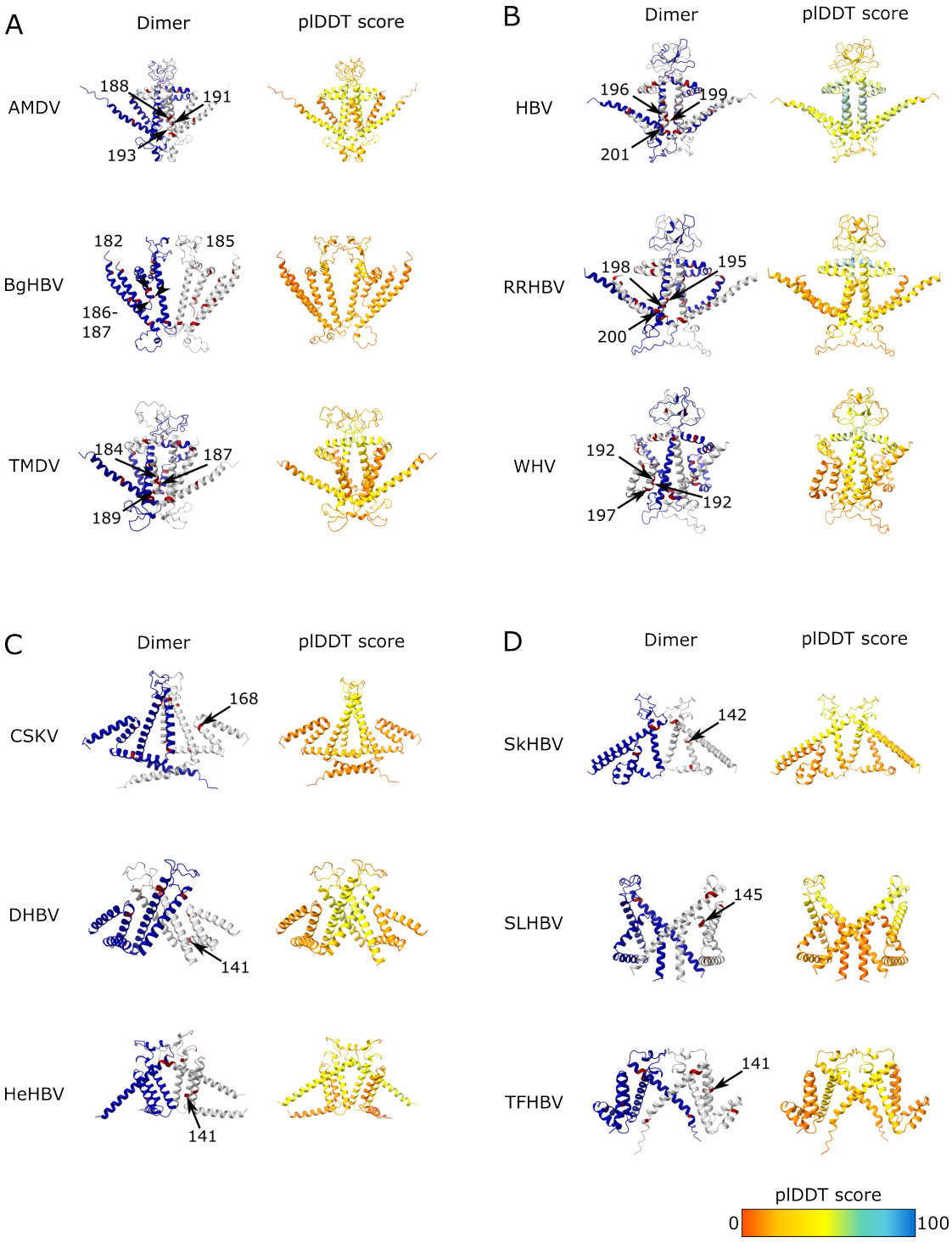

Figure 4.18: Legend shown on next page

Figure 4.18: Structure prediction of selected hepadnavirus S protein dimers. Structure prediction was performed using the AlphaFold2 algorithm. Structures of the S dimer are shown for A) Orthohepadnaviruses, B) Metahepadnaviruses, C) Para- and Avihepadnaviruses and D) Herpetohepadnaviruses. The left structure shows each monomer in blue and grey, respectively, and tryptophan residues in red. Residues being part of a potential TRD are marked with arrows. The right column shows structures colored according to the local distance difference test (plDDT) indicating the confidence of the predicted areas. The color scale runs from red (very low confidence) to blue (very high confidence).

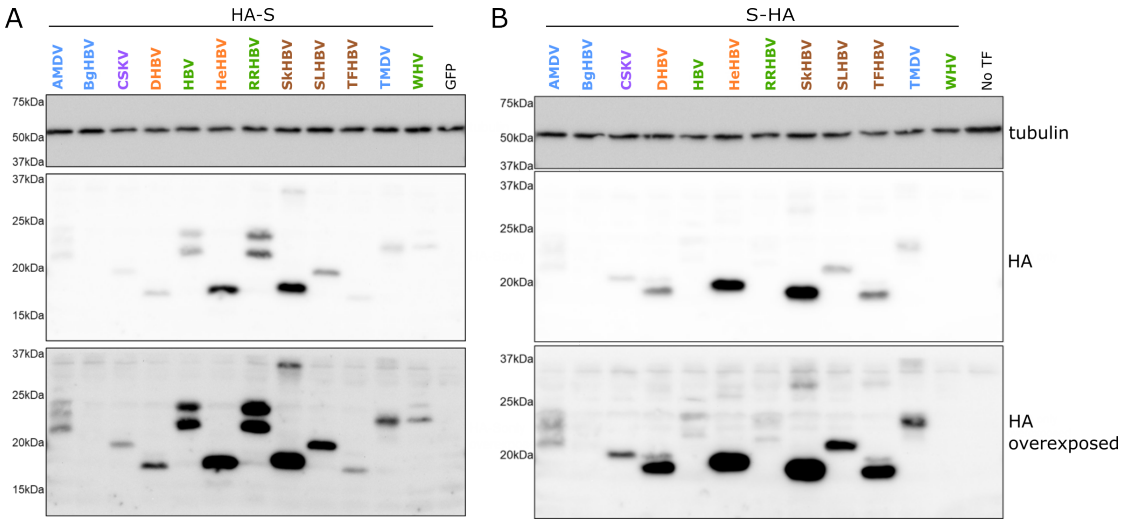

Figure 4.19: Intracellular production of hepadnaviral HA-tagged S-ORFs (western blot).
Huh7-wt cells were transiently transfected with constructs (500ng plasmid per 24-well) of various hepadnaviral S-ORFs carrying an HA-tag on their A) N-terminus (HA-S) or B) C-terminus (S-HA). Expression of tagged constructs was determined by western blot at d4p.t. The color scheme corresponds to the different genera: blue = Metahepadnavirus, green = Orthohepadnavirus, orange = Avihepadnavirus, brown = Herpetohepadnavirus, purple = Parahepadnavirus. N=1

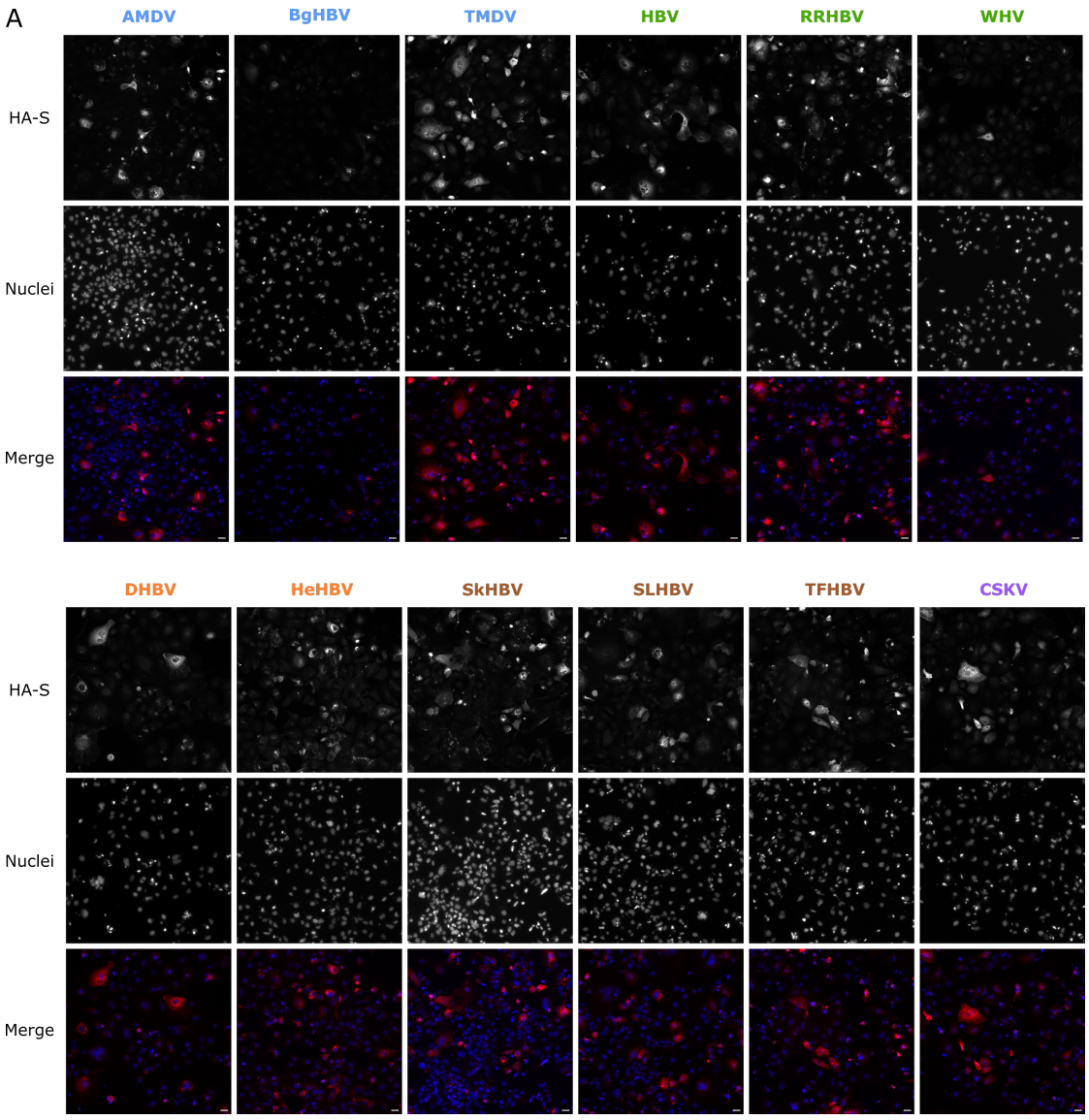

Figure 4.20: Intracellular production of hepadnaviral HA-tagged S-ORFs (IF, HA-S).
Huh7-wt cells were transiently transfected with constructs of selected hepadnaviral HA-tagged S-ORFs as described for Fig. 4.19. Expression of N-terminally tagged constructs was determined by IF at d4p.t. The color scheme corresponds to the different genera: blue = Metahepadnavirus, green = Orthohepadnavirus, orange = Avihepadnavirus, brown = Herpetohepadnavirus, purple = Parahepadnavirus. Scalebar: 100µm, N=1

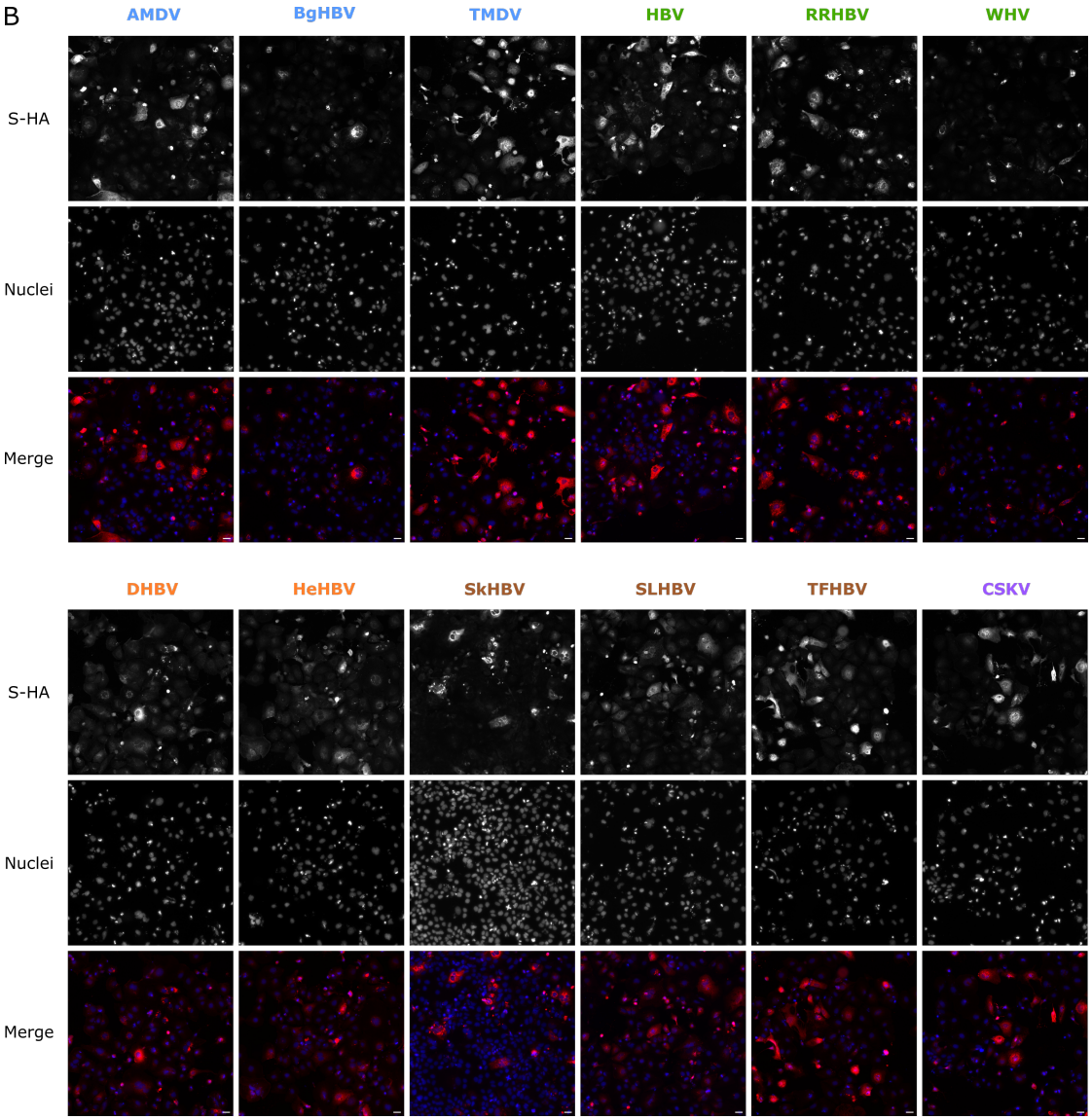

Figure 4.21: Intracellular production of hepadnaviral HA-tagged S-ORFs (IF, S-HA).
Huh7-wt cells were transiently transfected with constructs of selected hepadnaviral HA-tagged S-ORFs as described for Fig. 4.19. Expression of C-terminally tagged constructs was determined by IF at d4p.t. The color scheme corresponds to the different genera: blue = Metahepadnavirus, green = Orthohepadnavirus, orange = Avihepadnavirus, brown = Herpetohepadnavirus, purple = Parahepadnavirus.Scalebar: 100µm, N=1

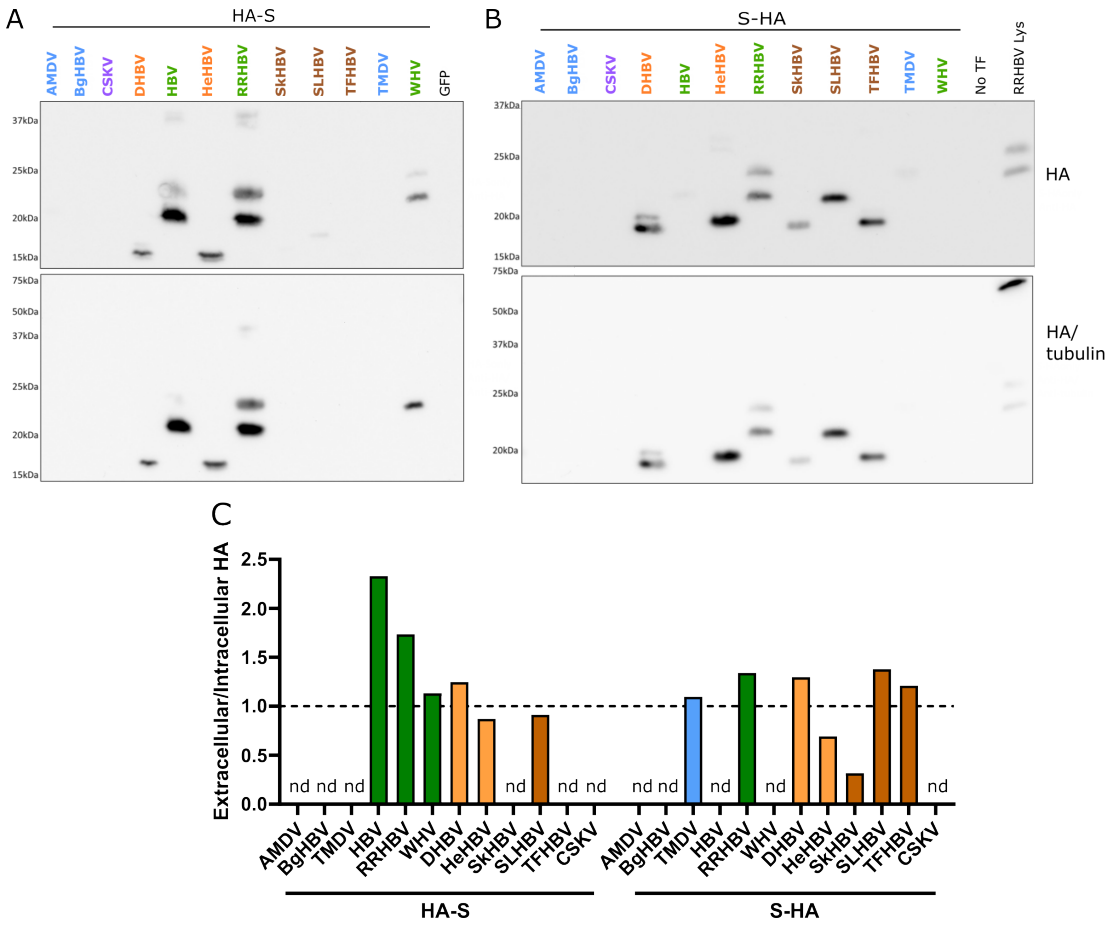

Figure 4.22: Tagged hepadnaviral SVPs do only get secreted for certain genera.

Supernatants from Huh7-wt transfected cells were harvested between d1-d11p.t. and concentrated using PEG-precipitation. The presence of extracellular HA-tagged constructs was determined by western blot. A) displays N-terminally tagged and B) C-terminally tagged constructs. As a positive control, the lysate of RRHBV-HA-Sonly was included on the gel. C) presents the ratio of extracellular to intracellular HA signal (based on the band with highest intensity if more than one band is observed). The dashed line represents a ratio of 1 indicating similar band intensity intra- and extracellular. If no signal was detected either extracellularly or intracellularly, no ratio was calculated, and bars were indicated with nd (not determined). The color scheme corresponds to the different genera: blue = Metahepadnavirus, green = Orthohepadnavirus, orange = Avihepadnavirus, brown = Herpetohepadnavirus, purple = Parahepadnavirus. N=1

4.3.3 Envelopment of HDV by hepadnaviral SVPs

Although not all tagged constructs were secreted, their untagged versions might still be able to provide helper function for HDV. This hypothesis can be tested by measuring levels of extracellular HDV RNA or HDAg after transfection even in the absence of antibodies specifically detecting untagged S protein. Therefore, I aimed for a pilot experiment investigating the envelopment capacity of these hepadnaviral S proteins (see Fig. 4.23). Huh7-wt cells were co-transfected with plasmids encoding the 1,1x HDV antigenome and untagged S protein of hepadnaviruses. Supernatants were harvested, concentrated by PEG-precipitation, and subjected to RNA isolation. The presence of HDV genome copies was detected by RT-qPCR. As a negative control to account for the assay background due to residual plasmid, HDV and GFP were co-transfected.

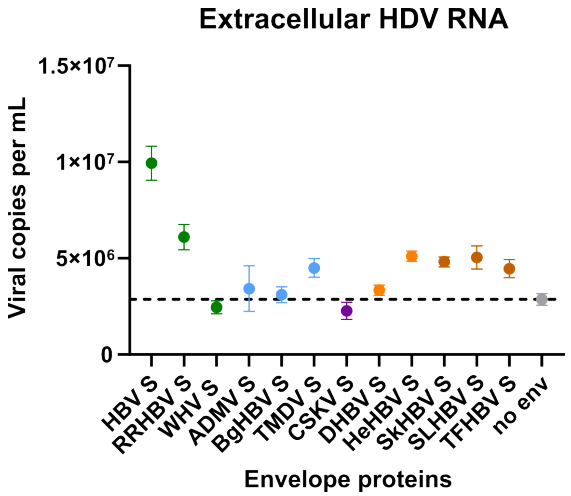

Figure 4.23: Potential envelopment of HDV by hepadnavirus envelope proteins. Huh7-wt cells were co-transfected with plasmids encoding for HDV and untagged hepadnaviral S-ORFs. The total amount of delivered DNA equaled 420ng per 24-well. Supernatants were harvested between d1-11p.t., concentrated by PEG-precipitation and further subjected to RNA isolation. Extracellular HDV RNA copies were determined using RT-qPCR. The dotted line represents the non-enveloped control of HDV/GFP transfection. Error bars indicate variation between three technical replicates. N=1

Fig. 4.23 illustrates that HBV and, to a lesser extent, RRHBV S could potentially envelop and secrete HDV, as expected. According to the literature, WHV S is also capable of HDV envelopment [141]. However, as demonstrated in Fig. 4.19, the levels of WHV S might be intrinsically lower in this setting resulting in decreased secretion levels of HDV particles. Notably, the presence of HDV genome was detected in the supernatants of various Avi- and Herpetohepadnaviruses (HeHBV, SkHBV, SLHBV, TFHBV) at low levels. Additionally, co-transfection of TMDV with HDV resulted in limited secretion of HDV RNA, while no HDV RNA could be detected in the supernatant

of the two other Metahepadnaviruses (AMDV, BgHBV). Repeating this experiment has thus far been unsuccessful due to unknown reasons, despite replication attempts in an alternative cell line (HEK293T) and incorporating an additional ELISA readout for HDAg (see Fig. 4.24).

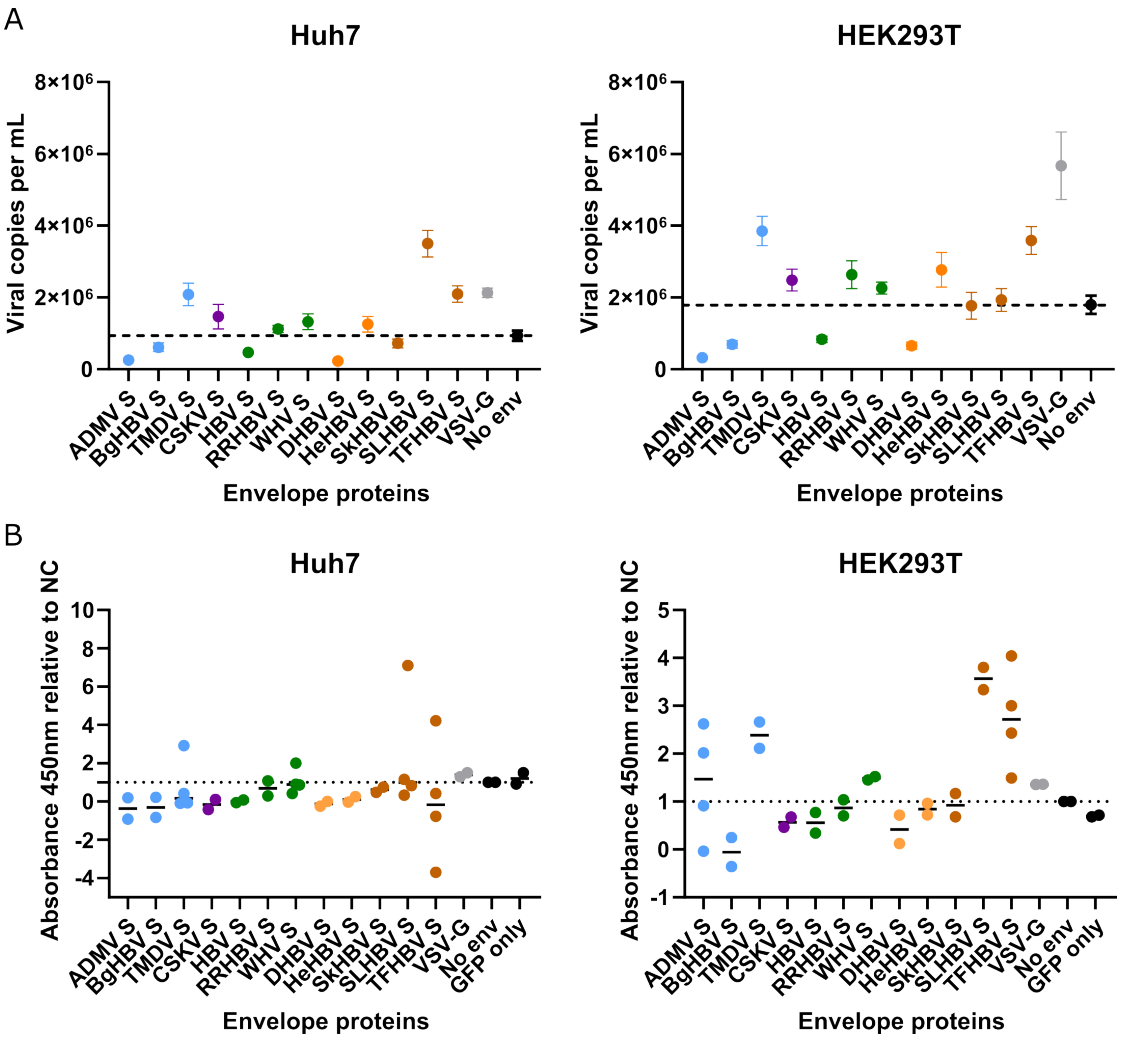

Figure 4.24: Repetition of potential envelopment of HDV by hepadnavirus envelope proteins. The experimental setting is similar to Fig. 4.23 but transfection was additionally performed in HEK293T cells and supernatants were harvested only until d9.p.t. From the last harvest, 500µL were directly inactivated with 1% TritonX-100 for later analysis using ELISA. Remaining supernatants were concentrated by PEG-precipitation and analysed by RT-qPCR. A) shows extracellular HDV RNA determined in concentrated supernatants by RT-qPCR and B) extracellular HDAg determined in non-concentrated supernatants by ELISA. ELISA was performed in duplicates and repeated in duplicates if values showed high variation in the first measurement. N=1

4.4 Studies on hepatitis virus host factors

A comprehensive analysis of host factors associated with HCV and HBV was planned to be included in this study and addressed in three different approaches. Firstly, I investigated the involvement of FGFR4 as a dependency factor for HCV. Secondly, I worked on an HBV reporter system to identify factors in human cells that are essential for HBV infection. Lastly, I assessed the potential role of CD302 and CR1L as restriction factors for HBV in murine cells. Unfortunately, the discontinuation of all three investigations was necessary due to the lack of supportive findings obtained from the conducted experiments, thereby restricting the possibility of pursuing further research on these particular subjects. The appendix (see section 7.1) includes more comprehensive experimental data that provides a more detailed description of the key results.

5 Discussion

The transmission of HDV has been primarily associated with HBV envelope proteins [110]. However, a single study has demonstrated that HDV can also be transmitted through human non-HBV envelope proteins [150]. In my study, I focused on investigating the transmission of HDV through human non-HBV viruses and non-human HBV-like viruses.

5.1 Envelopment of HDV by human non-HBV viruses

5.1.1 Establishment of a suitable cell culture model to study HDV envelopment by HCV

In a first step towards analysis of HCV mediated transmission of HDV, my objective was to establish a suitable cell culture model that is highly efficient and enables the simultaneous investigation of HDV and HCV within the same cell. In cell culture research, the analysis of HCV replication often involves the transfection of an *in vitro* transcribed subgenomic replicon. This replicon is a self-replicating RNA that can be modified by inserting different reporter genes such as luciferase or fluorescent proteins to assess replication efficiency [14]. In contrast, studies on HDV primarily rely on plasmid transfection, which delivers overlength sequences of antigenomic HDV. In this study, I successfully established an RNA transfection protocol for HDV that is compatible with the settings used for HCV transfection. It allows for robust investigation of co-replication and production of potentially infectious particles due to a high number of transfected cells. This protocol involves co-delivery of genomic HDV RNA and S-HDAg mRNA, a combination that has proven to be functional by other researchers as well [119].

Compared to infection based systems, this transfection protocol offers a major advantage in terms of the high number of cells becoming double positive for NS5A and HDAg (see Fig. 4.2). While in the Huh7 context HCV shows a high infection efficiency, studies involving HDV infection are often limited by the low number of infected cells. IF-based analysis has shown that with heparin purified virus and a high MOI, HDV infection only results in a maximum of approximately 20% of cells staining positive for HDAg [143]. Even cell lines that stably replicate and produce HDV [143] reach a plateau of approximately 30% HDAg positive cells in IF analysis (own preliminary data).
The transfection efficiency of HCV RNA, which is a already well established technique,

was expected to reach approximately 50%. The majority of these cells exhibited double positive staining for HDAg and NS5A (see Fig. 4.2), indicating a high level of co-transfected cells, that is mostly limited by the transfection efficiency of HCV RNA. The presence of intracellular viral RNA was efficiently detected by RT-qPCR. The IF staining proved to be highly reliable for detecting both intracellular viral proteins, HDAg and NS5A. However, some unspecific background was detected in the IF staining for NS5A, in particular at later time points when cell density was higher (see Fig. 4.5). It is important to note that in this study transfected cells were monitored for viral protein expression using IF until d6.p.t. Considering the half-life time of approximately 16h for NS5A [153] and 25h for HDAg [113], the detected signal most likely originates from newly synthesised proteins after transfection rather than from proteins produced from the input RNA. However, as the half-life times of the transfected RNA species were not determined, a contribution of the input RNA to the assessed protein expression cannot be fully excluded.

Taken together, the established system is nevertheless well suited for studying HCV/HDV co-replication and potential envelopment of HDV by HCV.

5.1.2 No efficient transmission of HDV by non-HBV envelope proteins

Investigation of replication efficiency did not reveal significant differences between single and co-transfected cells, neither for HCV nor HDV (see Fig. 4.3). This holds true upon infection with HDV and HCV as well and further aligns with previously published data [150]. Presence of both viruses in the same cell could be shown by IF staining for HDAg and NS5A. Notably, no significant difference in the amount of cells staining positive for either protein can be observed upon single or co-transfection or -infection of either HDV or HCV. In contrast, upon co-infection, the amount of double positive cells is significantly reduced compared to the expected values calculated by the co-infection coefficient (see Fig. 4.5). This unexpected result might be attributed to the inherently low number of HDAg positive cells in the infection experiment, which leads to low statistical power.

Interestingly, the formation of infectious particles was observed exclusively when HCV envelope proteins and the HCV genome were present. No evidence of HDV transmission was observed in conjunction with HCV envelope proteins. This finding holds true for both the co-transfection and the co-infection scenarios (see Figs. 4.4 & 4.6). These results combined with the distinct separation of IF stainings for HDAg and NS5A indicates that both viruses indeed replicate within the same cell. However, they remain confined to their respective compartments without interfering with each other. The absence of co-localisation between HDAg and NS5A aligns with previous findings indicating that HCV replication occurs within the virus induced membranous web [42], while HDV replication is exclusively confined to the nucleus [110]. Of note, as NS5A is part of the HCV replication complex, it is well suited for detection of viral replication sites. It was further shown, that it co-localises with E2 in close proximity to lipid droplets for HCV

assembly [107]. Nevertheless, NS5A cannot exclusively be used for estimating potential assembly sites of HCV enveloped HDV particles, as it is not part of the envelope. Still, as HCV E2 does not contain an NLS and was shown to localise to non-modified ER if not currently involved in an an active assembly process [107], the clear staining of HDAg in the nucleus indicates minimal chances for interaction with HCV envelope proteins.

The absence of HCV-mediated transmission of HDV, as observed in this study, contradicts published experimental data by Perez-Vargas et. al. [150]. However, it is consistent with the results of clinical studies [26, 152, 17]. It is estimated that if HCV-mediated transmission occurs, it is likely to be much less efficient compared to HBV-mediated transmission of HDV. This could potentially explain the absence of clinical evidence for the occurrence of HDV enveloped by HCV. Additionally, this might also account for the inability to observe transmission *in vitro* during co-infection (see Fig. 4.6), as the number of cells testing positive for both viruses might be insufficient to generate a significant number of infectious particles. However, the absence of HCV-mediated HDV transmission upon co-transfection experiments, where a large number of cells exhibits double positivity for HDV and HCV indicates an active or passive restriction mechanism preventing HCV-mediated transmission (discussed in more detail in section 5.1.3).

The previous study by Perez-Vargas et. al. further suggested that other envelope proteins such as VSV-G might have the potential to mediate transmission of HDV [150]. VSV-G is known for its very broad host cell tropism [52], making it an interesting candidate for investigating HDV transmission. Given the well established methods for plasmid transfection, a plasmid co-transfection experiment was conducted to explore the potential transmission of HDV by VSV-G (see Fig. 4.7).
The results of this experiment revealed that single cells could be infected with supernatants obtained from HDV/VSV-G co-transfected cells, indicating a potential VSV-G-mediated transmission of HDV. However, it is important to note that the efficiency of this transmission appeared relatively low, as only a small number of cells stained positive for HDAg following infection. It is worth mentioning that even when HDV was co-transfected with HBV envelope proteins, the transmission efficiency remained low, although higher than that observed for VSV-G. Nevertheless, statistical significance could not be determined, likely due to overall low efficiency observed throughout the experiment. Notably, no transmission of HDV by HCV envelope proteins was observed in this plasmid transfection system, which is in line with data obtained from RNA transfection and viral infection.
Interestingly, the initial transfection efficiency was similar among all tested envelope proteins. However, it was observed that the published ratio of 1:4 (genome:envelope) [150] for VSV-G and HDV resulted in a strong cytotoxic effect. In contrast, the transfection of HDV with other envelope proteins in this ratio did not affect cell viability. To address this issue, the amount of VSV-G encoding plasmid was reduced to a ratio of 1:1, which might further lead to the lower transmission efficiency compared to HBsAg.

The potential transmission of HDV by VSV-G might have limited relevance, despite being possible in the experimental setting. VSV is a virus that primarily infects live-

stock and only sporadically infects human beings. Given that the origin of HDV remains unclear but Delta-like agents seem to undergo frequent host jumps [13], one could speculate that the human HDV originated from an ancient zoonotic event. This might have occurred under close contact to livestock possibly facilitated by a VSV-like envelope, which still allows HDV susceptibility to VSV envelopment. However, the only known Delta-like agent identified in hoofed animals was found in the white deer [13], not in livestock. In addition, the white deer does not appear to be a natural host for VSV [32], indicating that it might not be the missing link for the transmission of HDV to humans.

In order to trace back the potential zoonotic origin of HDV and the development of its strict HBV dependency, further screening of host species for the presence of Delta-like agents and putative helper viruses is needed. Once identified, these Delta-like agents can be compared to HDV on genome sequence and protein level providing more insight into their evolutionary development. Envelopment capacity of putative helper viruses could further be explored in experimental settings similar to the ones used in this study. Still, as this hypothesis can neither been proven nor falsified at this point, other scenarios are at least equally likely. One possibility could connect to a potential evolutionary relationship between HDV and plant viroids. Striking similarities between those plant viroids and HDV have already been identified and discussed several years ago [187]. As they share not only their genome structure and replication strategy, but also e.g. the ability to redirect DNA dependent RNA polymerases to an RNA template, it could be hypothesised that they might have a common ancestor. Transmisison of such an ancestor to human beings or their ancestors might have happened in an hepadnavirus infected individual through the digestive tract [187].

5.1.3 Possible reasons why HDV does not use non-HBV envelope proteins

The absence of evidence for a non-HBV-mediated transmission, despite efficient co-replication, indicates the presence of a potential restriction that prevents this type of HDV transmission. This restriction might be actively regulated (e.g. a super-infection exclusion mechanism) or a more random coincidence (e.g. no chance for interaction between genome and envelope due to clear separation of viral replication cycles).

Super-infection exclusion mechanisms, which prevent infection of cells that are already infected, have been described for several viruses, including DHBV and HCV [202, 195]. These mechanisms might differ between distinct viruses and can operate at different stages of the viral relication cycle, including entry-related and later steps. For DHBV, the super-infection exclusion is mediated by the L protein, which leads to receptor down-regulation. This downregulation prevents binding and internalisation of additional particles using the same receptor [202]. Super-infection exclusion has also been postulated for HBV, although an HBV mediated downregulation of NTCP has not been observed thus far, indicating a different mechanism [111]. In the case of HCV, super-infection

exclusion is likely to occur at a later replication step, after entry and polyprotein processing [195].
The hypothesis of super-infection exclusion, which could lead to a low number of double positive cells, was considered due to the potential interference observed when cells were co-infected with HDV and HCV. This, in turn, would limit or even prevent HDV envelopment. However, super-infection of HDV or HCV transfected cells with the respective other virus did not lead to a reduced viral RNA copy number or amount of double positive cells (see Fig. 4.9). Calculation of the super-infection coefficient did not reveal significant differences and even showed a slight trend towards a higher number of double positive cells than expected. This observation was specifically made for HCV super-infection, which potentially increased the number of double infected cells by 50%. Given the high percentage of HDV transfected cells (approximately 90%) as established in Fig. 4.1, the chances of HCV infecting HDV negative cells are minimal. An increased SIC indicates that HCV is more likely to infect cells that are already replicating HDV. This might be attributed to factors such as an increased receptor expression, which has been shown to enhance HCV infection efficiency [94]. This effect is known to plateau at a certain level, potentially explaining the limited increase in SIC. However, it should be noted that an HDV mediated upregulation of CD81, a receptor for HCV, has not been reported and would need to be investigated to support this hypothesis.
In addition, it is important to consider that at high cell densities, an increased background fluorescence signal is observed for NS5A, as mentioned earlier. Although the algorithm for semi-automated image quantification was trained with multiple training images to correct for background fluorescence, it might still influence quantification and calculation of the SIC.

As mentioned above, the sites and mechanisms of replication for HDV and HCV are largely separated, limiting potential interaction sites between both viruses. The only commonly used pathway is the general secretory pathway employed for exiting the cell (see sections 1.1.2 & 1.1.3). However, it is important to consider that HCV replication happens in a highly shielded environment [42]. Packaging of HCV genomes likely occurs in very close proximity to these replication sites [8], minimising the transportation of viral RNA and potential triggering of the innate immune response. Consequently, the HDV RNP might not get access to HCV envelope proteins. Although presenting indirect evidence, as discussed above, the very strict localisation of HDAg to the nucleus and the lack of evidence for co-localisation of HDAg and NS5A support this hypothesis.
However, co-localisation was also not observed for HDAg and HBV envelope proteins in previous IF stainings. It can therefore not be fully excluded, that HDAg and HCV envelope proteins do not interact with each other.
In the context of HCV-mediated transmission of HDV in patients, HBV/HCV/HDV triple infected individuals could potentially serve as a source of these particles. Taking into consideration that HBV-mediated transmission is likely the most efficient route for HDV delivery, the co-localisation of HBV as an HDV transmitter, and HCV in liver samples should also be investigated. However, published data on this aspect is contradictory. Investigating HCV super-infection on HBV in a cell culture setting revealed

no evidence for viral interference [132]. In contrast, examining HBV super-infection on HCV in the chimpanzee model, both viruses are rarely found in the same cell but tend to occupy different spaces in the infected liver [209].

A third possibility why HDV cannot effectively make use of non-HBV envelope proteins might be related to its very specific interaction with HBsAg. The tight association of HDV to HBV appears unique to the human virus, as other Delta-like agents found in several animal species likely depend on different helper viruses [24]. The absence of a farnesylation site in BHDV, that might potentially spread using hepacivirus envelope proteins, led to the hypothesis that this mode of spread might only be possible due to the missing farnesylation. Conversely, human HDV might be compelled to rely on HBsAg-dependent transmission due to the presence of the farnesyl residue. However, inhibiting the farnesyltransferase by LFB did not result in the production of infectious HCV-enveloped HDV particles. This indicates that farnesylation of L-HDAg alone does not restrict non-HBV-mediated envelopment (see Fig. 4.12).
In contrast, the spread of HCV itself appears to be increased under LFB treatment, which was initally unexpected. In HCV infected cells, an upregulation of farnesyldiphosphate farnesyltransferase has been observed, leading to enhanced HCV propagation. Although this enzyme is involved in the lipid biosynthesis pathway and plays an important role for the HCV replication cycle [148], it is distinct from the enzyme responsible for transferring farnesyl residues to proteins like L-HDAg and is not targeted by LFB. However, both enzymes use the same substrate (farnesyldiphosphate). Therefore, inhibiting one enzyme might increase substrate availability for the other one, potentially enhancing propagation of HCV in LFB treated cells.

Another aspect that might contribute to the inability of HDV to utilise non-HBV envelope proteins is the expression of L-HDAg itself. It is currently unknown, whether BHDV makes use of its potential ADAR1 editing site, although ADAR enzyme orthologs are expressed in many vertebrates, including bats [138]. Along the same lines, it is hypothesised that L-HDAg as HBV specificity determinant might hinder HCV envelopment of HDV, possibly through steric hindrance or masking of potential binding sites. However, even a mutated HDV that is unable to produce L-HDAg while retaining its replication competence cannot be enveloped by HCV (see Figs. 4.13 & 4.14).
Unfortunately, there is no experimental evidence supporting the hypothetical spread of BHDV by hepacivirus envelope proteins so far. In a pilot experiment, I was able to show that BHDAg can be detected using the established anti-HDAg antibody and that BHDAg can be co-transfected with HA-tagged bat hepacivirus envelope proteins (data not shown). However, the receptor of this virus is not known, which presents a challenge for blind cell culture based infection experiments using particles obtained from co-transfection.

As the presence of HBV specificity determinants in the human HDV does not seem to prevent usage of non-HBV envelope proteins, I conducted further investigation into potential factors on the helper virus side. To this end, I screened envelope proteins of

HCV and VSV for the presence of a potential TRD. Applying a threshold of two tryptophan residues in close proximity (less than four AA apart), I identified one potential TRD in HCV E2 and VSV-G. However, in both cases, it seems that these tryptophan residues are located close to or partially within transmembrane domains. The TRD in HBV also exhibits close proximity to transmembrane domains, but it is believed to be located precisely between transmembrane domains III & IV [92]. In contrast, HCV E1E2 and VSV-G possess only one transmembrane domain in each protein, anchoring them in the membrane, while the main parts are ectodomains located outside of the particle [31, 30, 36]. The potential interaction between these tryptophan accumulation sites and HDAg, which clearly resides at the inner side of the particle, presents a challenge. This might help to explain the lack of evidence for HCV-mediated transmission of HDV, but further investigation is still required.
In contrast, although VSV-G mediated HDV transmission was possible with low efficiency, this protein is not believed to possess an accessible TRD, suggesting that packaging must have happened through a different pathway. One possibility is unspecific envelopment. VSV-G induces rapid fusion of various cellular membranes, leading to syncytia formation [165], and the production of extracellular vesicles. These vesicles, decorated with VSV-G, efficiently package and transport cargo located at intracellular membranes to potential target cells [124]. Given that the HDV RNP is located at intracellular membranes through its farnesylated L-HDAg, there is a high likelihood of packaging into these VSV-G pseudotyped particles. Consequently, it would be interesting to investigate, whether Lonafarnib treatment or the use of the L(-) HDV mutant can inhibit envelopment by VSV-G.
There might also be the possibility of a TRD-independent interaction between HDAg and envelope proteins. However, the structure of HDAg is not fully resolved and currently only includes the oligomerisation domain between AA 12-60 [222]. The majority of the protein is considered intrinsically disordered [5], which further complicates structure prediction using algorithm based approaches. Without a comprehensive understanding of the protein structure, prediction of potential interaction sites is challenging and cannot be performed at this stage.

5.2 Envelopment of HDV by non-human hepadnaviruses

The ability of non-human hepadnaviruses to envelop HDV has been demonstrated for the woodchuck model. In this model, replication of HDV and production of infectious HDV particles enveloped with WHV envelope proteins were observed [141]. However, attempts to envelop the woodchuck Delta-like agent with HBV envelope proteins failed to produce infectious particles, potentially due to the lack of an L-HDAg mediating interaction and envelopment with HBsAg [81].
In contrast to the woodchuck model, there is no evidence that DHBV, which is the best studied model for HBV, can provide helper function for HDV. This difference in helper function might be attributed to differences in the sequences of the S protein,

particularly the TRD. The TRD plays a crucial role in the interaction between L-HDAg and HBsAg for HDV envelopment [92]. Comparing the TRD sequences of different hepadnaviruse, it becomes evident that differences in this particular sequence are genus specific (see Fig. 4.16). Representatives of the genus Orthohepadnavirus (like WHV) and Metahepadnavirus have TRDs similar to HBV. In contrast, representatives from the other clades only possess the conserved tryptophan residue corresponding to Trp196 in HBV, but lack the following tryptophan residues. This difference in the TRD sequence might explain the ability of WHV to provide helper function for HDV and the inability of DHBV to do so.

In order to test the hypothesis that only hepadnaviruses presenting a TRD similar to HBV are able to provide helper function for HDV, I first aimed for generation of these hepadnaviral SVPs. The detection of tagged versions of the S protein was successfully achieved for representatives of all tested hepadnavirus clades by western blot, IF, or both techniques (see Figs. 4.19, 4.20 & 4.21). It is worth noting, that in western blot all proteins appeared at a smaller size than expected based on their calculated molecular weight. This phenomenon had been previously observed for HBsAg in our lab and was therefore not surprising.
The position at which successful tagging occurred varied between different genera. For HBV, previous studies have demonstrated that C-terminal tagging with GFP inhibits particle secretion, but allows secretion when a smaller tag like HA is used [102]. In contrast to published data, I could not observe intracellular production of C-terminally HA-tagged S in Orthohepadnaviruses. Interestingly, in Metahepadnaviruses, which are the closest related genus to Orthohepadnaviruses, the production of these S proteins appeared to be independent of the tag position. In these viruses, both N- and C-terminally tagged S proteins were produced intracellularly, but were not secreted. Notably, no intra- or extracellular S protein was detected in western blot analysis for BgHBV. In contrast, representatives of Avi- and Herpetohepadnaviruses showed a preference for C-terminal tagging, as it resulted in successful of intracellular production and secretion of SVPs.

Interestingly, a specific signal was observed upon staining HA in IF for all constructs. This was observed not only for BgHBV but also for Orthohepadnavirus S proteins tagged at the C-terminus, which were not detected in western blot. The intracellular distribution of the tagged proteins appeared to be widely dispersed in the cytoplasm, with certain regions exhibiting higher fluorescence intensity. It would be interesting to investigate, whether these regions colocalise with markers of specific organelles, such as ER, Golgi, Endosomes/MVBs, or vesicles of the autophagy pathway. This could provide insights into the potential exit routes used by these particles.
It is important to note that the comparison between western blot and IF yielded partially contradictory results. This discrepancy could be attributed to differences in the sensitivity of the two assays, which might explain the divergent findings. Furthermore, it is possible that incorrectly processed or aggregated S proteins can still be detected if they retain the correctly folded and accessible HA-tag. These aggregates might not be resolved under the reducing conditions used in western blot and could appear at higher

band size than expected. Since the membranes were only probed for HA within the expected size range of S proteins, there is the possibility of a loss of information regarding signals that could correspond to aggregated proteins.

Previous studies have demonstrated that tagging of S protein does not interfere with correct glycosylation despite potential misfolding [102]. The presene of a double band pattern, similar to what has been observed for HBV, where one band corresponds to the glycosylated form and the other one to the non-glycosylated form [86], indicates potential glycosylation of Orthohepadnavirus S proteins. This finding suggests that the membrane topology of these proteins might be correct, exposing the glycosylation sites to the ER lumen. In the case of DHBV, a potential glycosylation site has been reported but not utilised [157, 198]. Furthermore, a truncated version of the S protein of approximately 10kDa in size has been identified in purified DHBV SVP preparations, which likely facilitates proper transmembrane translocation and folding of DHBV S protein [61]. Interestingly, I could observe different running behaviour of the DHBV S protein depending on the position of the tag. N-terminal tagging resulted in the expected single protein band pattern, while C-terminal tagging led to the appearance of a second band. Assuming that the more prominent, lower band corresponds to the S protein, the upper band would represent a potentially glycosylated version. Treatment with endoglycosidase H, which removes sugar moieties, could help determining the origin of the second band. Alternatively, assuming the upper band represents the correct S protein of DHBV, the lower band might correspond to a truncated version. In this case, the production of normally produced S would be greatly reduced in DHBV and only possible with the C-terminal tag. However, the size of this band is closer to 15kDa than the expected 10kDa, pointing more support for the glycosylation hypothesis.

Not all species were detectable in concentrated supernatants of transfected cells, particularly Meta- and Parahepadnaviruses, despite their intracellular production being observed in most cases. One possible explanation is that the tag interferes with proper protein folding, leading to retention of the protein in the ER. This issue could potentially be overcome by using a different tag or altering the tag position. Another factor that could contribute to the lack of secretion is the absence of a signal sequence directing the proteins to the secretory pathway. However, for HBsAg it has been demonstrated that correct transmembrane topology is achieved through co-translational translocation, relying on internal signals that differ from a classical N-terminally cleaved signal peptide [40, 41, 173]. The precise definition of these signals remains challenging and requires mapping and screening in the remaining hepadnavirus genera.
Another reason for the non-detection of Meta- and Parahepadnaviruses could be their infection of fish, which have a lower body temperature compared to mammals or birds. It is possible, that these proteins do not undergo proper folding at the experimental conditions used in this study. Repetition of the experiment in fish cells could potentially address this issue, but has not yet been performed due to time reasons.

The quantification of the ratio between exta- and intracellular protein was challenging due to the incomplete secretion and weak intracellular detection of some constructs. In

addition, the separation of extra- and intracellular protein to different blots further complicated the interpretability of these results. It is important to approach these findings with caution, particularly for Meta- and Parahepadnaviruses, as they exhibited low or no intracellular production and no secretion of the S protein. Nevertheless, a clear trend emerges, with N-terminally tagged HBV and RRHBV being secreted very efficiently, while constructs for HeHBV or SkHBV showed only a small portion of produced protein reaching the supernatant, regardless of the tag position (see Fig. 4.22C). The remaining constructs generally displayed comparable levels of extra- and intracellular S protein, resulting in a ratio close to 1. This indicates that there is no significant shift towards either secretion or retention of these S proteins. Of note, the detection of extracellular S protein might indicate successful production of SVPs, but it does not prove this hypothesis. Therefore, the next step would be to visualise particles, for example using negative stain electron microscopy, once an efficient purification pipeline is established that allows recovery of SVPs.

Of note, the detection of extracellular tagged S protein for Metahepadnaviruses, which might have the highest likelihood after Orthohepadnaviruses to envelop HDV, was challenging. Nevertheless, as discussed above, this could be due to tag-dependent misfolding, leading to intracellular retention of the proteins. It is possible that untagged versions might still get secreted. However, the detection of untagged S proteins remains challenging, as specific antibodies targeting the different hepadnavirus S proteins are not available, and antibodies against HBV or DHBV S protein do not cross-react with other species.
To investigate the envelopment of HDV by non-human hepadnaviruses, a preliminary pilot experiment was conducted, focusing on the detection of extracellular HDV RNA (see Fig. 4.23). The results showed envelopment by HBV and RRHBV S proteins but not WHV, which aligns with expectations. Especially, assuming that the expression of WHV S protein is as low as compared to the tagged version, and that HDV envelopment by WHV S has only been shown in the animal experiment, an envelopment is unlikely. Surprisingly, some Avi- and Herpetohepadnaviruses, along with TMDV as representative of Metahepadnaviruses, exhibited the potential to envelop HDV.
Regrettably, this experiment encountered challenges due to high background signals from the initial plasmid transfection. Despite attempts to mitigate this issue through DNaseI treatment, the background detection persisted, thereby limiting the scope of meaningful interpretation. In addition, the repetition of this experiment yielded contradictory results, which were further confirmed by ELISA based detection of HDAg and performing the experiment in an additional cell line (see Fig. 4.24). The detection of extracellular HDAg by western blot was unsuccessful due to technical difficulties. The reasons behind the substantial discrepancies observed between the two experiments remain elusive. Transfection efficiency, as determined by GFP co-transfection, was comparable and therefore cannot explain the strong deviations. Potentially, the passage effects of the cell lines might have contributed to these discrepancies and this could be addressed through further repetitions of the experiment.

With respect to the question whether HDV might be able to use non-human hepadnaviruses and whether this might relate to its origin as a human pathogen, the above mentioned experiments clearly require repetition and refinement. However, given that HDV envelopment by WHV was demonstrated by others [141], one could still speculate that transmission to human beings might have happened or could happen again through an animal helper virus. Whether this transmission relies on a TRD, could be clarified in an experimental setting exchanging TRDs from different hepadnaviruses (e.g. Avi- and Orthohepadnaviruses) and investigating the capacity to provide helper function for HDV. In addition, screening of further animal species for presence of hepadnaviruses being able to provide an envelope for HDV might contribute to the understanding of HDV's origin and zoonotic potential.

6
Summary and outlook

In this study, I was able to show that HDV exhibits a preference for spread by HBV envelope proteins compared to other tested viruses. The main focus was on investigating the transmission of HDV by HCV. The findings suggest that there is likely no active mechanism restricting non-HBV envelopment. HDV and HCV were found to be capable of co-replication and infecting the same cells, without an evident super-infection exclusion mechanism. However, the interaction between HDV and HCV appears to be limited, as no co-localisation of viral proteins was observed. The absence of a TRD in HCV E1E2 or VSV-G, which is responsible for the interaction of HBsAg with farnesylated L-HDAg, further indicates why HDV cannot specifically utilise these proteins. These observations contradict previously published experimental data of a single study, which has not been confirmed independently thus far.

One intriguing aspect is that Delta-like agents, unlike HDV, probably do not rely on hepadnaviral envelopment. Removing determinants that are unique to HDV, such as L-HDAg and its farnesylation, did not render HDV susceptible to non-HBV envelopment. This indicates that a putative helper specificity of Delta-like agents is likely determined by other factors. Identifying additional Delta-like agents and, even more important, clarifying the role of helper viruses for these agents could help to improve the understanding of these questions. The role of putative helper viruses could experimentally be addressed by investigating various enveloped viruses for providing helper function for different Delta-like agents as described in this study.
In addition, creating chimeras of HDV and Delta-like agents containing different portions of each virus could provide further insights, whether differential helper dependency might be determined at different sites and whether these can be exchanged. This could further help to understand whether and how Delta-like agents co-evolved with their respective helper viruses. A key aspect contributing to a comprehensive understanding of why and how HDV developed its HBV specificity, is the identification of the time point when diversification from other Delta-like agents occurred and the specification towards the HBV helper emerged.

The issue of HDV envelopment by non-human hepadnaviruses as a potential origin in the human host remains unresolved in this study. There are indications that hepadnaviruses closely related to HBV might mediate envelopment of HDV, but further experiments are required to confirm this observation. In addition, refinement of experimental conditions and constructs is needed to investigate and improve secretion and morphological analysis of animal hepadnavirus SVPs and pseudotyped HDV.

In conclusion, non-HBV mediated spread of HDV appears to play a limited role in the human host. However, if HDV or Delta-like agents are able to use several helper viruses for spread, there is a risk of zoonotic events. Obtaining more information about the spread of Delta-like agents as well as non-human HBV pseudotyped HDV particles is therefore necessary to provide further insights into the putative zoonotic origin and potential of HDV, and the co-evolution between HDV and its helper viruses.

7 Acknowledgement

First of all, I would like to kindly thank Prof. Dr. Ralf Bartenschlager for giving me the great opportunity to do my PhD thesis in his group. I am very thankful for all the constructive meetings, discussions, opportunities, and the support I received in the last years. He always helped me to grow and develop towards a great level of independence.

I would also like to thank Prof. Dr. Stephan Urban and his group for giving me the opportunity to join their lab meetings and for contributing valuable input to my project.

Furthermore, I would like to thank Dr. Stefan Seitz for providing insights into the great world of HBV and ancient viruses and for his open ears and eyes facing puzzling scientific results.

I would like to thank Prof. Dr. Oliver Fackler for being my second referee and Prof. Dr. Martin Müller and Dr. Viet Loan Dao Thi for immediately agreeing on being part of the defense committee. And I would like to thank my Thesis Advisory Committee for fruitful discussions and support: Prof. Dr. Ralf Bartenschlager, Prof. Dr. Oliver Fackler, Dr. Steeve Boulant, Prof. Dr. Felix Hoppe-Seyler, Dr. Sabrina Schreiner and Dr. Stefan Seitz

I am grateful to the TRR179 for funding my research and offering very interesting seminars, retreats, and courses.

A warm-hearted thank you goes to all my colleagues from F170 and MolVirol - you made me enjoying coming to work every day. In particular, I would like to thank Pascal Mutz for his constant support from the first minute on and even after he left the group, and Vladimir Gonçalves Magalhães, who carefully proofread the thesis and gave very helpful suggestions for re-phrasing too complicated sentences. Special thanks also to Anastasia Bouteros, Aditi Dhawan, Firat Nebioglu, Shangqing Yang, Catherine Moreau, Sandra Wüst, Theresa Schindler, Nadine Gillich, Agnieszka Plociennikowska, Sebastian Stegmaier and Doroteja Ilic for great scientific discussions, proofreading this thesis, amazing coffeebreaks, open ears and your daily smile that made me feeling good throughout this journey.

Zuletzt möchte ich noch meiner Familie und meinen Freunden danken. Danke für Eure unendliche Unterstützung, die vielen Telefongespräche, die Aufmunterungen und Erinnerungen an die guten alten Zeiten, als man selbst noch promovierte. Ein unbezahlbares

Danke an Jakob, der zu jeder Zeit da ist, mich immer unterstützt und gemeinsam mit mir diesen Weg gegangen ist.

Bibliography

[1] D. P. Aden, A. Fogel, S. Plotkin, I. Damjanov, and B. B. Knowles. Controlled synthesis of HBsAg in a differentiated human liver carcinoma-derived cell line. *Nature*, 282:615–616, 12 1979.

[2] V. Agnello, G. Ábel, M. Elfahal, G. B. Knight, and Q.-X. Zhang. Hepatitis C virus and other Flaviviridae viruses enter cells via low density lipoprotein receptor. *Proceedings of the National Academy of Sciences*, 96:12766–12771, 10 1999.

[3] C. Aiken, J. Konner, N. R. Landau, M. E. Lenburg, and D. Trono. Nef induces CD4 endocytosis: Requirement for a critical dileucine motif in the membrane-proximal CD4 cytoplasmic domain. *Cell*, 76:853–864, 3 1994.

[4] D. Alfaiate, P. Dény, and D. Durantel. Hepatitis delta virus: From biological and medical aspects to current and investigational therapeutic options. *Antiviral research*, 122, 08 2015.

[5] C. Alves, H. Cheng, H. Roder, and J. Taylor. Intrinsic disorder and oligomerization of the hepatitis delta virus antigen. *Virology*, 407:333–340, 11 2010.

[6] American Society of Clinical Oncology. Liver Cancer Statistics, 2023. `https://www.cancer.net/cancer-types/liver-cancer/statistics`, last accessed 09.06.2023.

[7] C. Baechlein, N. Fischer, A. Grundhoff, M. Alawi, D. Indenbirken, A. Postel, A. L. Baron, J. Offinger, K. Becker, A. Beineke, J. Rehage, and P. Becher. Identification of a Novel Hepacivirus in Domestic Cattle from Germany. *Journal of Virology*, 89:7007–7015, 7 2015.

[8] R. Bartenschlager, F. Penin, V. Lohmann, and P. André. Assembly of infectious hepatitis C virus particles. *Trends in Microbiology*, 19:95–103, 2 2011.

[9] R. Bartenschlager and H. Schaller. Hepadnaviral assembly is initiated by polymerase binding to the encapsidation signal in the viral RNA genome. *The EMBO Journal*, 1:3413–3420, 1992.

[10] H. Barth, C. Schäfer, M. I. Adah, F. Zhang, R. J. Linhardt, H. Toyoda, A. Kinoshita-Toyoda, T. Toida, T. H. van Kuppevelt, E. Depla, F. von Weizsäcker, H. E. Blum, and T. F. Baumert. Cellular Binding of Hepatitis C Virus Envelope Glycoprotein E2 Requires Cell Surface Heparan Sulfate. *Journal of Biological Chemistry*, 278:41003–41012, 10 2003.

[11] P. Bellecave, J. Gouttenoire, M. Gajer, V. Brass, G. Koutsoudakis, H. E. Blum, R. Bartenschlager, M. Nassal, and D. Moradpour. Hepatitis B and C virus coinfection: A novel model system reveals the absence of direct viral interference. *Hepatology*, 50:46–55, 7 2009.

[12] S. Berg, D. Kutra, T. Kroeger, C. N. Straehle, B. X. Kausler, C. Haubold, M. Schiegg, J. Ales, T. Beier, M. Rudy, K. Eren, J. I. Cervantes, B. Xu, F. Beuttenmueller, A. Wolny, C. Zhang, U. Koethe, F. A. Hamprecht, and A. Kreshuk. ilastik: interactive machine learning for (bio)image analysis. *Nature Methods*, 16:1226–1232, 12 2019.

[13] L. M. Bergner, R. J. Orton, A. Broos, C. Tello, D. J. Becker, J. E. Carrera, A. H. Patel, R. Biek, and D. G. Streicker. Diversification of mammalian deltaviruses by host shifting. *Proceedings of the National Academy of Sciences of the United States of America*, 118:e2019907118, 1 2021.

[14] K. J. Blight and E. A. Norgard. *HCV Replicon Systems*. Horizon Biosciences, 2006.

[15] R. J. P. Brown, B. Tegtmeyer, J. Sheldon, T. Khera, Anggakusuma, D. Todt, G. Vieyres, R. Weller, S. Joecks, Y. Zhang, S. Sake, D. Bankwitz, K. Welsch, C. Ginkel, M. Engelmann, G. Gerold, E. Steinmann, Q. Yuan, M. Ott, F. W. R. Vondran, T. Krey, L. J. Ströh, C. Miskey, Z. Ivics, V. Herder, W. Baumgärtner, C. Lauber, M. Seifert, A. W. Tarr, C. P. McClure, G. Randall, Y. Baktash, A. Ploss, V. L. D. Thi, E. Michailidis, M. Saeed, L. Verhoye, P. Meuleman, N. Goedecke, D. Wirth, C. M. Rice, and T. Pietschmann. Liver-expressed Cd302 and Cr1l limit hepatitis C virus cross-species transmission to mice. *Science Advances*, 6, 11 2020.

[16] P. D. Burbelo, E. J. Dubovi, P. Simmonds, J. L. Medina, J. A. Henriquez, N. Mishra, J. Wagner, R. Tokarz, J. M. Cullen, M. J. Iadarola, C. M. Rice, W. I. Lipkin, and A. Kapoor. Serology-Enabled Discovery of Genetically Diverse Hepaciviruses in a New Host. *Journal of Virology*, 86:6171–6178, 6 2012.

[17] P. Cappy, Q. Lucas, N. Kankarafou, C. Sureau, and S. Laperche. No Evidence of Hepatitis C Virus (HCV)–Assisted Hepatitis D Virus Propagation in a Large Cohort of HCV-Positive Blood Donors. *The Journal of Infectious Diseases*, 223:1376–1380, 4 2021.

[18] E. Casanova, T. Lemberger, S. Fehsenfeld, T. Mantamadiotis, and G. Schütz. Complementation in the Cre recombinase enzyme. *genesis*, 37:25–29, 9 2003.

[19] M. T. Catanese, K. Uryu, M. Kopp, T. J. Edwards, L. Andrus, W. J. Rice, M. Silvestry, R. J. Kuhn, and C. M. Rice. Ultrastructural analysis of hepatitis C virus particles. *Proceedings of the National Academy of Sciences*, 110:9505–9510, 6 2013.

[20] Centers for Disease Control and Prevention. Fast facts on global Hepatitis B, 2022. `https://www.cdc.gov/globalhealth/immunization/diseases/hepatitis-b/data/fast-facts.html`, last accessed 08.06.2023.

[21] Centers for Disease Control and Prevention. Viral Hepatitis, 2023. `https://www.cdc.gov/hepatitis/abc/index.htm`, last accessed 09.06.2023.

[22] J. Chang, X. Nie, H. E. Chang, Z. Han, and J. Taylor. Transcription of Hepatitis Delta Virus RNA by RNA Polymerase II. *Journal of Virology*, 82:1118–1127, 2 2008.

[23] L.-J. Chang, P. Pryciak, D. Ganem, and H. E. Varmus. Biosynthesis of the reverse transcriptase of hepatitis B viruses involves de novo translational initiation not ribosomal frameshifting. *Nature*, 337:364–368, 1 1989.

[24] W. S. Chang, J. H. Pettersson, C. L. Lay, M. Shi, N. Lo, M. Wille, J. S. Eden, and E. C. Holmes. Novel hepatitis D-like agents in vertebrates and invertebrates. *Virus Evolution*, 5, 7 2019.

[25] M. Chao, S. Y. Hsieh, and J. Taylor. Role of two forms of hepatitis delta virus antigen: evidence for a mechanism of self-limiting genome replication. *Journal of Virology*, 64:5066–5069, 10 1990.

[26] I. Chemin, F. H. Pujol, C. Scholtès, C. L. Loureiro, F. Amirache, M. Levrero, F. Zoulim, J. Pérez-Vargas, and F. Cosset. Preliminary Evidence for Hepatitis Delta Virus Exposure in Patients Who Are Apparently Not Infected With Hepatitis B Virus. *Hepatology*, 73:861–864, 2 2021.

[27] P. J. Chen, G. Kalpana, J. Goldberg, W. Mason, B. Werner, J. Gerin, and J. Taylor. Structure and replication of the genome of the hepatitis delta virus. *Proceedings of the National Academy of Sciences*, 83:8774–8778, 11 1986.

[28] Q.-L. Choo, G. Kuo, A. J. Weiner, L. R. Overby, D. W. Bradley, and M. Houghton. Isolation of a cDNA clone Derived from a Blood-Borne Non-A, Non-B Viral Hepatitis Genome. *Science*, 244:359–362, 4 1989.

[29] H.-C. Chou, T.-Y. Hsieh, G.-T. Sheu, and M. M. C. Lai. Hepatitis Delta Antigen Mediates the Nuclear Import of Hepatitis Delta Virus RNA. *Journal of Virology*, 72:3684–3690, 5 1998.

[30] Y. Ci, Y. Yang, C. Xu, and L. Shi. Vesicular stomatitis virus G protein transmembrane region is crucial for the hemi-fusion to full fusion transition. *Scientific Reports*, 8:10669, 7 2018.

[31] L. Cocquerel, J.-C. Meunier, A. Pillez, C. Wychowski, and J. Dubuisson. A Retention Signal Necessary and Sufficient for Endoplasmic Reticulum Localization Maps to the Transmembrane Domain of Hepatitis C Virus Glycoprotein E2. *Journal of Virology*, 72:2183–2191, 3 1998.

[32] J. A. Comer, D. E. Stallknecht, and V. F. Nettles. Incompetence of White-Tailed Deer as Amplifying Hosts of Vesicular Stomatitis Virus for Lutzomyia shannoni (Diptera: Psychodidae). *Journal of Medical Entomology*, 32:738–740, 9 1995.

[33] V. M. Corman, A. Grundhoff, C. Baechlein, N. Fischer, A. Gmyl, R. Wollny, D. Dei, D. Ritz, T. Binger, E. Adankwah, K. S. Marfo, L. Annison, A. Annan, Y. Adu-Sarkodie, S. Oppong, P. Becher, C. Drosten, and J. F. Drexler. Highly Divergent Hepaciviruses from African Cattle. *Journal of Virology*, 89:5876–5882, 6 2015.

[34] R. A. Crowther, N. A. Kiselev, B. Böttcher, J. A. Berriman, G. P. Borisova, V. Ose, and P. Pumpens. Three-dimensional structure of hepatitis B virus core particles determined by electron cryomicroscopy. *Cell*, 77:943–950, 6 1994.

[35] S. Datta, S. Chatterjee, V. Veer, and R. Chakravarty. Molecular Biology of the Hepatitis B Virus for Clinicians. *Journal of Clinical and Experimental Hepatology*, 2:353–365, 12 2012.

[36] A. T. de la Peña, K. Sliepen, L. Eshun-Wilson, M. L. Newby, J. D. Allen, I. Zon, S. Koekkoek, A. Chumbe, M. Crispin, J. Schinkel, G. C. Lander, R. W. Sanders, and A. B. Ward. Structure of the hepatitis C virus E1E2 glycoprotein complex. *Science*, 378:263–269, 10 2022.

[37] J. A. Dill, A. C. Camus, J. H. Leary, F. D. Giallonardo, E. C. Holmes, and T. F. F. Ng. Distinct Viral Lineages from Fish and Amphibians Reveal the Complex Evolutionary History of Hepadnaviruses. *Journal of Virology*, 90:7920–7933, 9 2016.

[38] R. B. DuBridge, P. Tang, H. C. Hsia, P.-M. Leong, J. H. Miller, and M. P. Calos. Analysis of Mutation in Human Cells by Using an Epstein-Barr Virus Shuttle System. *Molecular and Cellular Biology*, 7:379–387, 1 1987.

[39] J. Dubuisson. Virology and cell biology of the hepatitis C virus life cycle-An update. *Journal of Hepatology*, 61:3–13, 11 2014.

[40] B. E. Eble, V. R. Lingappa, and D. Ganem. Hepatitis B surface antigen: an unusual secreted protein initially synthesized as a transmembrane polypeptide. *Molecular and Cellular Biology*, 6:1454–1463, 5 1986.

[41] B. E. Eble, D. R. MacRae, V. R. Lingappa, and D. Ganem. Multiple topogenic sequences determine the transmembrane orientation of the hepatitis B surface antigen. *Molecular and Cellular Biology*, 7:3591–3601, 10 1987.

[42] D. Egger, B. Wolk, R. Gosert, L. Bianchi, H. E. Blum, D. Moradpour, and K. Bienz. Expression of Hepatitis C Virus Proteins Induces Distinct Membrane Alterations Including a Candidate Viral Replication Complex. *Journal of Virology*, 76:5974–5984, 6 2002.

[43] Eiger Biopharmaceuticals. Lonafarnib/Ritonavir for HDV, 2023. `https://www.eigerbio.com/hepatitis-delta/`, last accessed 19.07.2023.

[44] B. Erbes. Analyse der L-Protein-vermittelten Superinfektionsresistenz bei der DHBV-Infektion; Promotionsarbeit, 2015.

[45] K. Esser, X. Cheng, J. M. Wettengel, J. Lucifora, L. Hansen-Palmus, K. Austen, A. A. R. Suarez, S. Heintz, B. Testoni, F. Nebioglu, M. T. Pham, S. Yang, A. Zernecke, D. Wohlleber, M. Ringelhan, M. Broxtermann, D. Hartmann, N. Hüser, J. Mergner, A. Pichlmair, W. E. Thasler, M. Heikenwalder, G. Gasteiger, A. Blutke, A. Walch, P. A. Knolle, R. Bartenschlager, and U. Protzer. Hepatitis B Virus Targets Lipid Transport Pathways to Infect Hepatocytes. *CMGH*, 16:201–221, 1 2023.

[46] European Medicines Agency. Hepcludex, 2020. `https://www.ema.europa.eu/en/medicines/human/EPAR/hepcludex`, last accessed 09.06.2023.

[47] M. J. Evans, T. von Hahn, D. M. Tscherne, A. J. Syder, M. Panis, B. Wölk, T. Hatziioannou, J. A. McKeating, P. D. Bieniasz, and C. M. Rice. Claudin-1 is a hepatitis C virus co-receptor required for a late step in entry. *Nature*, 446:801–805, 4 2007.

[48] M. J. Farquhar, K. Hu, H. J. Harris, C. Davis, C. L. Brimacombe, S. J. Fletcher, T. F. Baumert, J. Z. Rappoport, P. Balfe, and J. A. McKeating. Hepatitis C Virus Induces CD81 and Claudin-1 Endocytosis. *Journal of Virology*, 86:4305–4316, 4 2012.

[49] M. J. Farquhar and J. A. McKeating. Primary hepatocytes as targets for Hepatitis C virus replication. *Journal of Viral Hepatitis*, 15:849–854, 12 2008.

[50] S. M. Feinstone. History of the Discovery of Hepatitis A Virus. *Cold Spring Harbor Perspectives in Medicine*, 9:a031740, 5 2019.

[51] S. M. Feinstone, A. Z. Kapikian, R. H. Purcell, H. J. Alter, and P. V. Holland. Transfusion-Associated Hepatitis Not Due to Viral Hepatitis Type A or B. *New England Journal of Medicine*, 292:767–770, 4 1975.

[52] D. Finkelshtein, A. Werman, D. Novick, S. Barak, and M. Rubinstein. LDL receptor and its family members serve as the cellular receptors for vesicular stomatitis virus. *Proceedings of the National Academy of Sciences*, 110:7306–7311, 4 2013.

[53] C. Firth, M. Bhat, M. A. Firth, S. H. Williams, M. J. Frye, P. Simmonds, J. M. Conte, J. Ng, J. Garcia, N. P. Bhuva, B. Lee, X. Che, P.-L. Quan, and W. I. Lipkin. Detection of Zoonotic Pathogens and Characterization of Novel Viruses Carried by Commensal Rattus norvegicus in New York City. *mBio*, 5, 10 2014.

[54] A. Funk, M. Mhamdi, H. Will, and H. Sirma. Avian hepatitis B viruses: Molecular and cellular biology, phylogenesis, and host tropism. *China World J Gastroenterol*, 13:91–103, 2007.

[55] W. H. Gerlich. Medical Virology of Hepatitis B: how it began and where we are now. *Virology J*, 10:239, 7 2013.

[56] W. H. Gerlich and W. S. Robinson. Hepatitis B virus contains protein attached to the 5' terminus of its complete DNA strand. *Cell*, 21:801–809, 10 1980.

[57] K. Giersch, O. D. Bhadra, T. Volz, L. Allweiss, K. Riecken, B. Fehse, A. W. Lohse, J. Petersen, C. Sureau, S. Urban, M. Dandri, and M. Lütgehetmann. Hepatitis delta virus persists during liver regeneration and is amplified through cell division both in vitro and in vivo. *Gut*, 68:150–157, 1 2019.

[58] J. S. Glenn, J. M. Taylor, and J. M. White. In vitro-synthesized hepatitis delta virus RNA initiates genome replication in cultured cells. *Journal of Virology*, 64:3104–3107, 6 1990.

[59] T. L. Goldberg, S. D. Sibley, M. E. Pinkerton, C. D. Dunn, L. J. Long, L. C. White, and S. M. Strom. Multidecade Mortality and a Homolog of Hepatitis C Virus in Bald Eagles (Haliaeetus leucocephalus), the National Bird of the USA. *Scientific Reports*, 9:14953, 10 2019.

[60] R. Gosert, D. Egger, V. Lohmann, R. Bartenschlager, H. E. Blum, K. Bienz, and D. Moradpour. Identification of the Hepatitis C Virus RNA Replication Complex inHuh-7 Cells Harboring Subgenomic Replicons. *Journal of Virology*, 77:5487–5492, 5 2003.

[61] E. V. L. Grgacic and D. A. Anderson. St, a Truncated Envelope Protein Derived from the S Protein of Duck Hepatitis B Virus, Acts as a Chaperone for the Folding of the Large Envelope Protein. *Journal of Virology*, 79:5346–5352, 5 2005.

[62] P. Gripon, S. Rumin, S. Urban, J. L. Seyec, D. Glaise, I. Cannie, C. Guyomard, J. Lucas, C. Trepo, and C. Guguen-Guillouzo. Infection of a human hepatoma cell line by hepatitis B virus. *Proceedings of the National Academy of Sciences*, 99:15655–15660, 11 2002.

[63] P. Gripon, J. L. Seyec, S. Rumin, and C. Guguen-Guillouzo. Myristylation of the Hepatitis B Virus Large Surface Protein Is Essential for Viral Infectivity. *Virology*, 213:292–299, 11 1995.

[64] S. Gudima, J. Chang, G. Moraleda, A. Azvolinsky, and J. Taylor. Parameters of Human Hepatitis Delta Virus Genome Replication: the Quantity, Quality, and Intracellular Distribution of Viral Proteins and RNA. *Journal of Virology*, 76:3709–3719, 4 2002.

[65] S. Gudima, A. Meier, R. Dunbrack, J. Taylor, and V. Bruss. Two Potentially Important Elements of the Hepatitis B Virus Large Envelope Protein Are Dispensable for the Infectivity of Hepatitis Delta Virus. *Journal of Virology*, 81:4343–4347, 4 2007.

[66] J. T. Guo and J. C. Pugh. Topology of the large envelope protein of duck hepatitis B virus suggests a mechanism for membrane translocation during particle morphogenesis. *Journal of Virology*, 71:1107–1114, 2 1997.

[67] A. Gömer, R. J. P. Brown, S. Pfaender, K. Deterding, G. Reuter, R. Orton, S. Seitz, C.-T. Bock, J. M. V. Cavalleri, T. Pietschmann, H. Wedemeyer, E. Steinmann, and D. Todt. Intra-host analysis of hepaciviral glycoprotein evolution reveals signatures associated with viral persistence and clearance. *Virus Evolution*, 8, 3 2022.

[68] C. M. Hahn, L. R. Iwanowicz, R. S. Cornman, C. M. Conway, J. R. Winton, and V. S. Blazer. Characterization of a Novel Hepadnavirus in the White Sucker (Catostomus commersonii) from the Great Lakes Region of the United States. *Journal of Virology*, 89:11801–11811, 12 2015.

[69] K. M. Haines and D. D. Loeb. The sequence of the RNA primer and the DNA template influence the initiation of plus-strand DNA synthesis in hepatitis B virus. *Journal of Molecular Biology*, pages 370(3): 471–480, 7 2007.

[70] A. S. Hartlage, J. M. Cullen, and A. Kapoor. The Strange, Expanding World of Animal Hepaciviruses. *Annual Review of Virology*, 3:53–75, 9 2016.

[71] C. Herrscher, P. Roingeard, and E. Blanchard. Hepatitis B Virus Entry into Cells. *Cells*, 9, 6 2020.

[72] M. Hesterman, S. Furrer, B. Fallon, and M. Weller. Analysis of Hepatitis D Virus in Minor Salivary Gland of Sjögren's Disease. *Journal of Dental Research*, 8 2023.

[73] U. Hetzel, L. Szirovicza, T. Smura, B. Prähauser, O. Vapalahti, A. Kipar, and J. Hepojoki. Identification of a Novel Deltavirus in Boa Constrictors. *mBio*, 10:e00014–19, 4 2019.

[74] M. J. Heuschkel, T. F. Baumert, and E. R. Verrier. Cell Culture Models for the Study of Hepatitis D Virus Entry and Infection. *Viruses*, 13:1532, 8 2021.

[75] J. K. T. Ho, B. Jeevan-Raj, and H. J. Netter. Hepatitis B Virus (HBV) Subviral Particles as Protective Vaccines and Vaccine Platforms. *Viruses*, 12, 2 2020.

[76] J. Hoffmann, C. Boehm, K. Himmelsbach, C. Donnerhak, H. Roettger, T. S. Weiss, D. Ploen, and E. Hildt. Identification of -taxilin as an essential factor for the life cycle of hepatitis B virus. *Journal of Hepatology*, 59:934–941, 11 2013.

[77] S. Y. Hsieh, M. Chao, L. Coates, and J. Taylor. Hepatitis delta virus genome replication: a polyadenylated mRNA for delta antigen. *Journal of Virology*, 64:3192–3198, 7 1990.

[78] J. Hu and K. Liu. Complete and Incomplete Hepatitis B Virus Particles: Formation, Function, and Application. *Viruses*, 9, 3 2017.

[79] H.-C. Huang, C.-C. Chen, W.-C. Chang, M.-H. Tao, and C. Huang. Entry of Hepatitis B Virus into Immortalized Human Primary Hepatocytes by Clathrin-Dependent Endocytosis. *Journal of Virology*, 86:9443–9453, 9 2012.

[80] H.-C. Huang, C.-P. Lee, H.-K. Liu, M.-F. Chang, Y.-H. Lai, Y.-C. Lee, and C. Huang. Cellular Nuclear Export Factors TAP and Aly Are Required for HDAg-L-mediated Assembly of Hepatitis Delta Virus. *Journal of Biological Chemistry*, 291:26226–26238, 12 2016.

[81] M. Iwamoto, W. Saso, R. Sugiyama, K. Ishii, M. Ohki, S. Nagamori, R. Suzuki, H. Aizaki, A. Ryo, J. H. Yun, S. Y. Park, N. Ohtani, M. Muramatsu, S. Iwami, Y. Tanaka, C. Sureau, T. Wakita, and K. Watashi. Epidermal growth factor receptor is a host-entry cofactor triggering hepatitis B virus internalization. *Proceedings of the National Academy of Sciences of the United States of America*, 116:8487–8492, 4 2019.

[82] M. Iwamoto, Y. Shibata, J. Kawasaki, S. Kojima, Y. T. Li, S. Iwami, M. Muramatsu, H. L. Wu, K. Wada, K. Tomonaga, K. Watashi, and M. Horie. Identification of novel avian and mammalian deltaviruses provides new insights into deltavirus evolution. *Virus Evolution*, 7, 1 2021.

[83] B. Jiang, K. Himmelsbach, H. Ren, K. Boller, and E. Hildt. Subviral Hepatitis B Virus Filaments, like Infectious Viral Particles, Are Released via Multivesicular Bodies. *Journal of Virology*, 90:3330, 4 2016.

[84] V. Jirasko, R. Montserret, J. Y. Lee, J. Gouttenoire, D. Moradpour, F. Penin, and R. Bartenschlager. Structural and Functional Studies of Nonstructural Protein 2 of the Hepatitis C Virus Reveal Its Key Role as Organizer of Virion Assembly. *PLoS Pathogens*, 6:e1001233, 12 2010.

[85] C. L. Jopling, M. Yi, A. M. Lancaster, S. M. Lemon, and P. Sarnow. Modulation of Hepatitis C Virus RNA Abundance by a Liver-Specific MicroRNA. *Science*, 309:1577–81, 9 2005.

[86] R. Julithe, G. Abou-Jaoudé, and C. Sureau. Modification of the Hepatitis B Virus Envelope Protein Glycosylation Pattern Interferes with Secretion of Viral Particles, Infectivity, and Susceptibility to Neutralizing Antibodies. *Journal of Virology*, 88:9049–9059, 8 2014.

[87] J. Jumper, R. Evans, A. Pritzel, T. Green, M. Figurnov, O. Ronneberger, K. Tunyasuvunakool, R. Bates, A. Žídek, A. Potapenko, A. Bridgland, C. Meyer, S. A. A. Kohl, A. J. Ballard, A. Cowie, B. Romera-Paredes, S. Nikolov, R. Jain, J. Adler, T. Back, S. Petersen, D. Reiman, E. Clancy, M. Zielinski, M. Steinegger, M. Pacholska, T. Berghammer, S. Bodenstein, D. Silver, O. Vinyals, A. W. Senior, K. Kavukcuoglu, P. Kohli, and D. Hassabis. Highly accurate protein structure prediction with AlphaFold. *Nature*, 596:583–589, 8 2021.

[88] M. Junker-Niepmann, R. Bartenschlager, and H. Schaller. A short cis-acting sequence is required for hepatitis B virus pregenome encapsidation and sufficient for packaging of foreign RNA. *The EMBO Journal*, 9:3389–3396, 10 1990.

[89] A. Kapoor, P. Simmonds, G. Gerold, N. Qaisar, K. Jain, J. A. Henriquez, C. Firth, D. L. Hirschberg, C. M. Rice, S. Shields, and W. I. Lipkin. Characterization of a canine homolog of hepatitis C virus. *Proceedings of the National Academy of Sciences*, 108:11608–11613, 7 2011.

[90] A. Kapoor, P. Simmonds, T. K. H. Scheel, B. Hjelle, J. M. Cullen, P. D. Burbelo, L. V. Chauhan, R. Duraisamy, M. S. Leon, K. Jain, K. J. Vandegrift, C. H. Calisher, C. M. Rice, and W. I. Lipkin. Identification of Rodent Homologs of Hepatitis C Virus and Pegiviruses. *mBio*, 4, 5 2013.

[91] C. Koh, B. L. Da, P. Surana, A. Huang, D. Kapuria, Y. Rotman, A. Vittal, C. Gilman, G. Ben-Yakov, C. Lai, et al. A phase 2 study of Lonafarnib, Ritonavir and PEG-Interferon lambda for 24 weeks: Interim end-of-treatment results from the LIFT HDV study. In *Hepatology*, volume 70, pages 1483A–1483A. WILEY 111 RIVER ST, HOBOKEN 07030-5774, NJ USA, 2019.

[92] I. Komla-Soukha and C. Sureau. A tryptophan-rich motif in the carboxyl terminus of the small envelope protein of hepatitis B virus is central to the assembly of hepatitis delta virus particles. *Journal of virology*, 80:4648–4655, 5 2006.

[93] D. Konstantinou and M. Deutsch. The spectrum of HBV/HCV coinfection: epidemiology, clinical characteristics, viralinteractions and management. *Annals of gastroenterology*, 28:221–228, 4-6 2015.

[94] G. Koutsoudakis, E. Herrmann, S. Kallis, R. Bartenschlager, and T. Pietschmann. The Level of CD81 Cell Surface Expression Is a Key Determinant for Productive Entry of Hepatitis C Virus into Host Cells. *Journal of Virology*, 81:588–598, 1 2007.

[95] S. Kress, J. König, J. Schweizer, H. Löhrke, R. Bauer-Hofmann, and M. Schwarz. p53 mutations are absent from carcinogen-induced mouse liver tumors but occur in cell lines established from these tumors. *Molecular Carcinogenesis*, 6:148–158, 1992.

[96] M. Y. Kuo, M. Chao, and J. Taylor. Initiation of replication of the human hepatitis delta virus genome from cloned DNA: role of delta antigen. *Journal of Virology*, 63:1945–1950, 5 1989.

[97] M. Y. Kuo, J. Goldberg, L. Coates, W. Mason, J. Gerin, and J. Taylor. Molecular cloning of hepatitis delta virus RNA from an infected woodchuck liver: sequence, structure, and applications. *Journal of Virology*, 62:1855–1861, 6 1988.

[98] M. Y. Kuo, L. Sharmeen, G. Dinter-Gottlieb, and J. Taylor. Characterization of self-cleaving RNA sequences on the genome and antigenome of human hepatitis delta virus. *Journal of Virology*, 62:4439–4444, 12 1988.

[99] S. K. Ladner, M. J. Otto, C. S. Barker, K. Zaifert, G. H. Wang, J. T. Guo, C. Seeger, and R. W. King. Inducible expression of human hepatitis B virus (HBV) in stably transfected hepatoblastoma cells: a novel system for screening potential inhibitors of HBV replication. *Antimicrobial Agents and Chemotherapy*, 41:1715–1720, 8 1997.

[100] W. K. Lai, P. J. Sun, J. Zhang, A. Jennings, P. F. Lalor, S. Hubscher, J. A. McKeating, and D. H. Adams. Expression of DC-SIGN and DC-SIGNR on Human Sinusoidal Endothelium : A Role for Capturing Hepatitis C Virus Particles. *The American Journal of Pathology*, 169:200, 7 2006.

[101] C. Lambert and R. Prange. Dual Topology of the Hepatitis B Virus Large Envelope Protein. *Journal of Biological Chemistry*, 276:22265–22272, 6 2001.

[102] C. Lambert, N. Thomé, C. J. Kluck, and R. Prange. Functional incorporation of green fluorescent protein into hepatitis B virus envelope particles. *Virology*, 330:158–167, 12 2004.

[103] P. Lampertico, K. Agarwal, T. Berg, M. Buti, H. L. Janssen, G. Papatheodoridis, F. Zoulim, and F. Tacke. EASL 2017 Clinical Practice Guidelines on the management of hepatitis B virus infection. *Journal of Hepatology*, 67:370–398, 8 2017.

[104] C. Lauber, S. Seitz, S. Mattei, A. Suh, J. Beck, J. Herstein, J. Börold, W. Salzburger, L. Kaderali, J. A. Briggs, and R. Bartenschlager. Deciphering the Origin and Evolution of Hepatitis B Viruses by Means of a Family of Non-enveloped Fish Viruses. *Cell Host and Microbe*, 22:387–399.e6, 9 2017.

[105] M. Lauck, S. D. Sibley, J. Lara, M. A. Purdy, Y. Khudyakov, D. Hyeroba, A. Tumukunde, G. Weny, W. M. Switzer, C. A. Chapman, A. L. Hughes, T. C. Friedrich, D. H. O'Connor, and T. L. Goldberg. A Novel Hepacivirus with an Unusually Long and Intrinsically Disordered NS5A Protein in a Wild Old World Primate. *Journal of Virology*, 87:8971–8981, 8 2013.

[106] L. Lecoq, S. Wang, M. Dujardin, P. Zimmermann, L. Schuster, M. L. Fogeron, M. Briday, M. Schledorn, T. Wiegand, L. Cole, R. Montserret, S. Bressanelli, B. H. Meier, M. Nassal, and A. Böckmann. A pocket-factor–triggered conformational switch in the hepatitis B virus capsid. *Proceedings of the National Academy of Sciences of the United States of America*, 118:e2022464118, 4 2021.

[107] J. Y. Lee, M. Cortese, U. Haselmann, K. Tabata, I. Romero-Brey, C. Funaya, N. L. Schieber, Y. Qiang, M. Bartenschlager, S. Kallis, C. Ritter, K. Rohr, Y. Schwab, A. Ruggieri, and R. Bartenschlager. Spatiotemporal Coupling of the Hepatitis C Virus Replication Cycle by Creating a Lipid Droplet- Proximal Membranous Replication Compartment. *Cell Reports*, 27:3602–3617.e5, 6 2019.

[108] C. M. Leistner, S. Gruen-Bernhard, and D. Glebe. Role of glycosaminoglycans for binding and infection of hepatitis B virus. *Cellular Microbiology*, 10:122–133, 1 2008.

[109] F. A. Lempp, P. Mutz, C. Lipps, D. Wirth, R. Bartenschlager, and S. Urban. Evidence that hepatitis B virus replication in mouse cells is limited by the lack of a host cell dependency factor. *Journal of Hepatology*, 64:556–564, 3 2016.

[110] F. A. Lempp, Y. Ni, and S. Urban. Hepatitis delta virus: Insights into a peculiar pathogen and novel treatment options. *Nature Reviews Gastroenterology and Hepatology*, 13:580–589, 10 2016.

[111] F. A. Lempp, F. Schlund, L. Rieble, L. Nussbaum, C. Link, Z. Zhang, Y. Ni, and S. Urban. Recapitulation of HDV infection in a fully permissive hepatoma cell line allows efficient drug evaluation. *Nature Communications*, 10:2265, 5 2019.

[112] H. Liu, X. Hong, J. Xi, S. Menne, J. Hu, and J. C.-Y. Wang. Cryo-EM structures of human hepatitis B and woodchuck hepatitis virus small spherical subviral particles. *Science advances*, 8, 8 2022.

[113] K. Lo, S. B. Hwang, R. Duncan, M. Trousdale, and M. M. Lai. Characterization of mRNA for Hepatitis Delta Antigen: Exclusion of the Full-Length Antigenomic RNA as an mRNA. *Virology*, 250:94–105, 10 1998.

[114] V. Lohmann. Hepatitis C virus cell culture models: an encomium on basic research paving the road to therapy development. *Medical Microbiology and Immunology*, 208:3–24, 2 2019.

[115] V. Lohmann, J. O. Koch, and R. Bartenschlager. Processing pathways of the hepatitis C virus proteins. *Journal of Hepatology*, 24:11–9, 1996.

[116] S.-N. Lu, T.-M. Chen, C.-M. Lee, J.-H. Wang, H.-D. Tung, and J.-C. Wu. Molecular epidemiological and clinical aspects of hepatitis D virus in a unique triple hepatitis viruses (B, C, D) endemic community in Taiwan. *Journal of Medical Virology*, 70:74–80, 5 2003.

[117] G. X. Luo, M. Chao, S. Y. Hsieh, C. Sureau, K. Nishikura, and J. Taylor. A specific base transition occurs on replicating hepatitis delta virus RNA. *Journal of Virology*, 64:1021–1027, 3 1990.

[118] Y. Ma, M. Anantpadma, J. M. Timpe, S. Shanmugam, S. M. Singh, S. M. Lemon, and M. Yi. Hepatitis C Virus NS2 Protein Serves as a Scaffold for Virus Assembly by Interacting with both Structural and Nonstructural Proteins. *Journal of Virology*, 85:86–97, 1 2011.

[119] T. B. Macnaughton and M. M. Lai. *Hepatitis Delta Virus RNA Transfection for the Cell Culture Model*. Humana Press, 2004.

[120] T. B. Macnaughton and M. M. C. Lai. Genomic but Not Antigenomic Hepatitis Delta Virus RNA Is Preferentially Exported from the Nucleus Immediately after Synthesis and Processing. *Journal of Virology*, 76:3928–3935, 4 2002.

[121] T. B. Macnaughton, Y. J. Wang, and M. M. Lai. Replication of hepatitis delta virus RNA: effect of mutations of the autocatalytic cleavage sites. *Journal of Virology*, 67:2228–2234, 4 1993.

[122] A. Macovei, C. Radulescu, C. Lazar, S. Petrescu, D. Durantel, R. A. Dwek, N. Zitzmann, and N. B. Nichita. Hepatitis B Virus Requires Intact Caveolin-1 Function for Productive Infection in HepaRG Cells. *Journal of Virology*, 84:243–253, 1 2010.

[123] D. R. Macrae, V. Bruss, and D. Ganem. Myristylation of a duck hepatitis B virus envelope protein is essential for infectivity but not for virus assembly. *Virology*, 181:359–363, 3 1991.

[124] P.-E. Mangeot, S. Dollet, M. Girard, C. Ciancia, S. Joly, M. Peschanski, and V. Lotteau. Protein Transfer Into Human Cells by VSV-G-induced Nanovesicles. *Molecular Therapy*, 19:1656–1666, 9 2011.

[125] M. G. Mavilia and G. Y. Wu. HBV-HCV Coinfection: Viral Interactions, Management, and Viral Reactivation. *Journal of Clinical and Translational Hepatology*, 6:1–10, 9 2018.

[126] I. Mederacke, B. Bremer, B. Heidrich, J. Kirschner, K. Deterding, T. Bock, K. Wursthorn, M. P. Manns, and H. Wedemeyer. Establishment of a Novel Quantitative Hepatitis D Virus (HDV) RNA Assay Using the Cobas TaqMan Platform To Study HDV RNA Kinetics. *Journal of Clinical Microbiology*, 48:2022–2029, 6 2010.

[127] A. Merz, G. Long, M.-S. Hiet, B. Brügger, P. Chlanda, P. Andre, F. Wieland, J. Krijnse-Locker, and R. Bartenschlager. Biochemical and Morphological Properties of Hepatitis C Virus Particles and Determination of Their Lipidome. *Journal of Biological Chemistry*, 286:3018–3032, 1 2011.

[128] J. K. Millet, J. A. Jaimes, and G. R. Whittaker. Molecular diversity of coronavirus host cell entry receptors. *FEMS Microbiology Reviews*, 45, 5 2021.

[129] L. E. Modahl, T. B. Macnaughton, N. Zhu, D. L. Johnson, and M. M. C. Lai. RNA-Dependent Replication and Transcription of Hepatitis Delta Virus RNA Involve Distinct Cellular RNA Polymerases. *Molecular and Cellular Biology*, 20:6030–6039, 8 2000.

[130] D. Moradpour, C. Englert, T. Wakita, and J. R. Wands. Characterization of Cell Lines Allowing Tightly Regulated Expression of Hepatitis C Virus Core Protein. *Virology*, 222:51–63, 8 1996.

[131] D. Moradpour, F. Penin, and C. M. Rice. Replication of hepatitis C virus. *Nature Reviews Microbiology*, 5:453–463, 6 2007.

[132] P. Mutz, P. Metz, F. A. Lempp, S. Bender, B. Qu, K. Schöneweis, S. Seitz, T. Tu, A. Restuccia, J. Frankish, C. Dächert, B. Schusser, R. Koschny, G. Polychronidis, P. Schemmer, K. Hoffmann, T. F. Baumert, M. Binder, S. Urban, and R. Bartenschlager. HBV Bypasses the Innate Immune Response and Does Not Protect HCV From Antiviral Activity of Interferon. *Gastroenterology*, 154:1791–1804.e22, 5 2018.

[133] S. Nagashima, M. Takahashi, T. Kobayashi, T. Nishizawa, T. Nishiyama, P. P. Primadharsini, and H. Okamoto. Characterization of the Quasi-Enveloped Hepatitis E Virus Particles Released by the Cellular Exosomal Pathway. *Journal of Virology*, 91, 11 2017.

[134] H. Nakabayashi, K. Taketa, K. Miyano, T. Yamane, and J. Sato. Growth of human hepatoma cells lines with differentiated functions in chemically defined medium. *Cancer research*, 42:3858–63, 9 1982.

[135] M. Nassal. Hepatitis B viruses: Reverse transcription a different way. *Virus Research*, 134:235–249, 6 2008.

[136] M. Nassal. HBV cccDNA: viral persistence reservoir and key obstacle for a cure of chronic hepatitis B. *Gut*, 64:1972–1984, 12 2015.

[137] M. Nassal and A. Rieger. A Bulged Region of the Hepatitis B Virus RNA Encapsidation Signal Contains the Replication Origin for Discontinuous First-Strand DNA Synthesis. *Journal of Virology*, 70:2764–2773, 5 1996.

[138] National Center for Biotechnology Information (NCBI). ADAR - Adenosine deaminase RNA specific, Orthologs, 2023. `https://www.ncbi.nlm.nih.gov/gene/103/ortholog/?scope=89593`, last accessed 26.07.2023.

[139] N. Ndongo-Thiam, P. Berthillon, E. Errazuriz, I. Bordes, S. D. Sequeira, C. Trépo, and M.-A. Petit. Long-term propagation of serum hepatitis C virus (HCV) with production of enveloped HCV particles in human HepaRG hepatocytes. *Hepatology*, 54:406–417, 8 2011.

[140] H. J. Netter, M. H. Barrios, M. Littlejohn, and L. K. Yuen. Hepatitis Delta Virus (HDV) and Delta-Like Agents: Insights Into Their Origin. *Frontiers in Microbiology*, 12, 6 2021.

[141] H. J. Netter, J. L. Gerin, B. C. Tennant, and J. M. Taylor. Apparent helper-independent infection of woodchucks by hepatitis delta virus and subsequent rescue with woodchuck hepatitis virus. *Journal of Virology*, 68:5344–5350, 9 1994.

[142] C. J. Neufeldt, M. Cortese, E. G. Acosta, and R. Bartenschlager. Rewiring cellular networks by members of the Flaviviridae family. *Nature Reviews Microbiology*, 16:125–142, 2 2018.

[143] Y. Ni, Z. Zhang, L. Engelskircher, G. Verch, T. Tu, F. A. Lempp, and S. Urban. Generation and characterization of a stable cell line persistently replicating and secreting the human hepatitis delta virus. *Scientific Reports*, 9:1–14, 7 2019.

[144] M. Nomaguchi, M. Fujita, Y. Miyazaki, and A. Adachi. Viral Tropism. *Frontiers in Microbiology*, 3, 8 2012.

[145] B. O'Malley and D. W. Lazinski. Roles of Carboxyl-Terminal and Farnesylated Residues in the Functions of the Large Hepatitis Delta Antigen. *Journal of Virology*, 79:1142–1153, 1 2005.

[146] Q. Osseman, L. Gallucci, S. Au, C. Cazenave, E. Berdance, M. L. Blondot, A. Cassany, D. Bégu, J. Ragues, C. Aknin, I. Sominskaya, A. Dishlers, B. Rabe, F. Anderson, N. Panté, and M. Kann. The chaperone dynein LL1 mediates cytoplasmic transport of empty and mature hepatitis B virus capsids. *Journal of hepatology*, 68:441–448, 3 2018.

[147] S. Paraskevopoulou, F. Pirzer, N. Goldmann, J. Schmid, V. M. Corman, L. T. Gottula, S. Schroeder, A. Rasche, D. Muth, J. F. Drexler, A. C. Heni, G. J. Eibner, R. A. Page, T. C. Jones, M. A. Müller, S. Sommer, D. Glebe, and C. Drosten. Mammalian deltavirus without hepadnavirus coinfection in the neotropical rodent Proechimys semispinosus. *Proceedings of the National Academy of Sciences of the United States of America*, 117:17977–17983, 7 2020.

[148] E.-M. Park, L. N. Nguyen, Y.-S. Lim, and S. B. Hwang. Farnesyl-diphosphate farnesyltransferase 1 regulates hepatitis C virus propagation. *FEBS Letters*, 588:1813–1820, 5 2014.

[149] D. Paul, V. Madan, and R. Bartenschlager. Hepatitis C Virus RNA Replication and Assembly: Living on the Fat of the Land. *Cell Host & Microbe*, pages 569–579, 11 2014.

[150] J. Perez-Vargas, F. Amirache, B. Boson, C. Mialon, N. Freitas, C. Sureau, F. Fusil, and F. L. Cosset. Enveloped viruses distinct from HBV induce dissemination of hepatitis D virus in vivo. *Nature Communications*, 10, 5 2019.

[151] D. H. Persing, H. E. Varmus, and D. Ganem. Inhibition of Secretion of Hepatitis B Surface Antigen by a Related Presurface Polypeptide. *Science*, 234:1388–1391, 12 1986.

[152] L. S. Pflüger, J. S. zur Wiesch, S. Polywka, and M. Lütgehetmann. Hepatitis delta virus propagation enabled by hepatitis C virus—Scientifically intriguing, but is it relevant to clinical practice? *Journal of Viral Hepatitis*, 28:213–216, 1 2021.

[153] T. Pietschmann, V. Lohmann, G. Rutter, K. Kurpanek, and R. Bartenschlager. Characterization of Cell Lines Carrying Self-Replicating Hepatitis C Virus RNAs. *Journal of Virology*, 75:1252–1264, 2 2001.

[154] P. Pileri, Y. Uematsu, S. Campagnoli, G. Galli, F. Falugi, R. Petracca, A. J. Weiner, M. Houghton, D. Rosa, G. Grandi, and S. Abrignani. Binding of Hepatitis C Virus to CD81. *Science*, 282:938–941, 10 1998.

[155] A. Ploss, M. J. Evans, V. A. Gaysinskaya, M. Panis, H. You, Y. P. de Jong, and C. M. Rice. Human occludin is a hepatitis C virus entry factor required for infection of mouse cells. *Nature*, 457:882–886, 2 2009.

[156] A. G. Poison, B. L. Bass, and J. L. Casey. RNA editing of hepatitis delta virus antigenome by dsRNA-adenosine deaminase. *Nature*, 380:454–456, 4 1996.

[157] J. C. Pugh, J. J. Sninsky, J. W. Summers, and E. Schaeffer. Characterization of a pre-S polypeptide on the surfaces of infectious avian hepadnavirus particles. *Journal of virology*, 61:1384–90, 5 1987.

[158] P.-L. Quan, C. Firth, J. M. Conte, S. H. Williams, C. M. Zambrana-Torrelio, S. J. Anthony, J. A. Ellison, A. T. Gilbert, I. V. Kuzmin, M. Niezgoda, M. O. V. Osinubi, S. Recuenco, W. Markotter, R. F. Breiman, L. Kalemba, J. Malekani, K. A. Lindblade, M. K. Rostal, R. Ojeda-Flores, G. Suzan, L. B. Davis, D. M. Blau, A. B. Ogunkoya, D. A. A. Castillo, D. Moran, S. Ngam, D. Akaibe, B. Agwanda, T. Briese, J. H. Epstein, P. Daszak, C. E. Rupprecht, E. C. Holmes, and W. I. Lipkin. Bats are a major natural reservoir for hepaciviruses and pegiviruses. *Proceedings of the National Academy of Sciences*, 110:8194–8199, 5 2013.

[159] M. Rizzetto, M. G. Canese, J. L. Gerin, W. T. London, D. L. Sly, and R. H. Purcell. Transmission of the Hepatitis B Virus-Associated Delta Antigen to Chimpanzees. *Journal of Infectious Diseases*, 141:590–602, 5 1980.

[160] M. Rizzetto, B. Hoyer, M. G. Canese, J. W. Shih, R. H. Purcell, and J. L. Gerin. delta Agent: association of delta antigen with hepatitis B surface antigen and RNA in serum of delta-infected chimpanzees. *Proceedings of the National Academy of Sciences*, 77:6124–6128, 10 1980.

[161] Robert Koch Institut. Ratgeber Hepatitis E, 2015. `https://www.rki.de/DE/Content/Infekt/EpidBull/Merkblaetter/Ratgeber_HepatitisE.html`, last accessed 08.06.2023.

[162] Robert Koch Institut. Ratgeber Hepatitis B und D, 2016. `https://www.rki.de/DE/Content/Infekt/EpidBull/Merkblaetter/Ratgeber_HepatitisB.html?nn=2390060`, last accessed 08.06.2023.

[163] Robert Koch Institut. Ratgeber Hepatitis C, 2018. `https://www.rki.de/DE/Content/Infekt/EpidBull/Merkblaetter/Ratgeber_HepatitisC.html`, last accessed 09.06.2023.

[164] Robert Koch Institut. Ratgeber Hepatitis A, 2023. `https://www.rki.de/DE/Content/Infekt/EpidBull/Merkblaetter/Ratgeber_HepatitisA.html`, last accessed 08.06.2023.

[165] P. C. Roberts, T. Kipperman, and R. W. Compans. Vesicular stomatitis virus G protein acquires pH-independent fusion activity during transport in a polarized endometrial cell line. *Journal of virology*, 73:10447–57, 12 1999.

[166] I. Romero-Brey, A. Merz, A. Chiramel, J.-Y. Lee, P. Chlanda, U. Haselman, R. Santarella-Mellwig, A. Habermann, S. Hoppe, S. Kallis, P. Walther, C. Antony, J. Krijnse-Locker, and R. Bartenschlager. Three-Dimensional Architecture and Biogenesis of Membrane Structures Associated with Hepatitis C Virus Replication. *PLoS Pathogens*, 8:e1003056, 12 2012.

[167] D. Rupp. Establishing novel tools for studying Hepatitis C virus replication and pathogenesis; PhD thesis, 2017.

[168] W. S. Ryu, H. J. Netter, M. Bayer, and J. Taylor. Ribonucleoprotein complexes of hepatitis delta virus. *Journal of Virology*, 67:3281–3287, 6 1993.

[169] J. Schindelin, I. Arganda-Carreras, E. Frise, V. Kaynig, M. Longair, T. Pietzsch, S. Preibisch, C. Rueden, S. Saalfeld, B. Schmid, J.-Y. Tinevez, D. J. White, V. Hartenstein, K. Eliceiri, P. Tomancak, and A. Cardona. Fiji: an open-source platform for biological-image analysis. *Nature Methods*, 9:676–682, 7 2012.

[170] S. Schreiner and M. Nassal. A Role for the Host DNA Damage Response in Hepatitis B Virus cccDNA Formation—and Beyond? *Viruses*, 9, 5 2017.

[171] A. Schulze, P. Gripon, and S. Urban. Hepatitis B virus infection initiates with a large surface protein-dependent binding to heparan sulfate proteoglycans. *Hepatology*, 46:1759–1768, 12 2007.

[172] C. Seeger and W. S. Mason. Hepatitis B Virus Biology. *Microbiology and Molecular Biology Reviews*, 64:51–68, 3 2000.

[173] S. Seitz, J. Habjanič, A. K. Schütz, and R. Bartenschlager. The Hepatitis B Virus Envelope Proteins: Molecular Gymnastics Throughout the Viral Life Cycle. *Annual review of virology*, 7:263–288, 9 2020.

[174] S. Seitz, C. Iancu, T. Volz, W. Mier, M. Dandri, S. Urban, and R. Bartenschlager. A Slow Maturation Process Renders Hepatitis B Virus Infectious. *Cell Host and Microbe*, 20:25–35, 7 2016.

[175] L. Selzer and A. Zlotnick. Assembly and Release of Hepatitis B Virus. *Cold Spring Harbor Perspectives in Medicine*, 5, 12 2015.

[176] N. R. Sharma, G. Mateu, M. Dreux, A. Grakoui, F.-L. Cosset, and G. B. Melikyan. Hepatitis C Virus Is Primed by CD81 Protein for Low pH-dependent Fusion. *Journal of Biological Chemistry*, 286:30361–30376, 9 2011.

[177] M. Shi, X.-D. Lin, N. Vasilakis, J.-H. Tian, C.-X. Li, L.-J. Chen, G. Eastwood, X.-N. Diao, M.-H. Chen, X. Chen, X.-C. Qin, S. G. Widen, T. G. Wood, R. B. Tesh, J. Xu, E. C. Holmes, and Y.-Z. Zhang. Divergent Viruses Discovered in Arthropods and Vertebrates Revise the Evolutionary History of the Flaviviridae and Related Viruses. *Journal of Virology*, 90:659–669, 1 2016.

[178] Y. Shi, Y. Wu, W. Zhang, J. Qi, and G. F. Gao. Enabling the 'host jump': structural determinants of receptor-binding specificity in influenza A viruses. *Nature Reviews Microbiology*, 12:822–831, 12 2014.

[179] H. Stirk, J. Thornton, and C. Howard. A topological Model for Hepatitis B Surface Antigen. *Intervirology*, 33:148–158, 1992.

[180] C. Sureau, B. Guerra, and R. E. Lanford. Role of the large hepatitis B virus envelope protein in infectivity of the hepatitis delta virion. *Journal of Virology*, 67:366–372, 1 1993.

[181] C. Sureau, B. Guerra, and H. Lee. The middle hepatitis B virus envelope protein is not necessary for infectivity of hepatitis delta virus. *Journal of virology*, 68:4063–4066, 6 1994.

[182] C. Sureau and J. Salisse. A conformational heparan sulfate binding site essential to infectivity overlaps with the conserved hepatitis B virus a-determinant. *Hepatology (Baltimore, Md.)*, 57:985–994, 3 2013.

[183] Swiss Institute for Bioinformatics. Expasy translate tool, 2023. `https://web.expasy.org/translate/`, last accessed 29.07.2023.

[184] W. Szmuness, C. E. Stevens, E. J. Harley, E. A. Zang, W. R. Oleszko, D. C. William, R. Sadovsky, J. M. Morrison, and A. Kellner. Hepatitis B Vaccine. *New England Journal of Medicine*, 303:833–841, 10 1980.

[185] Z. H. Taji, P. Bielytskyi, M. Shein, M.-A. Sani, S. Seitz, and A. K. Schütz. Transient RNA Interactions Leave a Covalent Imprint on a Viral Capsid Protein. *Journal of the American Chemical Society*, 144:8536–8550, 5 2022.

[186] J. P. Tavanez, C. Cunha, M. C. Silva, E. David, J. Monjardino, and M. Carmo-Fonseca. Hepatitis delta virus ribonucleoproteins shuttle between the nucleus and the cytoplasm. *Rna*, 8:637–646, 5 2002.

[187] J. Taylor and M. Pelchat. Origin of hepatitis virus. *Future Microbiology*, 5:393–402, 3 2010.

[188] N. A. Terrault, A. S. Lok, B. J. McMahon, K. Chang, J. P. Hwang, M. M. Jonas, R. S. Brown, N. H. Bzowej, and J. B. Wong. Update on prevention, diagnosis, and treatment of chronic hepatitis B: AASLD 2018 hepatitis B guidance. *Hepatology*, 67:1560–1599, 4 2018.

[189] The Human Protein Atlas. SLC10A1, 2023. `https://www.proteinatlas.org/ENSG00000100652-SLC10A1/tissue`, last accessed 16.07.2023.

[190] V. L. D. Thi, C. Granier, M. B. Zeisel, M. Guérin, J. Mancip, O. Granio, F. Penin, D. Lavillette, R. Bartenschlager, T. F. Baumert, F.-L. Cosset, and M. Dreux. Characterization of Hepatitis C Virus Particle Subpopulations Reveals Multiple Usage

of the Scavenger Receptor BI for Entry Steps. *Journal of Biological Chemistry*, 287:31242–31257, 9 2012.

[191] J. Thézé, S. Lowes, J. Parker, and O. G. Pybus. Evolutionary and Phylogenetic Analysis of the Hepaciviruses and Pegiviruses. *Genome Biology and Evolution*, 7:2996–3008, 11 2015.

[192] C. Trépo, H. L. Chan, and A. Lok. Hepatitis B virus infection. *Lancet (London, England)*, 384:2053–2063, 12 2014.

[193] W.-C. Tsai, P. W.-C. Hsu, T.-C. Lai, G.-Y. Chau, C.-W. Lin, C.-M. Chen, C.-D. Lin, Y.-L. Liao, J.-L. Wang, Y.-P. Chau, M.-T. Hsu, M. Hsiao, H.-D. Huang, and A.-P. Tsou. MicroRNA-122, a tumor suppressor microRNA that regulates intrahepatic metastasis of hepatocellular carcinoma. *Hepatology*, 49:1571–1582, 5 2009.

[194] B. Tsatsralt-Od, M. Takahashi, T. Nishizawa, K. Endo, J. Inoue, and H. Okamoto. High prevalence of dual or triple infection of hepatitis B, C, and delta viruses among patients with chronic liver disease in Mongolia. *Journal of Medical Virology*, 77:491–499, 11 2005.

[195] D. M. Tscherne, M. J. Evans, T. von Hahn, C. T. Jones, Z. Stamataki, J. A. McKeating, B. D. Lindenbach, and C. M. Rice. Superinfection Exclusion in Cells Infected with Hepatitis C Virus. *Journal of Virology*, 81:3693–3703, 4 2007.

[196] S. Tsukuda and K. Watashi. Hepatitis B virus biology and life cycle. *Antiviral Research*, 182:104925, 10 2020.

[197] T. Tu, M. A. Budzinska, N. A. Shackel, and S. Urban. HBV DNA integration: Molecular mechanisms and clinical implications. *Viruses*, 9, 4 2017.

[198] UniProt. DHBV large envelope protein, accession number P17195, 2023. `https://www.uniprot.org/uniprotkb/P17195/entry#P17195-2`, last accessed 29.07.2023.

[199] S. Urban, R. Bartenschlager, R. Kubitz, and F. Zoulim. Strategies to Inhibit Entry of HBV and HDV Into Hepatocytes. *Gastroenterology*, 147:48–64, 7 2014.

[200] S. Urban and P. Gripon. Inhibition of Duck Hepatitis B Virus Infection by a Myristoylated Pre-S Peptide of the Large Viral Surface Protein. *Journal of Virology*, 76:1986–1990, 2 2002.

[201] S. Urban, C. Neumann-Haefelin, and P. Lampertico. Hepatitis D virus in 2021: virology, immunology and new treatment approaches for a difficult-to-treat disease. *Gut*, 70:1782–1794, 9 2021.

[202] K.-A. Walters, M. A. Joyce, W. R. Addison, K. P. Fischer, and D. L. J. Tyrrell. Superinfection Exclusion in Duck Hepatitis B Virus Infection Is Mediated by the Large Surface Antigen. *Journal of Virology*, 78:7925–7937, 8 2004.

[203] W. Wang, F. A. Lempp, F. Schlund, L. Walter, C. C. Decker, Z. Zhang, Y. Ni, and S. Urban. Assembly and infection efficacy of hepatitis B virus surface protein exchanges in 8 hepatitis D virus genotype isolates. *Journal of Hepatology*, 75:311–323, 8 2021.

[204] T. Watanabe, E. M. Sorensen, A. Naito, M. Schott, S. Kim, and P. Ahlquist. Involvement of host cellular multivesicular body functions in hepatitis B virus budding. *Proceedings of the National Academy of Sciences of the United States of America*, 104:10205–10210, 6 2007.

[205] A. M. Waterhouse, J. B. Procter, D. M. A. Martin, M. Clamp, and G. J. Barton. Jalview Version 2—a multiple sequence alignment editor and analysis workbench. *Bioinformatics*, 25:1189–1191, 5 2009.

[206] H. Wedemeyer, K. Schoeneweis, P. Bogomolov, V. Voronka, V. Chulanov, T. Stepanova, L. Allweiss, M. Dandri, J. Burhenne, W. Haefeli, et al. Final results of a multicenter, open-label phase 2 clinical trial (MYR203) to assess safety and efficacy of myrcludex B in combination with PEG-interferon Alpha 2a in patients with chronic HBV/HDV co-infection. *J Hepatol*, 70(Suppl 1):e81, 2019.

[207] M. L. Weller, M. R. Gardener, Z. C. Bogus, M. A. Smith, E. Astorri, D. G. Michael, D. A. Michael, C. Zheng, P. D. Burbelo, Z. Lai, P. A. Wilson, W. Swaim, B. Handelman, S. A. Afione, M. Bombardieri, and J. A. Chiorini. Hepatitis Delta Virus Detected in Salivary Glands of Sjögren's Syndrome Patients and Recapitulates a Sjögren's Syndrome-Like Phenotype in Vivo. *Pathogens and Immunity*, 1:12, 5 2016.

[208] M. D. Weltman, A. Brotodihardjo, E. B. Crewe, G. C. Farrell, M. Bililus, J. M. Grierson, and C. Liddle. Coinfection with hepatitis B and C or B, C and viruses results in severe chronic liver disease and responds poorly to terferon-a treatment. *Journal of Viral Hepatitis*, 2:39–45, 1 1995.

[209] S. F. Wieland, S. Asabe, R. E. Engle, R. H. Purcell, and F. V. Chisari. Limited Hepatitis B Virus Replication Space in the Chronically Hepatitis C Virus-Infected Liver. *Journal of Virology*, 88:5184–5188, 5 2014.

[210] H. Will, W. Reiser, T. Weimer, E. Pfaff, M. Buscher, R. Sprengel, R. Cattaneo, and H. Schaller. Replication Strategy of Human Hepatitis B Virus. *Journal of Virology*, 61:904–911, 3 1987.

[211] M. Wille, H. J. Netter, M. Littlejohn, L. Yuen, M. Shi, J.-S. Eden, M. Klaassen, E. C. Holmes, and A. C. Hurt. A Divergent Hepatitis D-Like Agent in Birds. *Viruses*, 10:720, 12 2018.

[212] Wordl Health Organization. Fact sheet Hepatitis C, 2023. `https://www.who.int/news-room/fact-sheets/detail/hepatitis-c`, last accessed 09.06.2023.

[213] World Health Organisation. Global Hepatitis Report. *https://www.who.int/publications/i/item/9789241565455*, 2017.

[214] World Health Organization. Fact sheet Hepatitis D, 2022. `https://www.who.int/news-room/fact-sheets/detail/hepatitis-d`, last accessed 09.06.2023.

[215] World Health Organization. Fact sheet Hepatitis B, 2023. `https://www.who.int/news-room/fact-sheets/detail/hepatitis-b`, last accessed 08.06.2023.

[216] H. Yan, G. Zhong, G. Xu, W. He, Z. Jing, Z. Gao, Y. Huang, Y. Qi, B. Peng, H. Wang, L. Fu, M. Song, P. Chen, W. Gao, B. Ren, Y. Sun, T. Cai, X. Feng, J. Sui, and W. Li. Sodium taurocholate cotransporting polypeptide is a functional receptor for human hepatitis B and D virus. *eLife*, 2012:1–28, 11 2012.

[217] D. Yang, C. Zuo, X. Wang, X. Meng, B. Xue, N. Liu, R. Yu, Y. Qin, Y. Gao, Q. Wang, J. Hu, L. Wang, Z. Zhou, B. Liu, D. Tan, Y. Guan, and H. Zhu. Complete replication of hepatitis B virus and hepatitis C virus in a newly developed hepatoma cell line. *Proceedings of the National Academy of Sciences*, 111, 4 2014.

[218] X.-L. Zhang, X.-Y. Yao, Y.-Q. Zhang, Z.-H. Lv, H. Liu, J. Sun, and J.-W. Shao. A Highly Divergent Hepacivirus Identified in Domestic Ducks Further Reveals the Genetic Diversity of Hepaciviruses. *Viruses*, 14:371, 2 2022.

[219] Z. Zhang, Y. Ni, F. A. Lempp, L. Walter, P. Mutz, R. Bartenschlager, and S. Urban. Hepatitis D virus-induced interferon response and administered interferons control cell division-mediated virus spread. *Journal of Hepatology*, 77:957–966, 10 2022.

[220] J. Zi, X. Gao, J. Du, H. Xu, J. Niu, and X. Chi. Multiple Regions Drive Hepatitis Delta Virus Proliferation and Are Therapeutic Targets. *Frontiers in Microbiology*, 13, 4 2022.

[221] B. F. Zuberi, S. Afsar, and M. S. Quraishy. Triple hepatitis: frequency and treatment outcome of co/super-infection of hepatitis C and D among patients of hepatitis B. *Journal of the College of Physicians and Surgeons–Pakistan : JCPSP*, 18:404–7, 7 2008.

[222] H. J. Zuccola, J. E. Rozzelle, S. M. Lemon, B. W. Erickson, and J. M. Hogle. Structural basis of the oligomerization of hepatitis delta antigen. *Structure*, 6:821–830, 7 1998.

Appendix

As indicated in section 4.4, a subsequent analysis was undertaken regarding host factors associated with HCV and HBV. The following section provides a description of the primary findings derived from these experiments

7.1 Studies on hepatitis virus host factors

7.1.1 FGFR4 as a potential dependency factor for HCV in HepaRG cells

Investigating triple infections of HBV/HCV/HDV *in vitro* is challenging due to the limited availability of cell culture models supporting replication of all three viruses. In fact, only primary human hepatocytes (PHH) can be infected with HBV, HCV, and HDV. However, infection efficiency is low in these cells, especially for HCV [49], and significant inter-batch and -patient variations are observed. HepaRG serve as the next closest model to PHH and support robust replication of HBV and HDV [62, 199]. They have also been shown to support HCV replication [139]. However, in our lab, we were unable to establish productive HCV replication in this cell line. A former member of our group identified FGFR4 as a potential dependency factor for HCV in HepaRG cells [167]. Therefore, I investigated the replication of a luciferase-tagged sgHCV in HepaRG cells overexpressing FGFR4 (HepaRG-FGFR4) upon RNA transfection. While this replicon efficiently induced replication in Huh7 cells, no luciferase activity could be observed in HepaRG and HepaRG-FGFR4 cells (see Fig. 7.1). Therefore, FGFR4 was not further explored as a potential HCV dependency factor in HepaRG cells.

7.1.2 Development of an HBV reporter system

Murine cells are not susceptible to HBV infection, potentially due to the absence of a necessary dependency factor [109]. In order to identify human host dependency factors, I aimed to construct an HBV reporter system. This system, originally developed by former lab members, involves inserting a reporter gene into the Pol/S ORF. A split Cre system was used as reporter gene, where the enzmye is divided into an N- and C-terminal part. When these parts come into close proximity, they associate and regain enzyme activity [18].
In the developed HBV reporter system, the reporter virus harbors the N-terminal part (NCre), while the reporter cells harbor the C-terminal part (CCre) along with a double

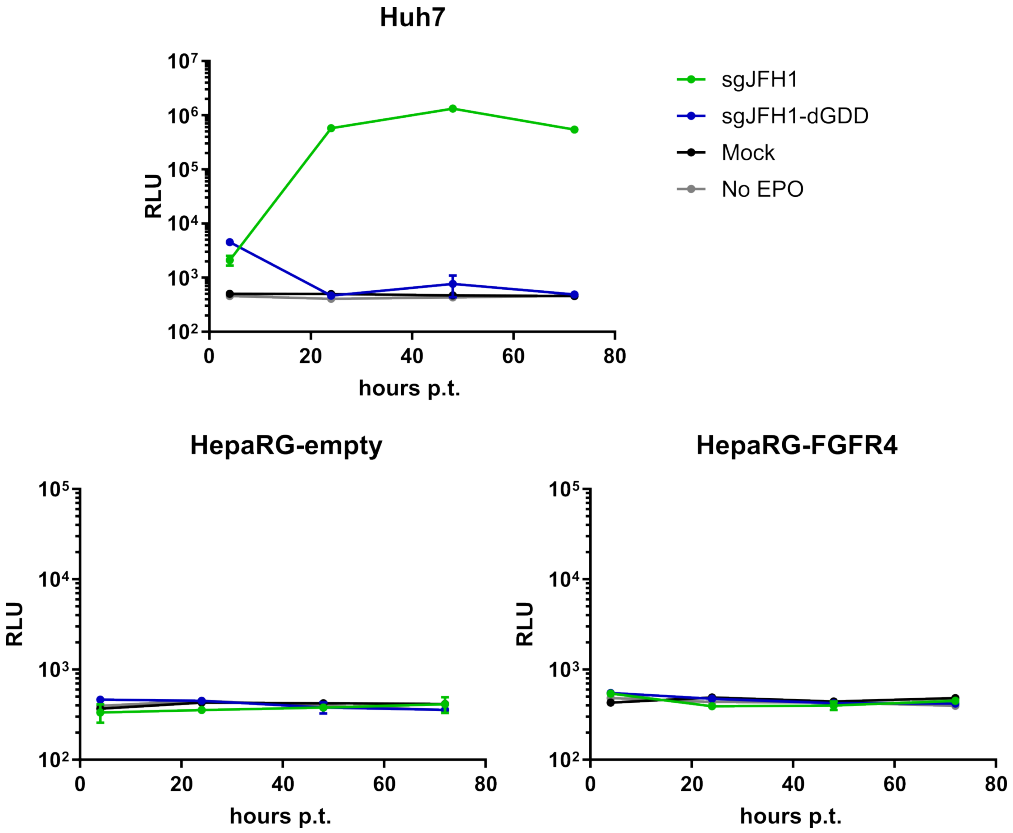

Figure 7.1: FGFR4 as potential HCV dependency factor. HepaRG-FGFR4 overexpressing, HepaRG-empty and Huh7-wt cells were transfected with 2,5µg *in vitro* transcribed RNA for sgHCV harboring Firefly luciferase or a replication deficient mutant (dGDD), without RNA or left untreated at all. Replication efficiency was determined measuring luciferase activity at depicted time points post transfection. Error bars indicate variation between three technical replicates. N=1

fluorescent reporter cassette. This cassette consists of DsRed flanked by LoxP sites, followed by GFP without a promoter, and an IRES-accessible Puromycin resistance cassette. In a non-infected cell, DsRed is expressed, and cells transduced with the reporter cassette can be selected by adding Puromycin. Upon successful infection with reporter virus, Cre is reconstituted, leading to recombination of the LoxP sites and excising the DsRed sequence. Consequently, GFP is expressed, causing infected cells to turn green. In order to screen for potential host factors, I aimed to overexpress a human library using lentiviral vectors in murine NTCP expressing cells, followed by infection with the reporter HBV.

I successfully generated reporter cells expressing the fluorescent reporter cassette, NTCP, and CCre. Transfection of an NCre plasmid confirmed the functionality of the reporter system, as demonstrated by microscopy and flow cytometry analysis (see Fig. 7.2). In order to produce the reporter virus, I successfully generated HepG2 and Huh7 helper cells overexpressing Pol and S ORFs required to transcomplement the defective reporter virus DNA (see Fig. 7.3). However, introducing the reporter HBV genome into these cells proved to be challenging. Despite attempting different delivery methods, such as circular or linear plasmid or transposon transfection, the production of reporter viruses remained unsuccessful. Consequently, this project was discontinued.

7.1.3 Potential restriction factors for HBV in murine cells

Two potential restriction factors for HCV replication in murine cells, CR1L and CD302, were recently identified [15]. These factors were hypothesised to potentially restrict HBV replication in murine cells as well. Therefore, I conducted an investigation into HBV replication by knocking down these factors in Hep56D.1-NTCP murine cells and overexpressing them in susceptible human HepG2-NTCP cells. The knockdown and overexpression were confirmed using RT-qPCR, and cells were subsequently infected with HBV. However, neither knockdown in murine cells nor overexpression in human cells showed any improvement or restriction of HBV replication (see Fig. 7.4). As a result, these factors were not further explored in this study.

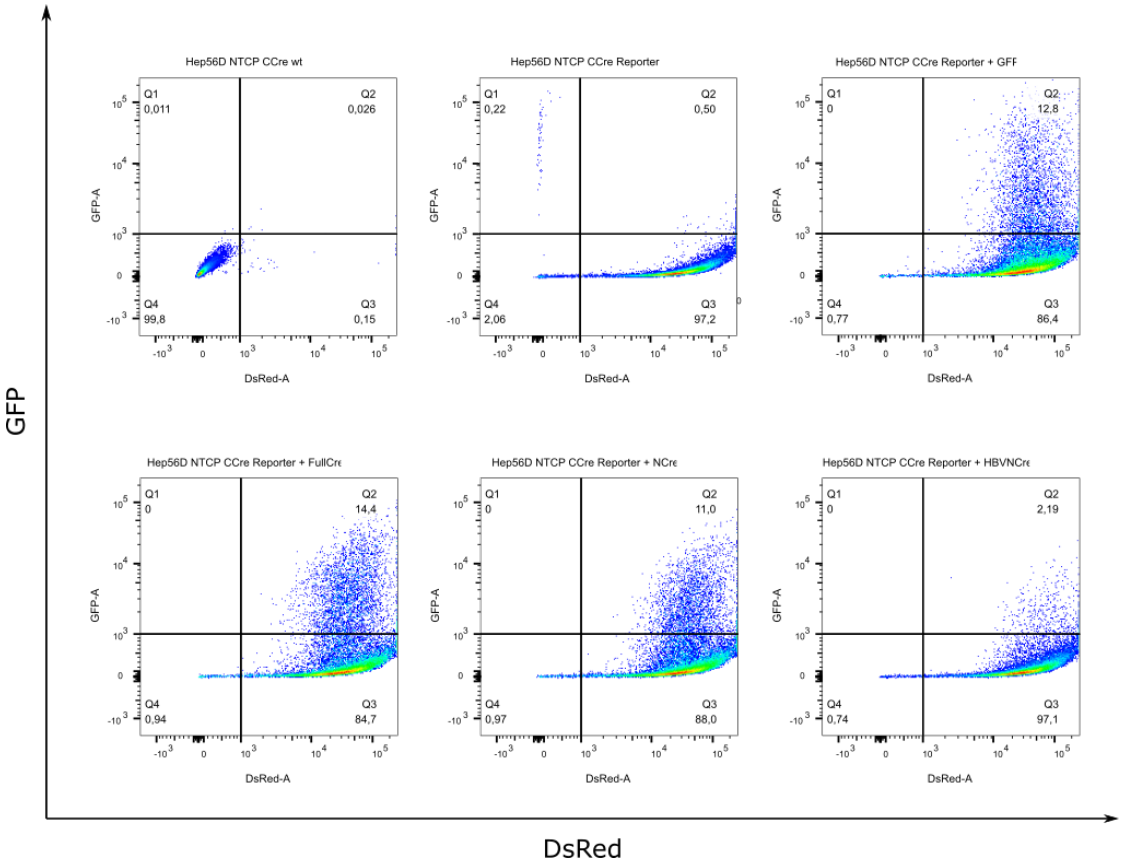

Figure 7.2: Reporter cells are functional. Cells stably expressing the double-fluorescent reporter cassette and CCre were transfected with 1µg plasmids per 6-well encoding for GFP, fullCre or HBV-NCre and expression of DsRed and GFP was investigated after fixation of cells by flow cytometry at d1p.t. N=1

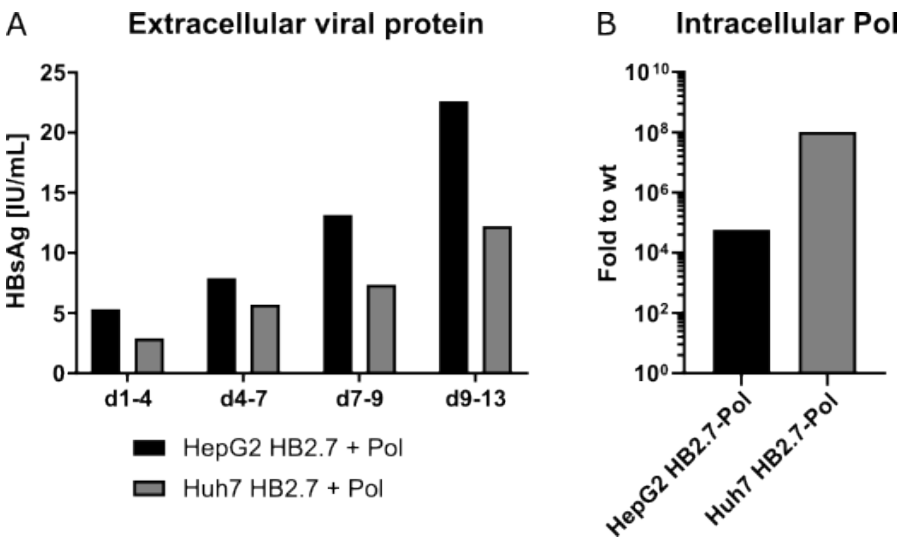

Figure 7.3: Production of HBsAg and Pol from helper cells. HepG2 or Huh7 cells were stably transduced with HB2.7 and HBV polymerase. After successful antibiotic selection, cells were tested for A) HBsAg secretion by ELISA between d1-13 and B) Pol production by RT-qPCR at d13; N=1

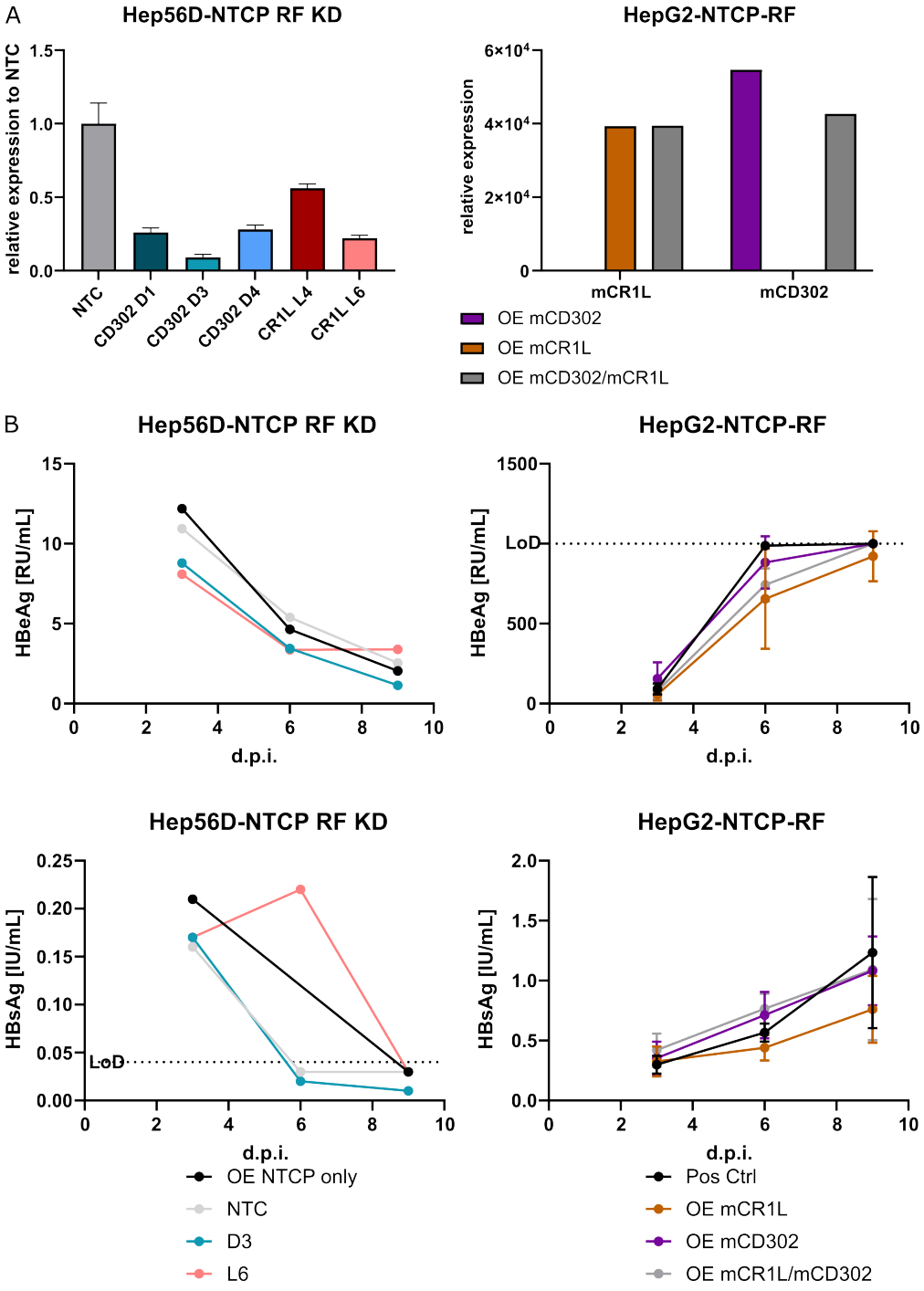

Figure 7.4: No effect of knockdown or overexpression of mCD302 and mCR1L on HBV infection. Both factors were knocked down via shRNA in Hep56.1D-NTCP or overexpressed using lentiviral transduction in HepG2-NTCP cells. A) Knockdown and overexpression efficiency was checked by RT-qPCR (data kindly provided by Aileen Krüger). Error bars indicate variation between three technical replicates. B) Productive infection with HBV (MOI 100 GE/cell) was checked by ELISA for HBeAg and HBsAg at indicated time points; Hep56.1D-NTCP N=1; HepG2-NTCP N=3